Production, characterization and upgrading of biomass-derived acetal-stabilized carbohydrates

Thèse N° 9508

Présentée le 19 juin 2019

à la Faculté des sciences de base
Laboratoire des procédés durables et catalytiques
Programme doctoral en chimie et génie chimique

pour l'obtention du grade de Docteur ès Sciences

par

Ydna Marie QUESTELL-SANTIAGO

Acceptée sur proposition du jury

Prof. V. Hatzimanikatis, président du jury
Prof. J. Luterbacher, directeur de thèse
Prof. Y. Román, rapporteur
Dr M. Rarbach, rapporteur
Prof. O. Kröcher, rapporteur

2019

ÉCOLE POLYTECHNIQUE
FÉDÉRALE DE LAUSANNE

Acknowledgments

I do not have in mind the precise moment when I started to consider doing a PhD. What I do remember, it is Professor María Curet-Arana taking some time from our course of Thermodynamics II to talk about our future careers and encourage us to continue studying. She was the author of one of the recommendation letters that launched my career path far from ordinary. I also remember Professor Arnaldo Carrasquillo-Jimenez, with whom I had my first research experience, warning me about the responsibilities that scientists have not only with science but with society. He gave me the book *On Being a Scientist: Responsible Conduct in Research*, which I still have. To these professors that marked my foundation, **thank you.**

My PhD journey started when I met professor Jeremy S. Luterbacher, who at the time was a postdoctoral researcher in the University of Wisconsin – Madison. After a full summer working under his supervision as an undergraduate researcher, he offered me the opportunity to become his PhD student at EPFL. Although I hesitated to accept, mainly due to the substantial distance with my family, Jeremy persuaded me by telling me that "most people who have taken the hardest decision, they have not regret it". For this and for all these years of constant guidance that have not led me to regret, **thank you.**

When I mentioned to my grandmother the idea of going to Switzerland, she told me that it was too far and that I could do my PhD in the University of Puerto Rico – Mayaguez (UPRM). After numerous efforts explaining why it is important to overpass horizons, she still says that UPRM offers PhD in Chemical Engineering. I **thank you,** *abuela,* because even though you did not understand my decision you were supportive and you sent me away to the other side of the world while secretly putting 40 USD in my hand "*por si acaso".*

Support always came unconditionally from *mami*, *papi, madrina* and Rebeca, since the moment I shared my intentions of doing a PhD in Switzerland, until going home by bike at two in the morning after an endless day in the lab. Frustrations were the order of the day, but they were always willing to listen and give me that extra push. **Thank you**, *mami*, for your prayers, **thank you,** *papi*, for your *"¿cómo estás?"*, **thank you,** *madrina*, for reiterating that I was doing the correct thing and **thank you,** Rebeca, for being there every time I was devastated.

Apart from flow reactors, extraction units and other weird setups, I had the fortune to build everlasting friendships. It would have been impossible to finish sane without the *BucksStar* breaks and the Sunday runs with Jher Hau, the *one-beer nights* with Masoud and Benjamin, the nonstop passive aggressive messages of Jessica and every other Florent's attempt of Spanish. **Thank you** for being the best colleagues and my friends.

Lastly, I would be careless not to share a little bit of the unforgivable flavor that this PhD has left me. I hope that the end of this page could dispense meaning as I understand it now…

Is there space for regrets?

My life could have been easier.
Life makes sense instead.

I could have been wealthy,
but I am richer instead.

My family would have missed me less.
We are stronger instead.

I could have conquered my limits,
but I increased them instead.

I was me,
now I am myself.

Abstract

Biomass is an attractive source of renewable carbon-based fuels and chemicals. Multiple research efforts are centered around integrated biorefineries, where all fractions of biomass are converted to fuels or chemical products. These efforts are focused around making biorefineries more economically competitive and sustainable. One of the major drawbacks is the incomplete utilization of biomass, specifically, lignocellulosic biomass, which is the largest terrestrial source of renewable carbon. Given the significant differences in the structure and reactivity of its components, the integrated depolymerization and subsequent upgrading of all the fractions involved has been challenging.

The depolymerization of lignocellulosic biomass is controlled by the kinetic competition between depolymerization and degradation reactions. Multiple strategies have relied in the modification of reaction conditions to mitigate this limitation, but are either expensive or have not fully overcome this issue. Here, I present the use of protecting group chemistry to reversibly stabilize biomass-derived carbohydrates during depolymerization by acetal formation with formaldehyde (FA). This stabilization technique, altered the kinetic paradigm by limiting sugar dehydration and further degradation. The depolymerization of beech wood using acid organosolv processes in the presence of FA led to recoveries of over 90% sugars with a final concentration of ~5wt%.

The produced acetal-stabilized biomass-derived sugars possess versatile properties compared to unmodified sugars, which motivated me to further investigate their reactivity. I found that diformylxylose (acetal-stabilized xylose, DX) produced an intermediate during its acid hydrolysis deprotection that promoted a 1,2-hydride shift that led to the low temperature production of furfural. Generally, this shift is catalyzed by Lewis acids, but its presence did not affect the

rate of reaction when DX was used as a starting material. Based on these findings and *Operando* NMR studies, a tandem hydrolysis-dehydration of DX to furfural, was proposed.

The benefits of using acetal-stabilized sugars was studied by performing a preliminary techno-economic analysis for the non-enzymatic production of ethanol and the direct upgrading of DX to xylitol. After taking account the solvent savings and the extra recovery steps of FA, a minimum selling price of $4.05 ($2014) of gasoline gallon equivalent was calculated. In the case of xylitol production, a proposed process was constructed around the volatility and unique reactivity of DX. The key advantages included the purification potential of DX by distillation rather than activated carbon adsorption and ion exchange chromatography, which is used for xylose purification, and a rate limiting step that was independent of hydrogen pressure, which minimized hydrogen requirements. The on stream study of the catalyst demonstrated an evolution of the active sites of Pt that led to an enhanced xylitol yield. This phenomenon is attributed to the formation of $Pt(OH)_2$ (detected by X-ray photoelectron spectroscopy), which accelerates the hydrolysis and hydrogenation reactions due to the proximal acid site to Pt^0.

In overall, I have demonstrated that acetal functionalization of carbohydrates can, not only increase yields by reducing sugar degradation but also reveal new reactivity that can be exploited to create novel catalytic upgrading pathways for the production of bio-based chemicals.

Keywords

lignocellulosic biomass, protecting group chemistry, acetal-stabilized carbohydrates, operando NMR, furfural, ethanol, catalytic production of xylitol, platinum on carbon, XPS

Résumé

La biomasse est une source de carbones renouvelables pour les carburants et produits chimiques. De nombreux efforts sont déployés autour des bio-raffineries, où la biomasse est convertie. Ces efforts sont axés sur la nécessité de rendre les bio-raffineries plus compétitives et durables. L'utilisation complète de la biomasse, en particulier de la biomasse lignocellulosique, constitue l'un des principaux défis. Compte tenu des importantes variations de structures et de réactivités parmi ses composants, la dépolymérisation ainsi que de la valorisation de toutes ses fractions s'est avéré techniquement difficile.

La dépolymérisation de la biomasse lignocellulosique est gouvernée par la compétition cinétique entre la déconstruction en monomères et la décomposition de ceux-ci. Les solutions explorées pour limiter ce problème ne sont, malheureusement, soit pas assez efficaces soit trop chères. Je présente, ici, l'utilisation de groupes protecteurs à base de formaldéhyde (FA) pour stabiliser les glucides sous forme d'acétals pendant l'étape de dépolymérisation, de manière réversible, limitant leur décomposition. La dépolymérisation du hêtre en milieu organique et en présence de FA a permis une récupération allant jusqu'à 90% des glucides avec une concentration finale d'environ 5% massique.

Le produit, stabilisé sous forme d'acétal, est significativement plus volatile que son homologue non protégé, ce qui m'a poussé à étudier leurs différences en termes de réactivité. J'ai déterminé que le xylose stabilisé (diformylxylose, DX) forme un intermédiaire pendant sa déprotection hydrolytique qui favorise le transfert d'hydrure en 1,2-permettant la production à basse température de furfural. En général, ce type de réaction est catalysé par des sites acides de Lewis. Cependant, la présence ou non de ce type de sites n'a eu aucun effet sur la cinétique de réaction lorsque le DX est utilisé comme réactif de départ. Guidée par cet indice et les résultats obtenus

par RMN *operando*, un mécanisme impliquant un tandem hydrolyse-déshydratation du DX en furfural fut proposé.

Les bénéfices de l'utilisation de sucre stabilisés en acétals fut étudié par analyse technico économique pour la production non enzymatique d'éthanol et la valorisation directe du DX en xylitol. Après avoir pris en considération l'économie de solvant et les étapes supplémentaires de récupération du FA, un prix minimum de vente de 4.05$ (2014) par équivalent de gallon d'essence fut calculé. Dans le cas de la production du xylitol, un procédé fut établit autour de la volatilité et de la réactivité unique du DX. Les principaux avantages qui en découlent sont la purification du DX qui pourrait potentiellement être fait par distillation plutôt que par adsorption sur charbon actif, et le besoin amoindri en hydrogène du fait que l'étape cinétiquement limitante est indépendante de la pression en H_2. Les essais catalytiques en flot continue indiquent une évolution des sites actifs en Pt qui mène à une amélioration du rendement en xylitol. Ce phénomène est attribué à la formation de $Pt(OH)_2$ (détecté par spectrométrie à photo électron X), qui accélère l'hydrolyse et l'hydrogénation du fait de la proximité des sites acides avec Pt^0.

En résumé, j'ai démontré que la fonctionnalisation de glucides en acétals permet, d'augmenter le rendement en réduisant la dégradation des sucres ainsi que de révéler de nouvelle voies de conversion catalytique pour la production de produits chimiques issue de biomasse.

Mots clef

biomasse lignocellulosique, chimie des groupes protecteurs, glucides stabilisés par des acétals, RMN operando, furfural, éthanol, production catalytique de xylitol, platine sur carbone, XPS.

Table of contents

List of Figures

List of Tables

List of Equations

$$F_{DG\ isomer} = \frac{MW_{DG\ isomer} \cdot ECN_{DX}}{MW_{DX} \cdot ECN_{DG\ isomer}} \cdot F_{DX}$$

$$M_{DG\ isomer} = \frac{A_{DG\ isomer\ in\ injection}}{F_{DG\ isomer}}$$

$$n_{DG\ isomer} = \frac{M_{DG\ isomer}}{MW_{DG\ isomer}}$$

$$n_{i_{glucose}} = \frac{M_{pretreated\ solids} \cdot x_{glucan} \cdot y_{glucose/glucan}}{MW_{glucose}}$$

$$Y_{DG\ isomer} = \frac{(n_{DG\ isomer} \cdot V_{sample})}{n_{i_{glucose}}} \cdot 100\%$$

List of Symbols

- $A_{DG\ isomer\ in\ injection}$ [pA min]: peak area of the diformylglucose isomer in the GC-FID chromatogram
- [A]: concentration of acid
- Biomass [ton h^{-1}]: mass flow of wood
- Ea_i [J mol^{-1}]: the activation energy of the reaction in question
- $ECN_{DG\ isomer}$: effective carbon number of diformylglucose
- ECN_{DX}: effective carbon number of diformylxylose
- $F_{DG\ isomer}$ [pA min mg^{-1}]: response factor of the diformylglucose isomer
- F_{DX} [pA min mg^{-1}]: response factor of diformylxylose based on a calibration curve
- k_i [s^{-1}]: kinetic constant where *i* is the reaction in question
- $k_{i,0}$ [s^{-1}]: pre-exponential factor
- $M_{DG\ isomer}$ [mg]: mass (milligrams) of the diformylglucose isomer in GC injection (in 1 µL)
- $M_{pretreated\ solids}$ [mg]: mass (milligrams) of packed pretreated solids in the reactor bed (air dried basis)
- $MW_{DG\ isomer}$[mg $mmol^{-1}$]: molecular weight of the DG isomer (204.06 mg $mmol^{-1}$)
- MW_{DX}[mg $mmol^{-1}$]: molecular weight of diformylxylose (174.05 mg $mmol^{-1}$)
- $MW_{glucose}$[mg $mmol^{-1}$]: molecular weight of glucose (180.16 mg $mmol^{-1}$)

- $n_{DG\ isomer}$ [mmol]: millimoles of the diformylglucose isomer in GC injection (in 1 μL)
- n_i: acid exponent (empirically determined)
- $n_{i_{glucose}}$ [mmol]: initial millimoles of packed glucose- equivalents as pretreated solids in the reactor bed
- R [J K^{-1} mol^{-1}]: universal gas constant, 8.314
- R1: wood pretreatment reactor
- R2: treated cellulose reactor
- Ratio: solvent to biomass ratio
- Solids [ton h^{-1}]: mass flow of treated cellulose
- T [K]: reaction temperature
- V_{sample} [mL]: total sample volume of collected liquid from flow-through reactor
- x_{glucan} [mg mg^{-1}]: glucan content in pretreated solids (air dried basis)
- $y_{glucose/glucan}$ [mg mg^{-1}]: conversion factor of glucose to glucan (1/0.9)
- $Y_{DG\ isomer}$ [%]: yield of diformylglucose isomers based on the packed pretreated solids in the reactor bed

Chapter 1: Introduction

In this thesis, I first review the current status, where most of the global energy and carbon demand is primarily fulfilled by fossil resources. I then discuss biomass as a renewable feedstock for the substitution of fossil carbon with a particular emphasis on lignocellulosic materials. I then briefly discuss the principal transformations and depolymerization routes in biorefineries considering different types of biomass. I notably provide a specific overview of the kinetic limitation that shape the depolymerization of lignocellulosic biomass and a summary of approaches that modify depolymerization reactions to overcome the kinetic limitation region. Later, I outline the objectives of my doctoral thesis, followed by my research work. Finally, I present overall conclusions with respect to the objectives and some recommendations for follow-up work.

This chapter contains parts of a published book chapter in the *Royal Society of Chemistry (RSC)* as **Questell-Santiago, Y.M.** and Luterbacher, J.S. Chapter 2: Introduction to High Pressure CO_2 and H_2O Technologies in Sustainable Biomass Processing, in *High Pressure Technologies in Biomass Conversion,* **2017**, 9-36. doi: 10.1039/9781782626763-00009[1]. The selected content is reproduced here with a few formatting changes and permission from RSC.

1.1 Global energy and carbon demand: Current scenario

Petroleum is a major raw material for the production of fuels, chemicals and materials used in our daily lives. The continuous growth in the consumption of these products requires an increased exploitation of fossil resources. In turn, this exploitation has led to environmental and economic issues linked to climate change, resource depletion and political instabilities due to the unequal distribution of fossil deposits.[2] The global primary energy consumption has increased at a constant rate of 2.4%/year ± 0.08% since 1850 and shows no sign of slowing

down.[3] The global community, aware of the dangers linked to diminishing fossil reserves and climate change mainly due to CO_2 emissions, is encouraging the development of renewable carbon sources through several agreements and policies.[4] In order to achieve full sustainability, it is essential the consolidation of all types of renewable sources of energy and carbon. In 2017 the world's total energy consumption was 13.5 billion tons of oil equivalent (2.2% growth with respect to 2016) and only 10.4% of this energy was supplied by renewables.[5] According to the International Energy Agency (IEA) and the 2ºC scenario (increase in global temperature that would lead to catastrophic climate change), bioenergy will play an important role in the total annual CO_2 emission saving by contributing 17% of the future final energy demand in 2060.[6,7] In this scenario, biofuels will be required to provide nearly 30 ExaJoules (EJ) of total transport final energy demand. The two biggest contributions will be to jetfuel (12 EJ) and bunker fuel (9 EJ) because, for these fuels, and with current technology, biomass represents the only viable alternative feedstock.

Using biomass and organic wastes as a feedstock for renewable carbon represents a promising and sustainable alternative to fossil carbon.[8] Biomass, in particular, is a neutral carbon source as it is part of a closed carbon cycle where the released CO_2 by biomass usage is subsequently captured by plants (Figure 1.1). However, the full exploitation of biomass is associated with many challenges including the development of suitable conversion technologies both from an ecological and economic standpoint coupled with political support issues. The production of fuels from biomass has been criticized due to the so-called fuel *vs*. food competition.[9,10] The risk that large-scale biomass exploitation could drive up the price of competing food crops has favored the substitution of primarily jet fuel and carbon-based materials with their bio-based alternatives. Jet fuels are difficult or sometimes impossible to substitute with other renewable

source of energy such as sustainably produced electricity due to the highly specific performance properties that are required.[11] These fuels are considered more valuable than other transportation fuels and their demand is significantly lower which leads to less competition issues for land used in food production. For these reasons, the production of jet fuel and carbon-based chemicals from biomass has attracted less controversy and has helped promote the concept of an integrated biorefinery.[12]

This concept is defined as the production of at least one energy product (besides heat and electricity), the production of at least one high value chemical or materials, along with large volumes of low-grade products in a single biomass conversion plant.[13] Unfortunately, current conversion technologies are usually designed for a specific type of biomass and can suffer from low yields, high energy requirements and elevated operational costs which makes difficult the integration of bioproducts in the competitive market.[14,15]

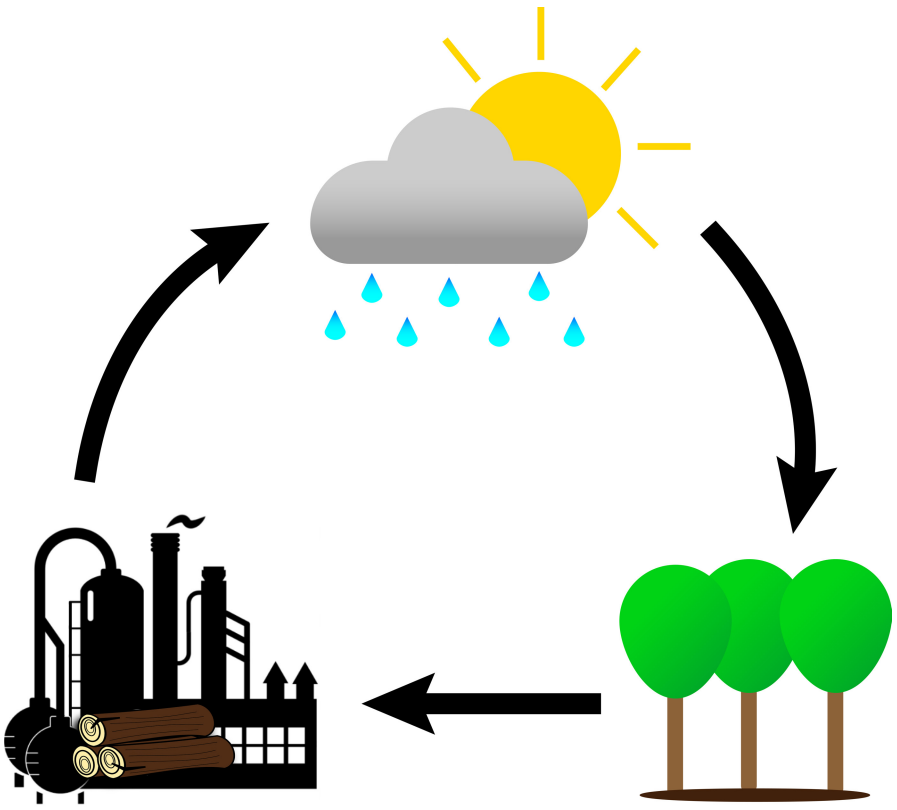

Figure 1.1 | Representation of the closed carbon cycle in biomass utilization.

1.2 Biomass as feedstock

Biomass refers to a renewable organic material created biologically and is defined as "substance wholly comprised of living or recently living (non-fossil) material".[16] This concept includes an extensive range of materials, e.g. whole or parts of, plants, trees, animals, microorganisms and aquatic organisms, which are classified as edible and non-edible crops. When considered as a source of fuel, biomass is sub-classified into three categories referred to as first, second or third generation biofuels.[16,17] First generation biofuels or bioproducts refer to fuels and chemicals made from edible crops that are used for the production of compounds containing starch (e.g. corn, flower, etc.), sugar, vegetable oil, lipids and/or proteins.

Second generation biofuels or bioproducts refer to molecules made from lignocellulosic materials, which are non-edible crops, mainly composed of polysaccharides. Lignocellulosic material tends to be more difficult to convert to fuels, but usually provides more material per plant growth area and requires less fertilizer to grow.[18,19] Both of these attributes lead most experts to agree that second generation biofuels and bioproducts are more sustainable than their first generation equivalents. Lignocellulosic material/biomass is mainly composed by three biopolymers: cellulose, hemicellulose and lignin. Chemicals produced or extracted from microalgae have sometimes been referred to as third generation biofuels and bioproducts. Algae has mainly been considered for the production of oil and lipids.[17,20] Figure 1.2 shows the chemical structure of the main components of the feedstock used for the three generations of bio-based molecules.

As discussed above, biomass has the potential to replace fossil-based feedstock for the production of chemical intermediates and fuels. However, the chemical structure and composition of biomass is considerably different from that of crude oil, which is the major conventional fossil

feedstock.[21] Hence, all biomass processing employ reforming steps to produce direct or indirect petrochemical replacements.

1.2.1 First generation biofuels and bioproducts – Edible crops

First generation biofuels and bioproducts are produced from biomass with significant edible fractions, such as corn, sugar cane, wheat, palm oil and rapeseed. These feedstocks are the primary sources of starch, sugars and vegetable oil, mainly used to produce energy products that include biogas, bioethanol and biodiesel.[13] Biogas is produced by the anaerobic digestion of mixtures of starch, manure and other organic wastes, and is use for the production of electricity and in some countries as transportation fuel, after purification and pressurization of the resulting methane. In such cases, starch, free sugars, oils and proteins can generally be converted to gas by microorganisms but other inedible biomass fractions generally remain untouched. Bioethanol is recovered from the fermentation of simple sugars derived from sugarcane, sugar beet and starch crops. Simple sugars are fermented directly, while amylase enzymes are generally added to the starch-based biomass before fermentation to break down the starch to simple sugars.

Currently, bioethanol is the largest biofuel produced worldwide with a total world production of 105.5 billion liters of bioethanol in 2017.[22] The largest producer of bioethanol in 2017 was the USA with a production of 60 billion liters, Brazil was second with 28.5 billion liters and China third with 3.3 billion liters. Another transportation fuel with a large worldwide production capacity is biodiesel, which is produced from oil-based crops including palm oil, rapeseed and soybean. The three world leaders in biodiesel production in 2017 were Europe (12.7 billion liters), the USA (5.9 billion liters) and Brazil (4.3 billion liters).[22]

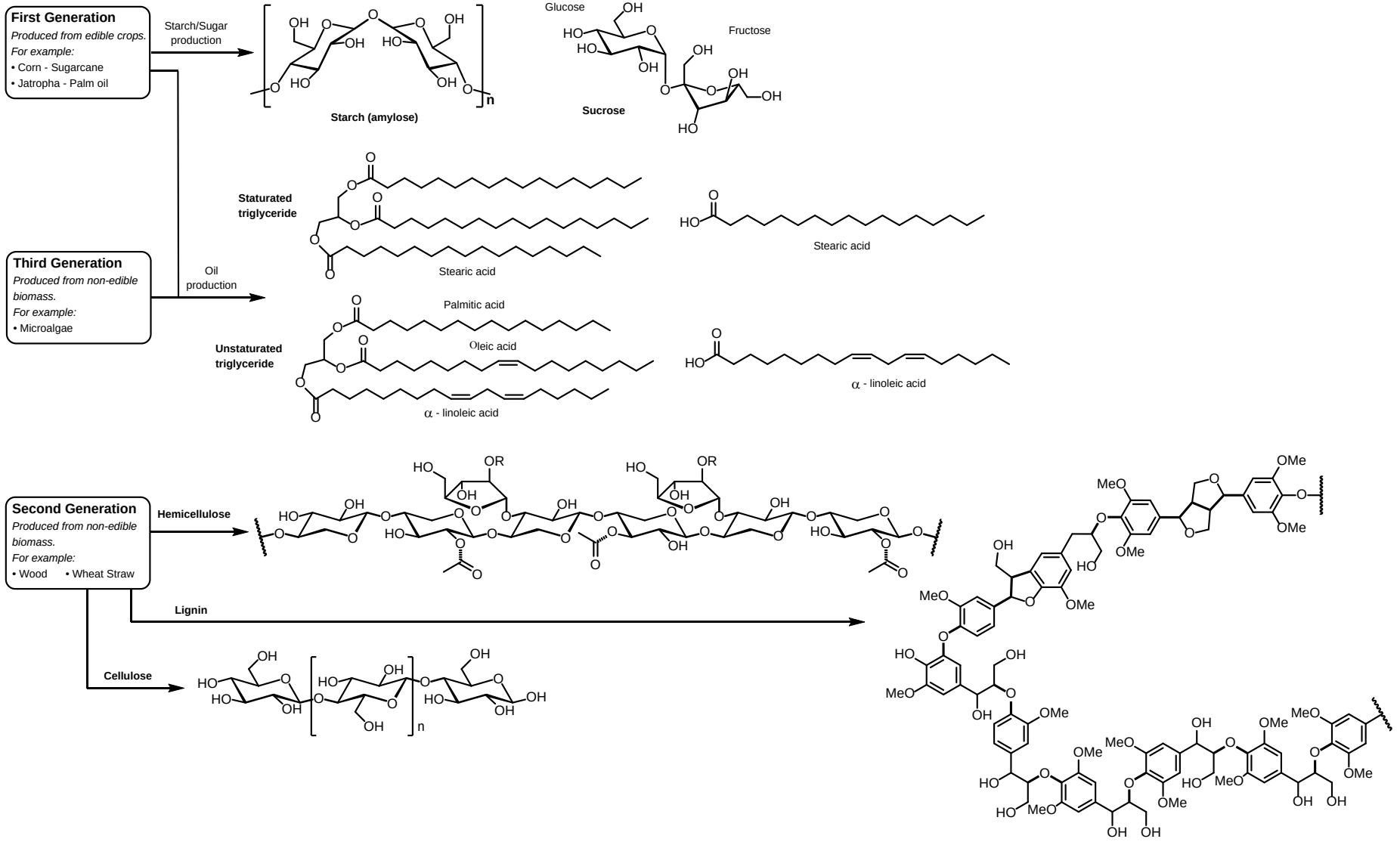

Figure 1.2 | Main components of all three biomass categories.

The chemical structures that produce first generation biofuels and bioproducts are very easy to convert to biofuels due to their ease of depolymerization and high content within the relevant plant structure (which is why these plants are considered edible). However, first generation products have several issues including their competition with food, their limited availability, their high fertilizer use and, therefore, their minimal savings in terms of CO_2 emissions compared to their fossil equivalent. For these reasons, the final bioenergy demand in 2060 is not expected to be met by edible crops and is rather expected to be supplied almost entirely from second and third generation biofuels and bioproducts.[7]

1.2.2 Second and third generation of biomass – Non-edible crops

Lignocellulosic biomass, microalgae and organic wastes are usually described as non-edible crops. Agriculture and forestry residues are examples of lignocellulosic biomass. The bulk of terrestrial biomass is represented by lignocellulosic materials, mainly composed by three natural biopolymers: cellulose, hemicellulose and lignin. Their content varies between 30-50% cellulose, 20-35% hemicellulose and 15-30% lignin.[2,23] The cellulose fraction is exclusively composed by β-D-glucopyranose moieties linked lineary via β-1,4-glycosidic bonds.[24,25] The interaction between these chains induces the formation of rigid and semi-crystalline fibers through hydrogen and van der Waals bonds, making it insoluble in most conventional solvents.[26,27] These polymer chains can have a polymerization degree up to 10'000 units in woody biomass.

Hemicellulose is an amorphous hetero-polymer with branches and short lateral chains containing five different types of sugars (D-galactose, D-mannose, D-glucose, L-arabinose and D-xylose), xylose being the most abundant.[28–30] The hydroxyl groups of these sugars could be partially substituted with acetyl groups and, other minor sugars such as L-rhamnose and a-L-

fucose could be present. The degree of polymerization is significantly lower compared to glucose, it varies from 50 to 300 units.[31] Lignin is also an amorphous hetero-polymer with a three dimensional structure, composed by methoxylated phenylpropanoid units.[31,32] Because of its lower oxygen content compared to cellulose and hemicellulose (30 wt% oxygen in lignin versus 49 wt% in cellulose), lignin accounts for about 40% of the biomass heating value. [2,33]

In the plant cell wall, lignin surrounds hemicellulose and cellulose, while cellulose fibers are interlaced with hemicellulose (Figure 1.3).[24] As a result, most biomass conversion routes begin with the extraction of lignin and some hemicellulose sugars to expose the remaining polysaccharides for further transformations. Each of the fractions in lignocellulosic biomass have the potential to replace petroleum-based derivatives including fuels, materials and fine chemicals.[34,35] Given their structure and reactivity differences, an integrated conversion into their corresponding monomers is highly challenging and energetically demanding. In addition, due to their structural differences, these three biopolymers also have different potential applications. Biomass-derived carbohydrates are mostly thought of as potential platform molecules for the production of renewable fuels and materials by both biological and chemical upgrading, while lignin-derived monomers are thought of as precursors for renewable aromatic chemicals and drop-in fuels due to their lower oxygen content.[36,37]

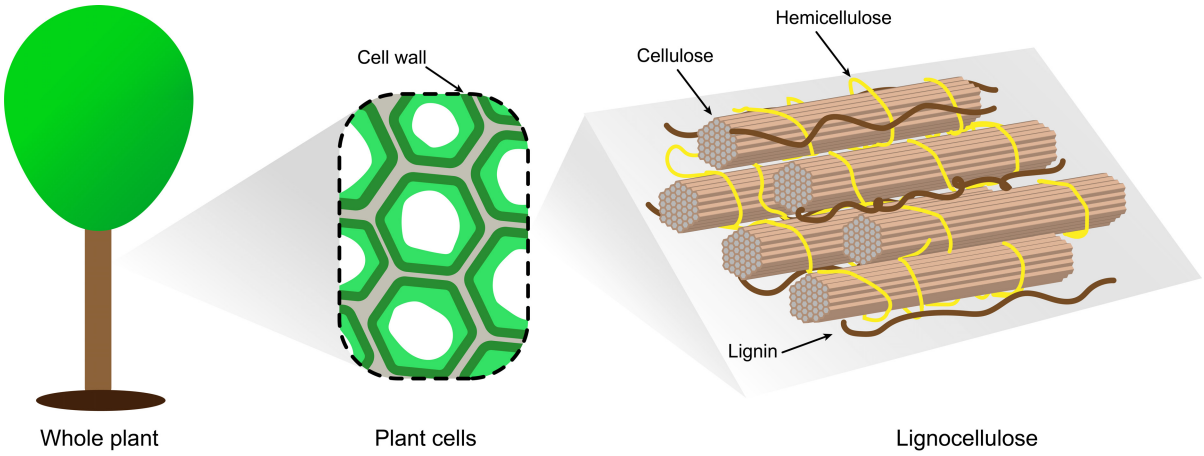

Figure 1.3 | Representation of the structure of lignocellulosic biomass in plant cells.

Organic wastes are another feedstock for so-called second generation biofuels and bioproducts and mainly refer to sewage sludge, pulp and paper mill sludge, food waste, manure and other agricultural residues, which are composed of carbohydrates, proteins, lipids and lactose.[38,39] These feedstocks can be directly processed or pretreated prior to conversion for the production of biogas, hydrogen and C_2 to C_4 hydrocarbons.[39–41] Given the wide compound variety in organic wastes, upgrading routes mainly rely on biological processes such as anaerobic digestion or harsh chemical processes to reduce the molecular weight (gasification).

Microalgae (sometimes referred to as the feedstock for third generation biofuels and bioproducts) are generally considered for the production of biodiesel from extracted lipids by catalytic or enzymatic transesterification.[42] Due to their higher photosynthetic efficiency, they have an impressive potential for the production of biofuels in comparison to lignocellulosic biomass. Algae also has an impressive potential for lipid production. However, these properties are difficult to achieve simultaneously. As a comparison, sugarcane can produce up to 4,892 kg of bioethanol per hectare,[43] while microalgae could, if its potential is realized, produce 52,000-121,100 kg of biodiesel per hectare.[44] This has led to considerable interest in algae research in the last two decades, but this potential has never been achieved at an industrial scale mainly due to the high energy and nutrients requirements in cultivation plants.[44,45] Microalgae can also be used as a source of natural dyes, antioxidants, carbohydrates and other fine chemicals.[44] After extraction, the remaining algae can be processed into ethanol, methane, livestock feed and fertilizer.

1.3 The biorefinery concept

A biorefinery is a facility where a sustainable process integrates the production of fine chemicals, materials, biofuels and heat/power from biomass while minimizing the quantity of leftover

material after treatment. The concept of a biorefinery is analogues to today's petroleum refineries, where multiple carbon-based products and fuels are produced from crude oil and wastes are minimized.[13] Proposed biorefinery processes employ a wide range of technologies to fractionate biomass into valuable compounds (polysaccharides, sugars, oils, lipids, proteins) and for subsequent upgrading in several steps. Feedstock fractionation is a crucial step due to the heterogeneity of the biomass and the multiple functional groups that are present.

Currently, most bioproducts produced from edible crops are manufactured in single product chains and not within a biorefinery concept. Because these plants have already been built, so far, the main focus of facilities that convert edible crops has been to further optimize their processes for single product production and reduce costs rather than implement new technologies.[46] On the other hand, biorefineries based on second and third generation biofuels and bioproducts have the opportunity to exploit many more routes and achieve larger scales due to a larger 'effective' biomass yield per cultivation area, since they rely on the whole plant as feedstock (first generation commodities use only a small portion of plants, e.g. the extractable oil).[13] Such scales could also allow the implementation of new conversion technologies that only become economical at very large scales. Nevertheless, the development of viable biomass conversion platforms or biorefineries will require the selective conversion of biomass's constitutive biopolymers into high-value chemicals and fuels using cost-competitive processes (Figure 1.4).[47–49]

1.3.1 Biorefinery products

Presently, the petrochemical industry refines crude oil into fractions that include naphtha (from which all the major bulk chemicals are derived), gasoline, kerosene, gas oil and residues.[50] The processes employed in the refinery industry include numerous cracking and refining catalysts

as well as distillation as the dominant separation strategy. An important characteristic and advantage of the naphtha fraction compared to biomass, is its low oxygen content. Most bulk chemicals produced in refineries are derived from molecules containing no oxygen such as ethylene, propylene, C_4-olefins and the aromatics benzene, toluene and xylene (BTX).[50]

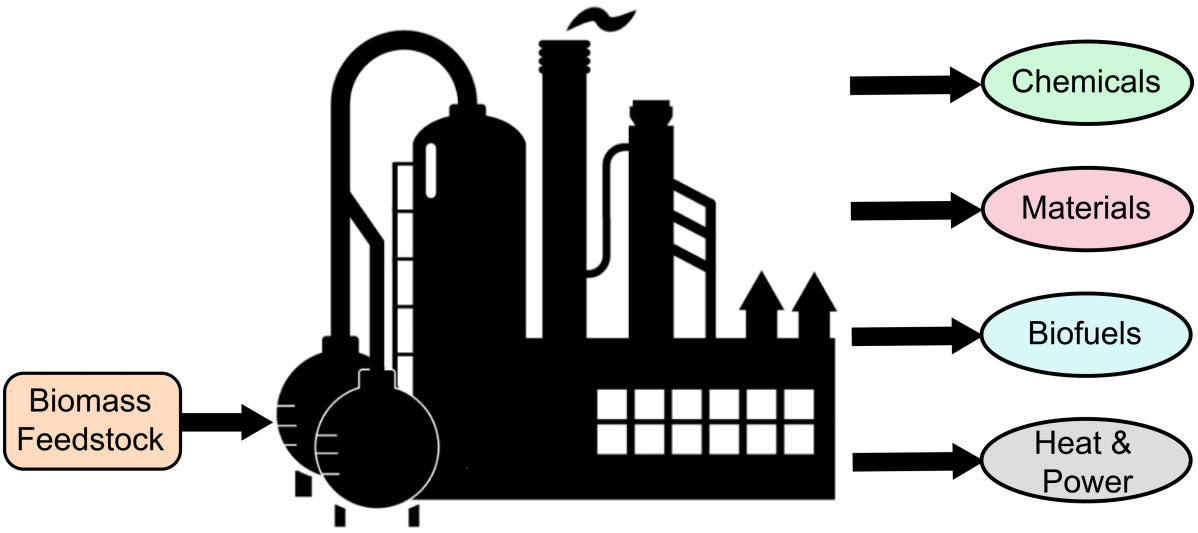

Figure 1.4 | Representation of an integrated biorefinery.

In principle, most petrochemical refinery platform molecules could be derived from renewable carbon sources. Unfortunately, this is currently only possible at relatively low yields and high costs.[50] For this reason, it has been proposed that the biorefinery industry produce a number of petrochemical substitutes through a different selection of simple platform molecules that are different from those currently used in the petrochemical industry.[13] Given the chemical complexity of biomass, there is a range of platform chemicals that could be produced from one type of feedstock depending on the chosen processing strategy. Nevertheless, several of these building block chemicals are expected to be derived from the carbohydrate fraction of biomass, which, due to it being a major component of all types of biomass, is likely to play a crucial role in future biorefineries. In 2004, the US Energy Department identified twelve building block chemicals of major importance that could be produced from sugar by biological or chemical

conversions.[34] These twelve sugar-based building block chemicals are shown in Figure 1.5 along with the main chemicals and products (in bold) that can be easily derived from these intermediates and that are likely to be found in an integrated biorefinery.

A major focus of this thesis is the catalytic production of xylitol, which is one of the twelve sugar-based building block chemicals. Xylitol has no petrochemical alternative.[34] This polyol is commercially used as a natural sweetener in the food industry and in the pharmaceutical industry due to its insulin-independent metabolism and anticariogenecity properties.[51,52] It is also used in personal health products such as toothpaste and mouthwash, and more recently, it has been suggested as a platform molecule for the production of alkanes, aromatics, propylene glycol, ehtyele glycol, glycerol, xylaric acid, lactic acid, hydroxyfurans and hydrogen.[2,53] Given the numerous applications of xylitol, it production has increased more than forty-fold in 40 years.[53] In 2016, the estimated global market for xylitol was valued at US$725.9 million and it is expected to overpass US$1 Billion by 2022. Although it is produced from lignocellulose biomass (a cheap and abundant raw material around the planet), its growth potential is limited by its costly manufacturing process due to the high energy consumption in the hydrogenation and purification steps.[51–54]

1.3.2 Main biorefinery processes

The initial and unavoidable processes in most biorefineries will involve the fractionation, depolymerization and (in some cases) deoxygenation of biomass components. Since biomass is already highly oxidized, several hydrogenation and/or dehydration transformations are usually required. These transformations are key steps for the conversion of biomass into building block molecules and value-added compounds. These processes can be classified into two main categories depending on the nature of biomass transformation: physical or chemical treatments.

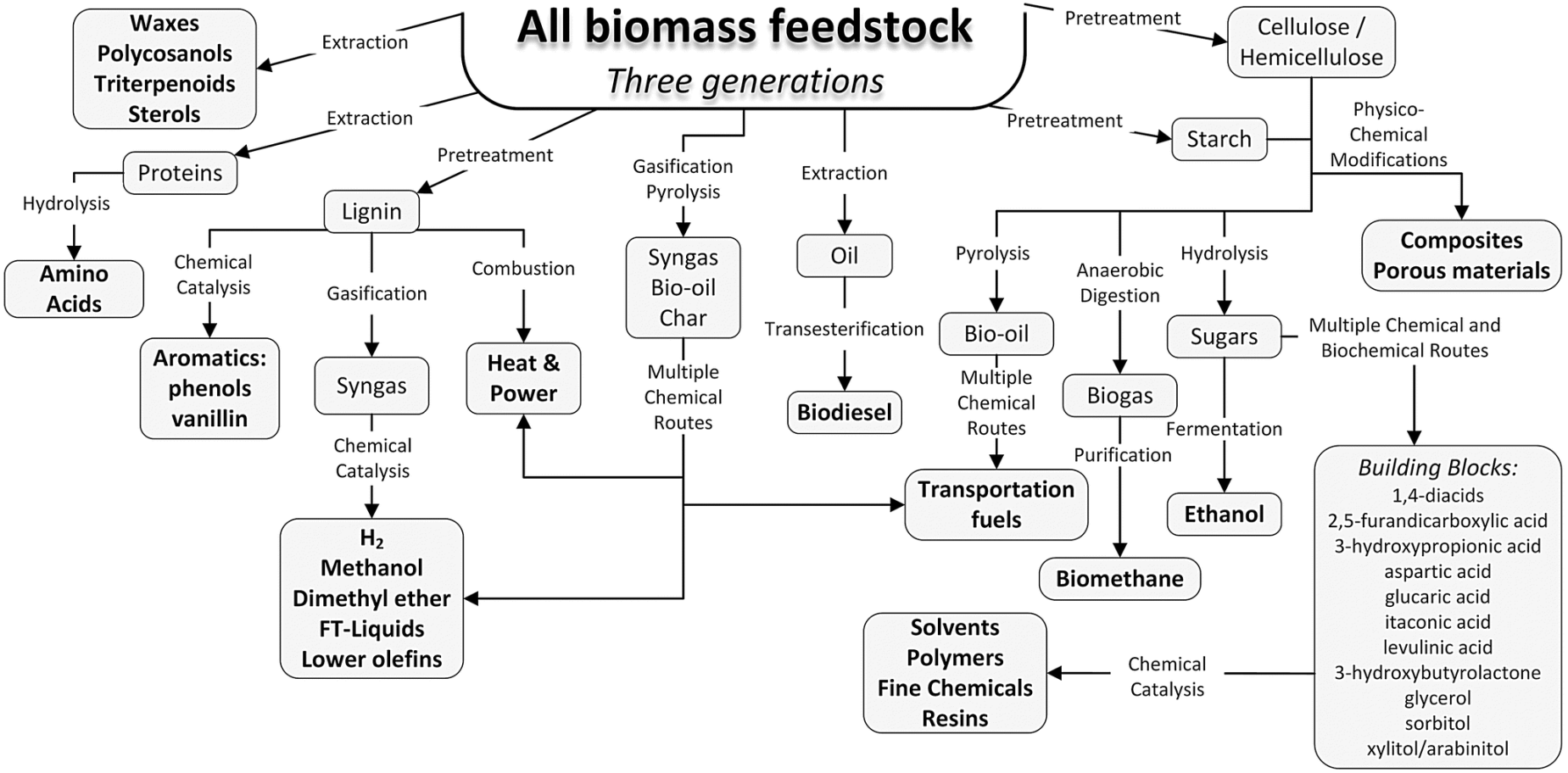

Figure 1.5 | Principal conversion routes and products of all biomass feedstock.

Physical treatment. Physical or mechanical processes are usually the first step in biorefineries and serve as a preconditioning, although they are not always required.[13] These processes do not change the composition of the biomass, but only lead to particle size reduction or separation of the feedstock components. Biomass size reduction refers to changes in particle size, shape or bulk density within specific ranges depending on further conversion processes requirements. Separation procedures can consist of increasing the concentration of valuable compounds without the transformation of their components by extractions methods, mainly using organic solvents or supercritical fluids.

Chemical treatment. Chemical processes involve changes in the chemical structure of one or more of the molecules by introducing high temperatures or catalytic species into the reaction media. For the purpose of this thesis, these processes are classified as thermochemical and catalytic. Thermochemical pathways are defined as rapid and largely driven by high temperatures rather than the presence of catalysts. These thermochemical processes have been used for the production of syngas, bio-oil, bio-char/bio-coal and power from biomass[55] and include gasification, pyrolysis and dry/wet torrefaction. Gasification consists of keeping biomass at high temperatures (>700°C) with limited oxygen concentration to produce hydrogen, methane, syngas, and/or power. Hydrogen and methane can also be in liquid conditions at high pressure if hydrothermal gasification (HTG) conditions are used. HTG operates within the subcritical or supercritical region of water (374°C and 22.1 MPa) usually with a catalyst and generally uses biomass feedstocks with a high water content, e.g. manure, that benefit most from avoiding a pre-drying step in the process.[39,56]

Syngas is an important intermediate in several biorefinery processes that could lead to multiple fuels or chemicals.[57] The Fisher-Tropsch (FT) process is a well-known route for the upgrading

of syngas into long chain liquid hydrocarbons including alkanes and short alcohols (C_1 to C_3) by multiple catalytic syntheses using mostly cobalt and iron-based catalysts.[58] Other catalysts such as nickel and ruthenium have shown high catalytic activity in FT processes, but under operational conditions nickel can promote methanation, which is undesirable, while ruthenium is much more expensive. Higher alcohols (C_4 to C_{10}), used as additives in the reformulation of gasoline[59] and for the production of C_2 to C_4 olefins,[60] are also produced from syngas using a range of catalyst combinations.

Pyrolysis can be described as the processing of biomass at temperatures between 300°C and 600°C in the absence of oxygen, to produce bio-oil, charcoal and light gases similar to syngas. Bio-oil is usually the most desirable product and its production can be maximized by applying what is known as fast pyrolysis conditions (which involves rapid heating up to 500°C and short residence times at high temperatures, e.g. seconds)[55]. Bio-oil can be upgraded to mixtures of molecules that can be used as transportation fuels or chemicals. However, the high production of char and coke, and the important hydrogen consumption still remain problematic.[13] Dry torrefaction, sometimes referred to as a mild pyrolysis, is performed under an inert environment at atmospheric pressure with a retention time around one hour at low temperatures (within 200°C to 300°C or 180 to 260°C in the case of wet torrefaction (WT)).[61,62] In both conditions the main product is bio-char or bio-coal, which is used as a feedstock for combustion or gasification. The advantage of this char over raw biomass is that its characteristics are more stable and that it has a higher energy density, which makes its transportation less environmentally and economically burdensome.

Catalyzed chemical reactions play a vital role in the production and upgrading of platform molecules to petrochemical equivalents and they can be found at various stages of biomass

conversion. The most common catalyzed reactions that occur in biorefineries are hydrolysis, dehydration, hydrogenation and transesterification. Hydrolysis is catalyzed by acids, alkalis or enzymes to depolymerize polysaccharides, proteins and, in some cases, lignin to their corresponding carbohydrates, amino acids and lignin monomers. This reaction is generally seen at the beginning of the process, known as biomass pretreatment.[63] This pretreatment step is a major contributor to the cost of biorefineries that produce second generation (2G) bioethanol, from non-edible biomass.[63,64] At the upgrading stage, dehydration and hydrogenation reactions are important deoxygenation reactions downstream in the process. Other important chemical reactions are transesterification, used to produce biodiesel from lipids or oils by an acid or base-catalyzed reaction with a short alcohol, Fisher-Tropsch synthesis, methanation and steam reforming, which involve syngas conversion in the gas phase and are used to produce hydrocarbons, methane or hydrogen, respectively.[13]

Of all the biochemical reactions currently implemented in various industries, there are three principal types found in biorefineries: fermentation, anaerobic digestion and enzymatic reactions. Fermentation and anaerobic digestion involve live cells whereas enzymatic-based reactions usually involve cell free mixtures of proteins. Fermentation generally refers to the production of specific non-volatile chemicals such as alcohols, organic acids or even alkanes from carbohydrates. CO_2 is almost always a co-product of fermentative processes. Anaerobic digestion refers to processes that in the absence of oxygen produce methane, CO_2, hydrogen, organic acids and hydrogen from carbohydrate and proteins found in biomass and organic wastes. Enzymes are usually used to facilitate the deconstruction of various polymers including polysaccharides and proteins.

1.3.3 Lignocellulosic biorefinery

There are different types of biorefineries, which are classified according to their feedstock or intermediates.[14] These are: sugar biorefinery, starch biorefinery, vegetable oil biorefinery, algal lipid biorefinery, lignocellulosic biorefinery and synthesis gas biorefinery. In the specific case of the lignocellulosic biorefinery, installations have been studied and even run since the beginning of the 20th century.[65] However, complete lignocellulosic material utilization is still far from implemented.[66,67] Two examples of processes found in lignocellulosic biorefineries that have been thoroughly studied are presented below (Figure 1.6):[14]

- *2G Bioethanol Plant* - produces bioethanol by fermentation of monomeric sugars, biogas by anaerobic digestion and steam and power from the burning of remaining lignin.

- *Chemicals Focused Plant* - produces three streams of fractionated biomass (lignin, xylose and cellulose) to consecutively upgrade them separately. Usually the upgrading routes leads to the fermentation of sugars and burning of lignin.

Both of these approaches use technologies centered around the preservation and upgrading of carbohydrates while lignin is completely degraded.[66,67] This issue is caused by the kinetics of depolymerization and degradation reactions that governs biomass deconstruction at most industrially practical conditions, which often lead to degradation reactions outpacing depolyermization reactions. In this case, lignin degradation outpaces its extraction, making it a poor upgrading substrate, which leads to its use as a low value fuel. There are depolymerization strategies that have bypassed these limitations. However, they often utilize complex systems with high process costs, that are often not fully compatible with all biomass fractions. In the following sections, I detail the limitations that are introduced by kinetics and how they control the chemical deconstruction of biomass-derived polysaccharides and lignin.

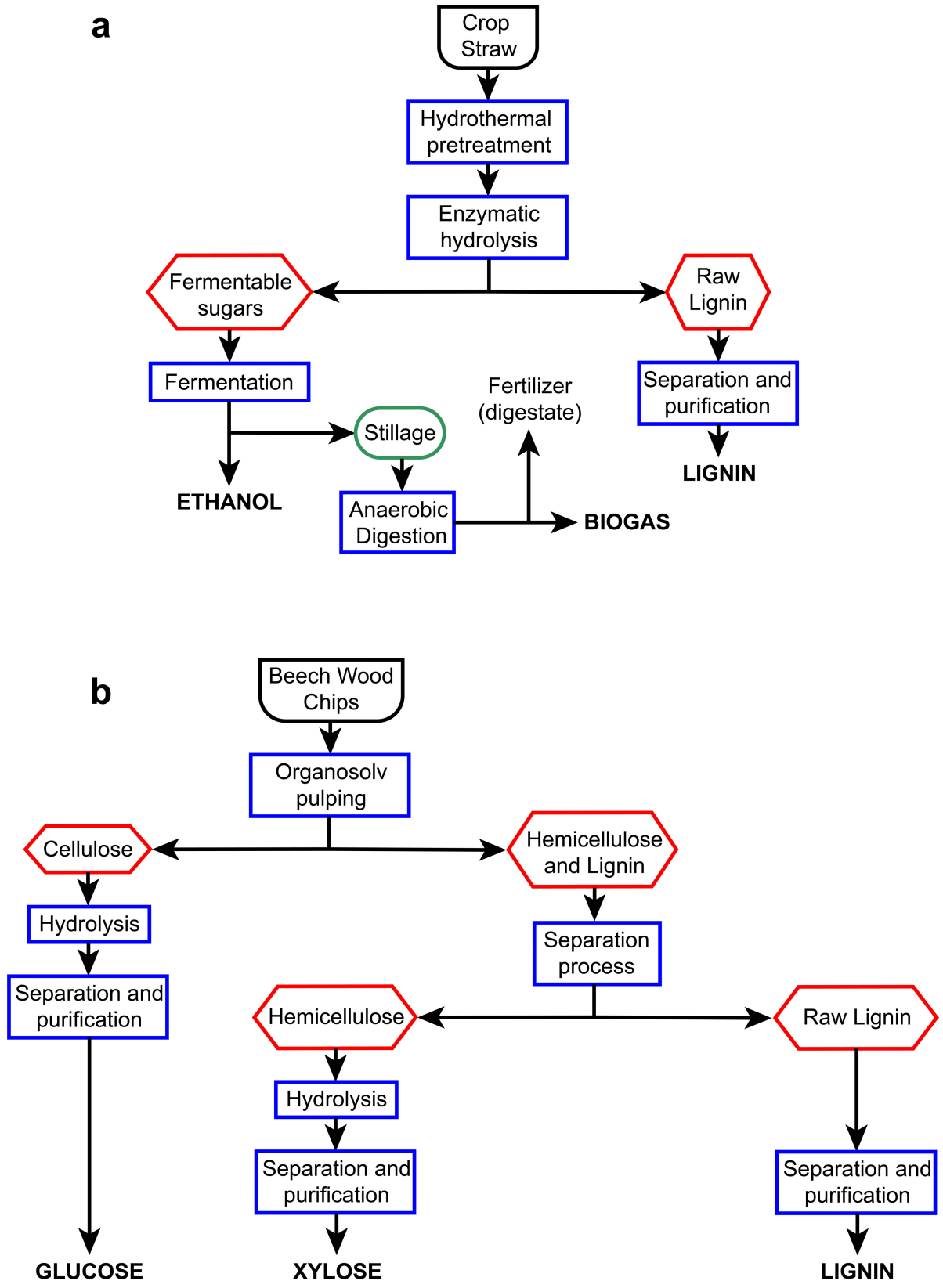

Figure 1.6 | Two biorefinery approaches. Adapted from Wagemann and Tippkötter.[14] a) Second generation bioethanol plant from crop straw. b) Chemical biorefinery plant of beech wood chips.

1.4 The kinetics of polysaccharides and lignin depolymerization

1.4.1 Polysaccharides

The initial step of biomass conversion generally consists of the transformation of its biopolymers into single carbohydrates from cellulose and hemicellulose, and phenylpropanoid monomers from lignin through ether bond cleavage.[68] Ether cleavage can be easily performed in inexpensive systems through hydrolysis including using just pure water (autohydrolysis) or extremely dilute acid (pH = ~2.5).[69,70] However, these acidic conditions also catalyze dehydration and condensation reactions, which lead to randomly repolymerized polymers that contain extremely recalcitrant C-C bonds known as humins and condensed- or technical-lignins (Figure 1.7).[71,72] This kinetic competition between depolymerization and degradation reactions always limits the production of carbohydrates and lignin monomers.

In the depolymerization of polysaccharides, there is a large kinetic region where carbohydrate monomer degradation rates outpace hemicellulose and cellulose depolymerization lowering sugar yields (Figure 1.7 b and c). This region overlaps with many accessible and practical reaction conditions in terms of temperature, residence time and acid concentration. The acid hydrolysis of glycosidic bonds (ether bonds found in polysaccharides) can be described by a pseudo first-order rate law that depends on the H_3O^+ ion concentration, the temperature and the chemical environment of the bond.[73,74] Specifically, the hydrolysis reactions of hemicellulose and cellulose catalyzed by mineral acid can be modeled as two sequential reactions:[75–79]

$$\text{Hemicellulose} \xrightarrow{k_1} \text{Xylose} \xrightarrow{k_2} \text{Degradation products} \qquad \text{Equation 1.1}$$

$$\text{Cellulose} \xrightarrow{k_1} \text{Glucose} \xrightarrow{k_2} \text{Degradation products} \qquad \text{Equation 1.2}$$

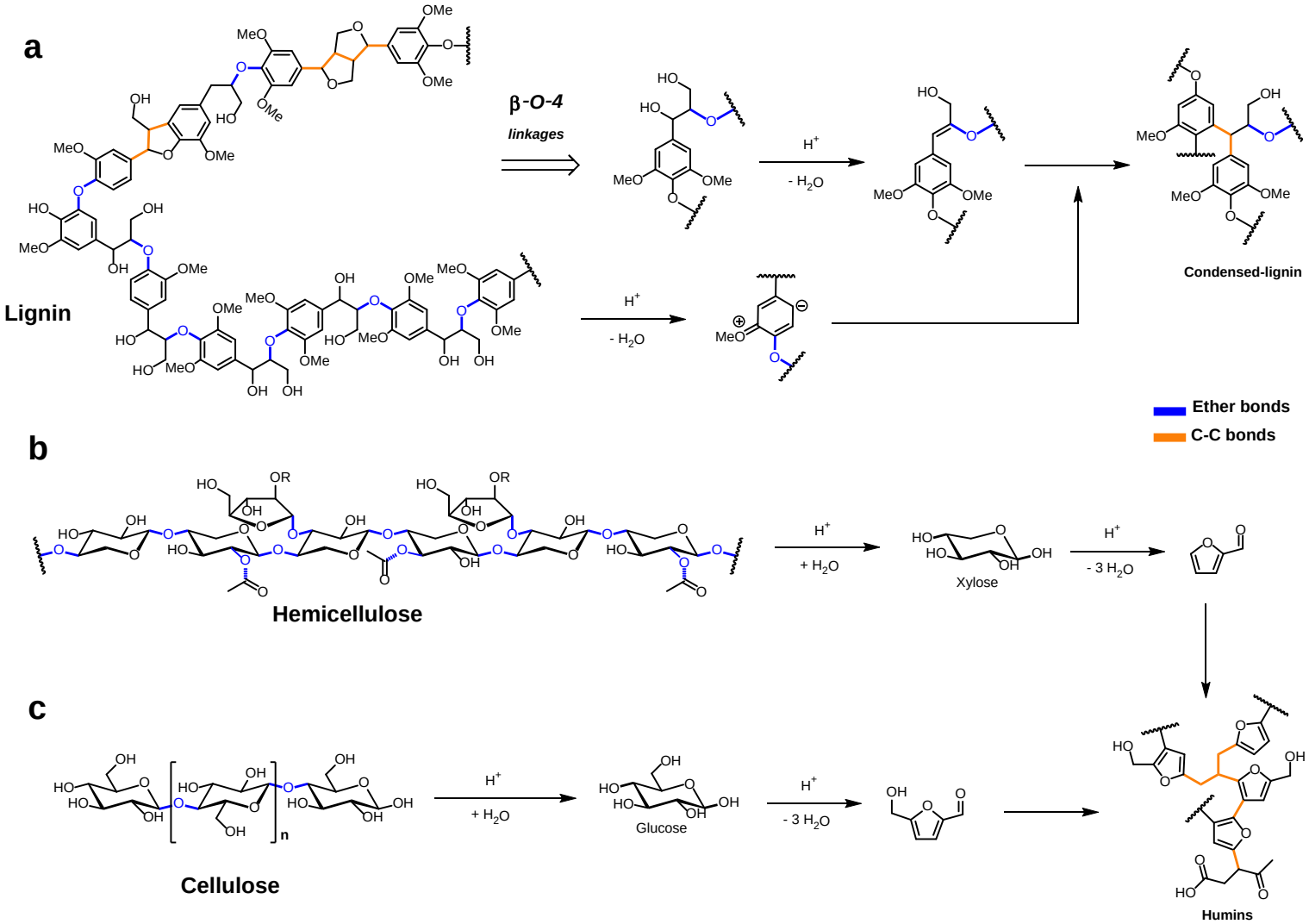

Figure 1.7 | Depolymerization of lignocellulosic biomass by the conventional acid hydrolysis. a) Depolymerization and condensation of lignin fragments in acid conditions. b) Acid hydrolysis of hemicellulose into xylose, dehydration of xylose into furfural and condensation of furfural into humins. c) Acid hydrolysis of cellulose into glucose, dehydration of glucose into 5-HMF and 5-HMF into humins. Ether and C-C are highlighted in blue and orange, respectively.

The kinetic constants of these models are influenced by the acid concentration and the temperature in the system, and can be represented by the following Arrhenius equation:

$$k_i=[A]^{ni}\ k_{0,i}\ \exp\left(\frac{Ea_i}{RT}\right) \qquad \text{Equation 1.3}$$

where *i* is the reaction in question (1, 2, etc.), n_i is the acid exponent (empirically determined) and [A] is the concentration of acid (which is commonly sulfuric acid).

These hydrolysis models are useful to demonstrate the kinetic limitations of acid catalyzed polysaccharide depolymerization under easy accessible reaction conditions. In particular, the maximum carbohydrate yield that can be achieved at given acid concentrations and temperatures can be easily extracted (Figure 1.8). Maximum xylose yields from hemicellulose can be reached within minutes at temperatures below 200°C under dilute conditions and are nearly quantitative.[69,75] In comparison, much higher temperatures (>220°C) are required to reach maximal yields for cellulose for similar residence times and those maximal yields are much lower (<60%). This difference demonstrates that the kinetic region of interest is far narrower for cellulose, which is due to the restricted access to ether bonds induced by its crystallinity.[28,80] Because of this, dual stage hydrolysis processes are usually used when trying to maximize the yield of both soluble carbohydrates, i.e. first hemicellulose at a lower temperature and then cellulose at harsher conditions.

The predominant degradation pathway of sugars is through the dehydration of carbohydrates into furans, furfural and 5-hydroxymethylfuran. Furans are highly reactive molecules that tend to condensate between each other to produce insoluble solid wastes known as humins.[81] Humins are randomly crosslinked macromolecules with a carbon content between 50-66 wt%,

containing 29-46 wt% oxygen with the rest being hydrogen.[82,83] Their formation introduces large process efficiency losses since their only current use is the production of heat and electricity by combustion. Some recent work have studied using humins to produce sustainable hydrogen[82] or activated carbon[83], but these strategies are still far from being industrial achievable.

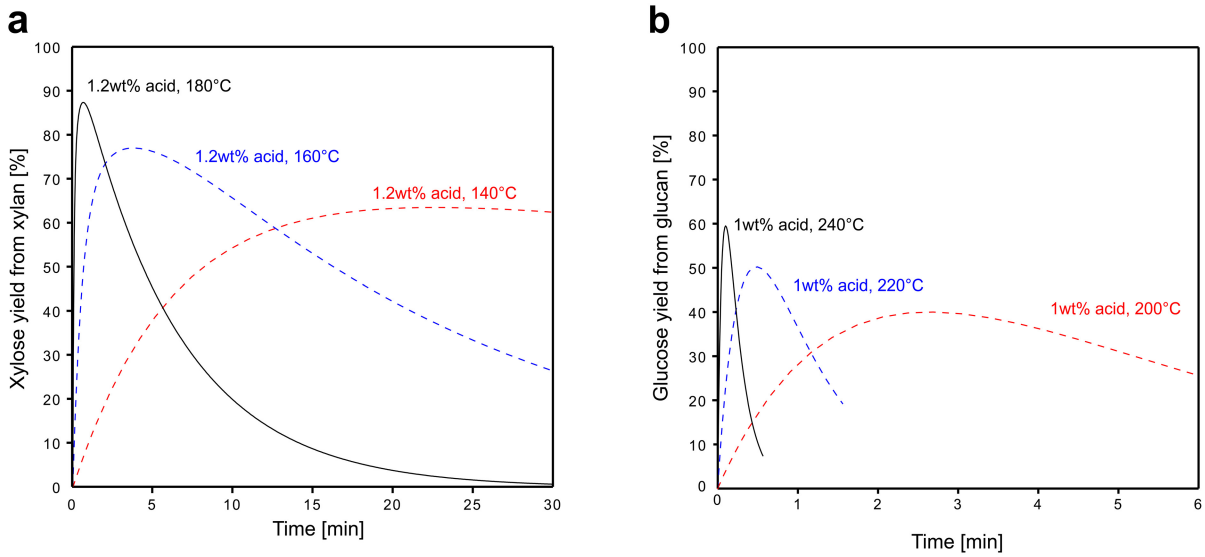

Figure 1.8 | Depolymerization of xylan (a) and glucan (b) into their corresponding monosaccharides with dilute acid hydrolysis of hardwood. Adapted from Luterbacher et al.[2]. Xylan kinetic data were obtained from Esteghlalian et al.[75] and glucan data were obtained from Fagan et al.[77].

1.4.2 Lignin

Lignin is generally formed by the radical coupling between coniferyl, sinapyl, and phydroxyphenyl alcohol.[84–86] These couplings give lignin a rigid and hydrophobic structure with different interunit linked by C-C and C-O bonds that provide resistance to microbial attacks. The most abundant bond and relatively delicate portion of the lignin is the β-aryl ether unit also known as β-O-4 linkage.[23,84,87] This linkage contains a benzylic secondary hydroxyl at the Cα position and a primary hydroxyl at Cγ position. The main challenge in the depolymerization of lignin is associated with the need to stabilize highly reactive lignin fragments produced from the cleavage the β-O-4 linkages (Figure 1.7a).[66] Otherwise, these fragments rapidly lead to the formation of new C-C bonds, which, due to their recalcitrance to cleavage, decreases lignin

monomer yields.[66,87,88] This kinetic competition between the cleavage of β-O-4 linkages and the formation of new C-C bonds controls upgrading yields. About 1/4 to 1/2 of the interunit linkages in a typical native lignin are already recalcitrant C-C linkages, which limits the theoretical yield of lignin monomers.[72,87] Assuming that these C-C linkages are randomly distributed and neglecting end effects, the theoretical monomer yield can be roughly estimated as the square of the ether content in the lignin bonds.[36] Therefore, the key for an efficient lignin depolymerization should be the preservation or the rapid stabilization of these bonds. Several strategies including reductive fractionation,[66,89,90] oxidation of lignin [88,91–94], mild conditions using ammonia [95–97], IL[98–100] or solvent use (organosolv) [101–104], that have attempted to mitigate the degradation of lignin within this context. These technologies were recently reviewed by Schutyser et al.[23]

In the next section, I briefly discuss most common chemical depolymerization strategies and discuss how their development was shaped by the interplay of depolymerization and degradation kinetics. Enzymatic hydrolysis does not encounter this kinetic issue as the catalytic site (enzyme pocket) only catalyzes the cleavage of glycosidic bonds.[105,106] In this case, the hydrolysis of cellulose is influenced by the structural features of cellulose, interaction of enzymes with cellulose fibers and enzymes inhibition (denaturalization). As with other technologies, this approach presents several challenges and limitations, including notably the cost of enzyme production, and has been extensively reviewed by several groups.[107–110]

1.5 Strategies for high yield polysaccharides depolymerization

1.5.1 Concentrated acid

Concentrated acid is the oldest known technique to depolymerize biomass at high yields. The first recorded attempt to depolymerize biomass was using concentrated sulfuric acid back in

the early 1800s by Braconnot.[111,112] It was found that the produced aqueous solution was fermentable leading to the conclusion that it contained glucose. As the interest in biomass depolymerization increased, so did the research related to these technologies.[65,113] Concentrated mineral acids are known for their potential to swell and decrystallize cellulose, which facilitates subsequent hydrolysis reactions.[114–116] The large amount of unsolvated proton ions can disrupt the hydrogen bonds in the crystalline structure of cellulose by forming strong hydrogen linkages with cellulose hydroxyl groups. [73,117,118] As result, cellulose is completely dissolved leading to an amorphous structure. This change in structure lowers the activation energy in cellulose hydrolysis (Figure 1.9), leading to a shift in the depolymerization kinetics.[78]

The polysaccharides acid hydrolysis and degradation rate constants can be represented by an Arrhenius equation that contains an acid exponent (Equation 3). Based on published data, the acid exponent for hydrolysis reactions is usually greater than that of the degradation reactions.[75,76,119] This difference can serve to modulate the kinetic competition between these two reactions. Increases in the acid concentration will accelerate the rate of depolymerization more than degradation reactions. Consequently, the usage of concentrated mineral acids is one solution to shift the kinetic limits in polysaccharide depolymerization by both decrystallizing cellulose and selectively accelerating the hydrolysis reaction rate. Processes based on concentrated acid have the advantages of being able to almost quantitatively recover the sugars and thus have low formation of bio-inhibitors. They also proceed with a high reaction rate and at mild operational conditions with a low temperature and pressure.[65,73,120] On the other hand, they suffer from high operational and capital cost due to the need for acid recovery and corrosion resistant materials. Although only very few processes are based on this technology due to the aforementioned drawbacks, the high sugar yield is still an attractive feature.[121,122] Because

sugars are recovered near quantitatively, concentrated acid hydrolysis has become a standard method for measuring polysaccharide composition in biomass.[123]

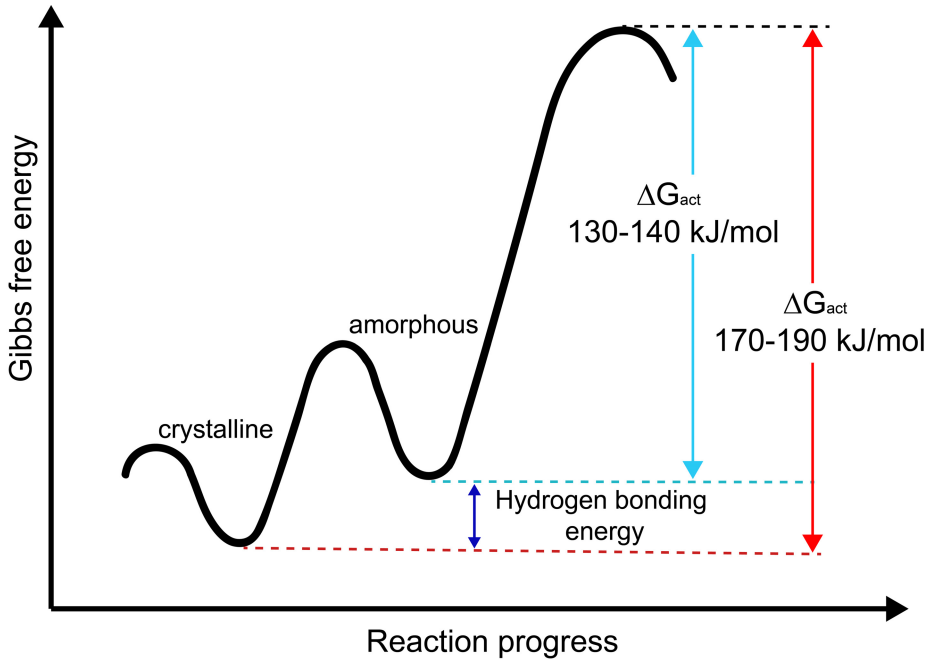

Figure 1.9 | Energy diagram of the hydrolysis of amorphous and crystalline cellulose. Adapted from Shuai and Luterbacher.[124]

1.5.2 Ionic Liquids

Ionic liquids (ILs) can be defined as organic salts with melting points below 373K. ILs have numerous applications including in catalysis, biocatalysis, electrochemistry and green chemistry.[125–127] They were introduced in biomass conversion because of their low volatility and unique solvent properties. IL-based pretreatments can effectivity fractionate biomass by extracting lignin and hemicellulose, and, similarly to concentrated acid, decrystallize and solubilze cellulose.[98,128,129] Contrary to other traditional biomass solvents, IL can dissolve these macromolecules by changing their structure to cations and anions. This makes ILs a powerful and environmentally friendly cellulose-dissolving solvent. ILs can completely dissolve cellulose by breaking hydrogen bonds between cellulose strands. Once cellulose is solubilized, the activation energy of cellulose hydrolysis is significantly decreased, as in the case of concentrate

mineral acids (Figure 1.9).[130–132] However, to achieve this hydrolysis, a careful balance of the water content in solution has to be achieved because water is needed for hydrolysis but too much water will lead to precipitation of the cellulose and reformation of the hydrogen bonding. Typically, after dissolution, the hydrolysis process is done by slowly adding water in order to cleave the glycosidic bonds without precipitating the cellulose.[131]

ILs do not only dissolve cellulose, but also lower the activation energy of cellulose hydrolysis by stabilizing transition state intermediates. One of the key steps in the hydrolysis of cellulose is the formation of oxocarbenium ions,[133,134] which requires around 50-60 kJ/mol. However, the apparent activation energy for this reaction in aqueous environments is about 120-130 kJ/mol. This difference in energy suggests that the formation of oxocarbenium ions is highly unfavorable in the aqueous environment, which could be explained by the preferred planar geometry of the pyranose ring around the $C=O^+$ (Figure 1.10).[135,136]

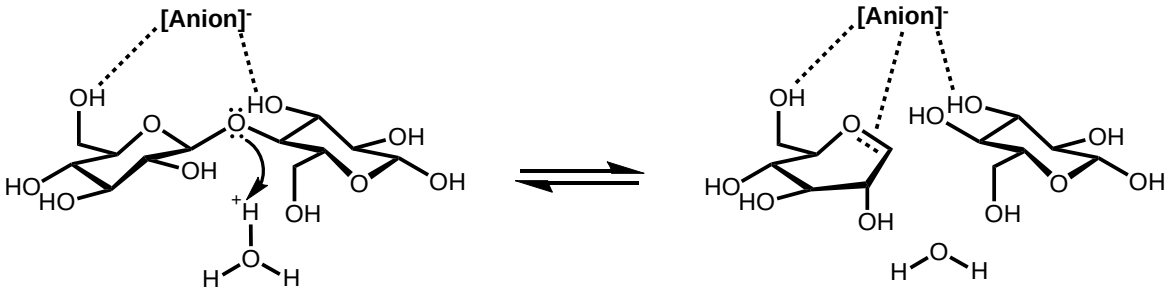

Figure 1.10 | Stabilization of the oxocarbenium ions produced by the cleavage of a glycoside bond in ionic liquids. Adapted from Shuai and Luterbacher[124].

It has been proposed that the strongly ionic environment of ILs stabilizes the positive charge of oxocarbenium ions lowering the Gibbs free energy of the transition state.[134] This effect leads ILs to enable the saccharification of cellulose at temperatures where no reaction would have occurred in pure water.[130] Currently, most research in IL-based processes are focused on opti-

mization and the production of low-cost ILs.[98,137] The main drawback for the industrial implementation of this technology is the cost of ILs recovery and purification, which remains much too high.[138,139]

1.5.3 Hydrothermal and dilute acid

In contrast to concentrated acid, hydrothermal and dilute acid processes for polysaccharide depolymerization focus on the deconstruction of biomass at high temperatures and short residence times. These parameters are based on the temperature dependence of the polysaccharides hydrolysis and degradation rate constants (Equation 3). Given that the activation energy for hydrolysis reactions is greater than that of decomposition reactions, increasing the reaction temperature "activates" the hydrolysis more than decomposition (Figure 1.11 a).[69,76,140]

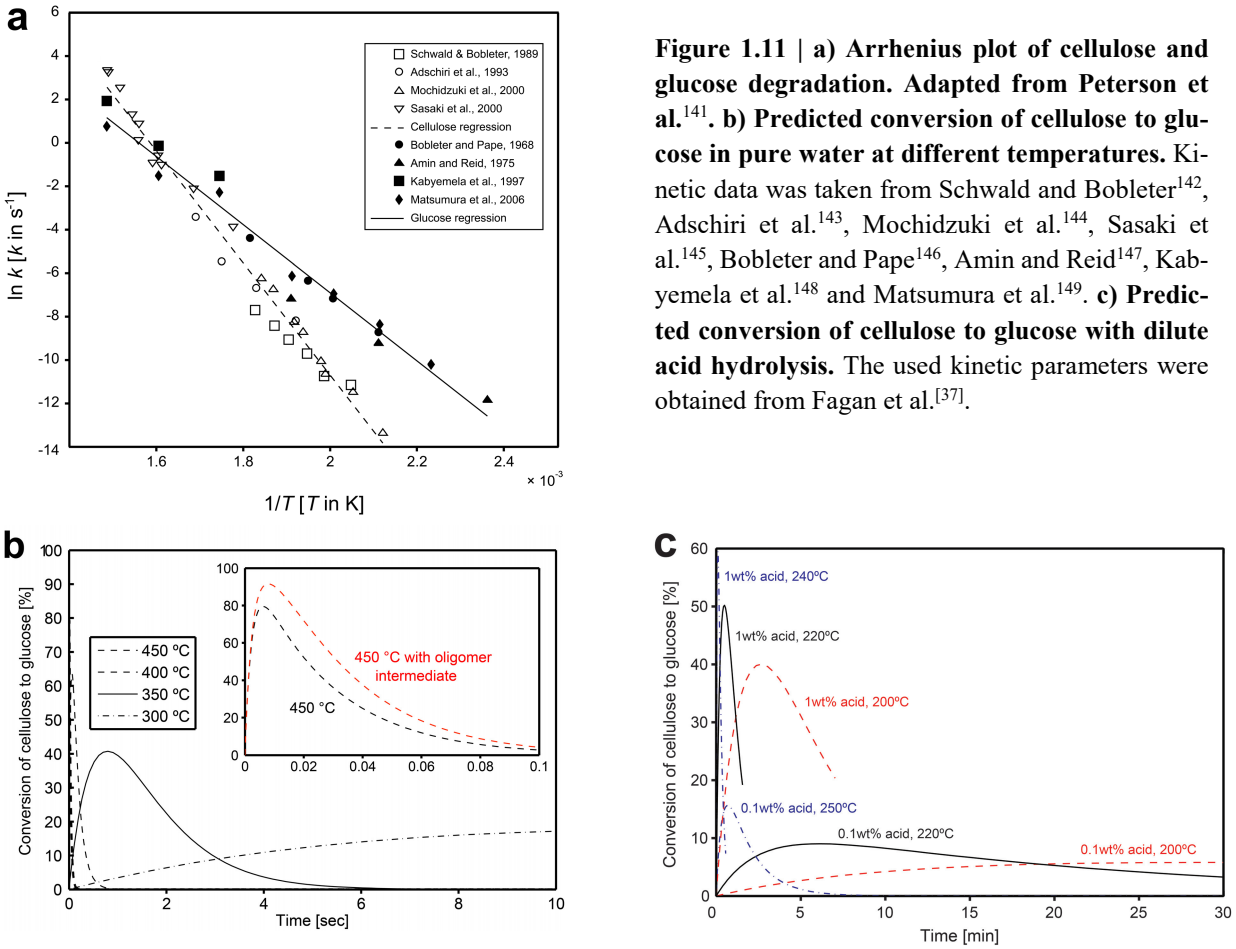

Figure 1.11 | a) Arrhenius plot of cellulose and glucose degradation. Adapted from Peterson et al.[141]. b) Predicted conversion of cellulose to glucose in pure water at different temperatures. Kinetic data was taken from Schwald and Bobleter[142], Adschiri et al.[143], Mochidzuki et al.[144], Sasaki et al.[145], Bobleter and Pape[146], Amin and Reid[147], Kabyemela et al.[148] and Matsumura et al.[149]. **c) Predicted conversion of cellulose to glucose with dilute acid hydrolysis.** The used kinetic parameters were obtained from Fagan et al.[37].

Hydrothermal conditions (i.e. without additional acid) can be used because at temperatures higher than 500K, the equilibrium concentration of protons in water is enough even to catalyze cellulose hydrolysis (pK_w= 11.31-11.20).[150] However, in systems without acid, temperatures ca. 625K have to be reached before the hydrolysis of cellulose begins to have a higher reaction rate compared to glucose degradation.[141] Because at these conditions rates are very fast, high temperature processes require very short residence time in order to achieve interesting results. Using the same kinetic model for cellulose in Equation 2, it is possible to predict yields of 40% and 80% for systems at 620 K and 720 K for 1 s or 10 ms of retention time, respectively (Figure 1.11 b).[2] These predictions are consistent with experimental data reported by several research groups with a total sugar yield between 60-95% obtained at 640-675 K for 10 ms to 2 s.[151–153]

Moreover, it is possible to combine the advantages of elevated temperature with increases in proton concentrations by addition of small quantities of acid. This approach is known as dilute acid hydrolysis and has been used in lignocellulosic biorefineries focused on ethanol production.[14,67] This technique has the benefit of reaching the same carbohydrate yield as in the hydrothermal process at significantly lower temperature (Figure 1.11 b and c). Despite the technical difficulties that these systems present, mainly due to their high pressure drop and short residence time, they have been commercialized using two-stage chemical hydrolysis processes.[67,153–158] A subset of these processes use a single stage dilute acid hydrolysis as a pretreatment, where lignin and hemicellulose are partially depolymerized and extracted, cellulose is hydrolyzed by enzymes in a second step. This technique takes advantage of the mild dilute acid conditions required to hydrolyze hemicellulose only and leave cellulose behind for enzymes.

1.5.4 Organosolv

The organosolv pretreatment consists of the partial depolymerization of biomass where lignin and hemicellulose are separated from cellulose using a reaction mixture of water with a co-solvent.[49,159,160] Cellulose can then be chemically hydrolyzed by a subsequent harsher organosolv process or biologically by enzymes. Most commonly used solvents are tetrahydrofuran, acetone, ethanol, methanol, γ-valerolactone and 1,4-dioxane. Usually, these reaction mixtures contain an acid catalyst in fairly low concentrations (< 5 wt%). Acid organosolv pretreatments are well-known for their high lignin removal (70% to 95%), low catalyst loading, mild reaction temperature and decrease in cellulose crystallinity (relatively easy to hydrolyze).[159,161–163] These reaction systems benefit from solvent effects that enhance and accelerate the depolymerization of lignin and polysaccharides.[124,164] This is mostly due to the medium-polar environment of the reaction mixture induced by the co-solvent and the variable Gibbs free energies of protons solvation.

The medium-polarity environment of these solvents is ideal to dissolve depolymerized fragments of condensed and un-condensed lignin, which also influence the reactivity of cellulose by avoiding surface blocking. Almost all the cellulose remains insoluble (solids) after this type of pretreatment due to low acid concentration and mild reaction temperature. However, its morphology changes significantly. The treated cellulose shows some decrease in crystallinity, high surface area and high pore volume. Although the solvent mixture used in organosolv processes do not have the ability to completely dissolve cellulose, the changes in morphology and the high lignin removal after pretreatments facilitate the hydrolysis of cellulose by both, chemical and biological approaches (enzymes).[68,159,163,165,166]

On the other hand, the solvation effects on the protons catalyzing the reaction in the solvent increase their Gibbs free energy while not affecting the free energy of the transition state as

drastically. The overall effect lowers the reaction's activation energy and facilitates mild reaction temperatures (350 to 420 K) and low catalyst loading in acid organosolv pretreatments.[164] These mild conditions can also partially preserve the β-O-4 linkages in lignin even enough degradation generally occurs to significantly affect lignin upgradeability.[23,101] The co-solvent could be polar protic or polar aprotic, but aprotic solvents are preferred since they feature this proton solvation effect much more significantly than water and other protic solvents.[124] The increase in the activity of destabilized protons reduces the activation energy of both proton-catalyzed hydrolysis and dehydration reactions.[167] However, the acceleration is more significant for depolymerization reaction, which helps the process. As result, this solvent effect has been considered as the main reason for observed decreases in the formation rate of humins.[159,161,162,167]

This approach offers an option to mitigate, if not completely overcome, the kinetic competition between lignin and polysaccharides depolymerization and their degradation. The main disadvantages of this technology are considered to be the solvent recovery and recycling as well as risks associated with its stability and flamability.[160,168] Nevertheless, techno-economic analyses have shown this approach to be economical competitive for the production of the second generation of ethanol, furfural and pulp compare to current market prices.[14,49]

Each of the technologies that have been discussed, influences the polysaccharide depolymerization kinetic by one or more of the three key factors that affects the cleavage of glycosidic bonds (concentration and accessibility of H_3O^+, reaction temperature and the chemical environment of the bond) (Table 1). In this thesis, I am interested in developing techniques, where instead of trying to influence this glycosidic cleavage, I will try to prevent the formation of degradation products via dehydration and repolymerization reactions. One approach to do so

would be to stabilize reactive intermediates that are produced after depolymerization reactions. This approach, which is analogous to protection group chemistry, introduces a new reaction within the conventional reaction network of acid hydrolysis of polysaccharides that competes with dehydration reactions.

Table 1. Summary of lignocellulosic biomass deconstruction technologies and their influence in the kinetic.

Technology	Influence in kinetics by:			
	Proton ions accessibility	Temperature	Activation Energy (bond environment)	Additional Reaction
Concentrated Acid	**X**		**X**	
Hydrothermal and Dilute Acid		**X**		
Organosolv	**X**		**X**	
Ionic Liquids	**X**		**X**	
Protective Group Chemistry in Organosolv	**X**		**X**	**X**

1.6 Protecting group chemistry

Protecting groups are used routinely in organic synthesis to temporarily block a specific portion of a molecule from reacting and provide chemoselectivity in subsequence reactions.[169,170] Functionalities that are commonly protected are: hydroxyl (including 1,2 and 1,3-diols), amino, carboxyl, carbonyl, alkyne C-H, phosphate and thiol groups. A suitable protecting group should fulfill a number of requirements that accommodate the chemical environment where it is being implemented.[169] The group should have minimal functionality to selectively produce a protected and stable molecule with good yield. It must be able to selectively detach using vastly available and non-toxic reagents while not further reacting with the exposed functional group. Finally, once the protecting group is removed, it should be easily separable from the reaction

media. Due to the great control protection chemistry brings to synthesis of multifunctional molecules, it has been extensively studied in the past century,[171] and now days, some might consider it a chemistry discipline in its own right, where the focus is around designing new protecting groups.[169] There are innumerable applications for protecting group chemistry, but they are rarely implemented at large industrial scales and can be criticized due to additional materials and steps, which include protection and deprotection.[172] Yet, there are some cases such as the production of Oseltamivir (Tamiflu™)[173] and Sucralose (Splenda™)[174], where the benefit of chemoselectivity offered by protecting group compensates these processes considerations.

1.6.1 Protecting group chemistry in carbohydrates

The usage of protective group chemistry in carbohydrates is a traditional approach that began in the 19th century, first to characterize them and later to synthesize oligosaccharides and rare monosaccharides.[175–179] This chemistry notably, led to the historical synthesis of L-ascorbic acid also known as vitamin C by N. Haworth.[180,181] Due to the multifunctionality and potential that carbohydrates possess in organic synthesis, innumerous protecting groups and novel strategies have been developed for over the last century to exploit their benefits.[170,182–184]

The hydroxyl groups in carbohydrates can also be seen as 1,2- and 1,3-diols. There is an extensive variety of reagents that could be used to protect diols, but the most common and reactive protecting groups for diols are aldehydes.[185] In the case of carbohydrates, they are known to react with aldehydes and ketones in a presence of an acid-catalysts to produce acetals and ketals.[186,187] These protection reactions are generally equilibrium reactions and produce water. Therefore, because of le Chatelier's principle, they often proceed far more efficiently in the

presence of limited amounts of water. Hence, in the context of biomass depolymerization, acid-catalyzed organosolv processes have the right conditions to perform these reactions.

1.6.2 Protective group chemistry in lignocellulosic biomass

Recently, it was found that when an aldehyde is added to an acid organosolv pretreatment (using an aprotic co-solvent), hemicellulose-derived sugars and lignin react with the aldehyde producing acetal-stabilized sugars and lignin fragments (Figure 1.12).[32,88] These modified carbohydrates cannot undergo dehydration, thus, eliminating the primary pathway to humin formation. Depending on the chosen aldehyde, the formation of this acetal can result in a new stereogenic center and generate two isomers.[188] However, this stereogenic center is lost upon deprotection. Moreover, this strategy is not only known to assist polysaccharides, but also fully protect and preserve the β-O-4 bonds in depolymerized lignin fragments (Figure 1.12).[32,88,188,189] Lignin stabilization using this chemistry is discussed in more detail elsewhere.[88,188,190]

To my knowledge, the stabilization of biomass-derived carbohydrates using protecting groups has only been previously executed by forming acetal and ketal sugars.[32,68,88,191–193] The first attempt in the ketalization of biomass-derived carbohydrates was in an acetone-based acid organosolv pretreatment containing 70-90% acetone and dilute mineral acids.[192] Similar to aldehydes, acetone reacts with carbohydrates producing ketal sugars, which can help the depolymerization kinetic outrun the dehydration of sugars.[192,193] However, the recovery of acetone is quite challenging due to the formation of condensed products (mainly due to the high temperature of the process), and the large volumes required in these processes conditions.

In another case, acetone helped improve the quality of bio-oil by protecting carbohydrates from degradation. This was done at ≤ 120°C using microwave radiation. The produced bio-oil shows a substantial increase in thermochemical stability and solubility with gasoil.[191] Similar to previous examples, this process requires large acetone volume since it is used as the only solvent. Another issue is the recovery of acetone due to the formation of acetone condensed products (4-15 wt%) and the integration of the ketal group in protected sugars into the final product (25 wt% of acetone is transformed into gasoline products).[191] This led to an overall acetone recovery of ca. 60 wt%. Bio-oil is commonly produced from pyrolysis or fast pyrolysis at high to moderate temperature (473-973 K). At those conditions, biomass is converted into a dark brown liquid with highly oxygenated compounds which are quite unstable (and tend to produce coke) and insoluble in hydrocarbons.[191,194] These products result from the pyrolysis conditions being within this kinetic zone where the formation of degradation products and unstable intermediates are favored over simple sugars. Known strategies to limit the formation of such products during pyrolysis were reviewed by Kan et al.[194]. The use of acetone in acid organosolv biomass pretreatment was recently investigated.[88] However, the rate of the protection reactions at the pretreatment temperature were similar to that of the degradation reactions leading to similar yields compared to control experiments.

In summary, it seems that protective groups chemistry is a promising tool to achieve an integrated biomass depolymerization at practical reaction conditions that are kinetically unfavourable. This approach has been barely studied in real biomass, current results were not completely effective. Further investigations could provide novel routes for the valorization of lignocellulosic biomass. Although aldehydes have been considered as the most common and effective protecting groups for diols, they have not been applied in biomass-derived carbohydrates.

Therefore, there is a clear opportunity to study the potential of aldehydes, beginning with formaldehyde, the simplest and cheapest aldehyde to stabilize carbohydrates and overcome the kinetic competition between polysaccharides depolymerization and degradation. In line with the aforementioned disadvantages of acetone-based processes, I will use formaldehyde as an additive rather than a solvent (limited amounts) and study possibilities for its recovery.

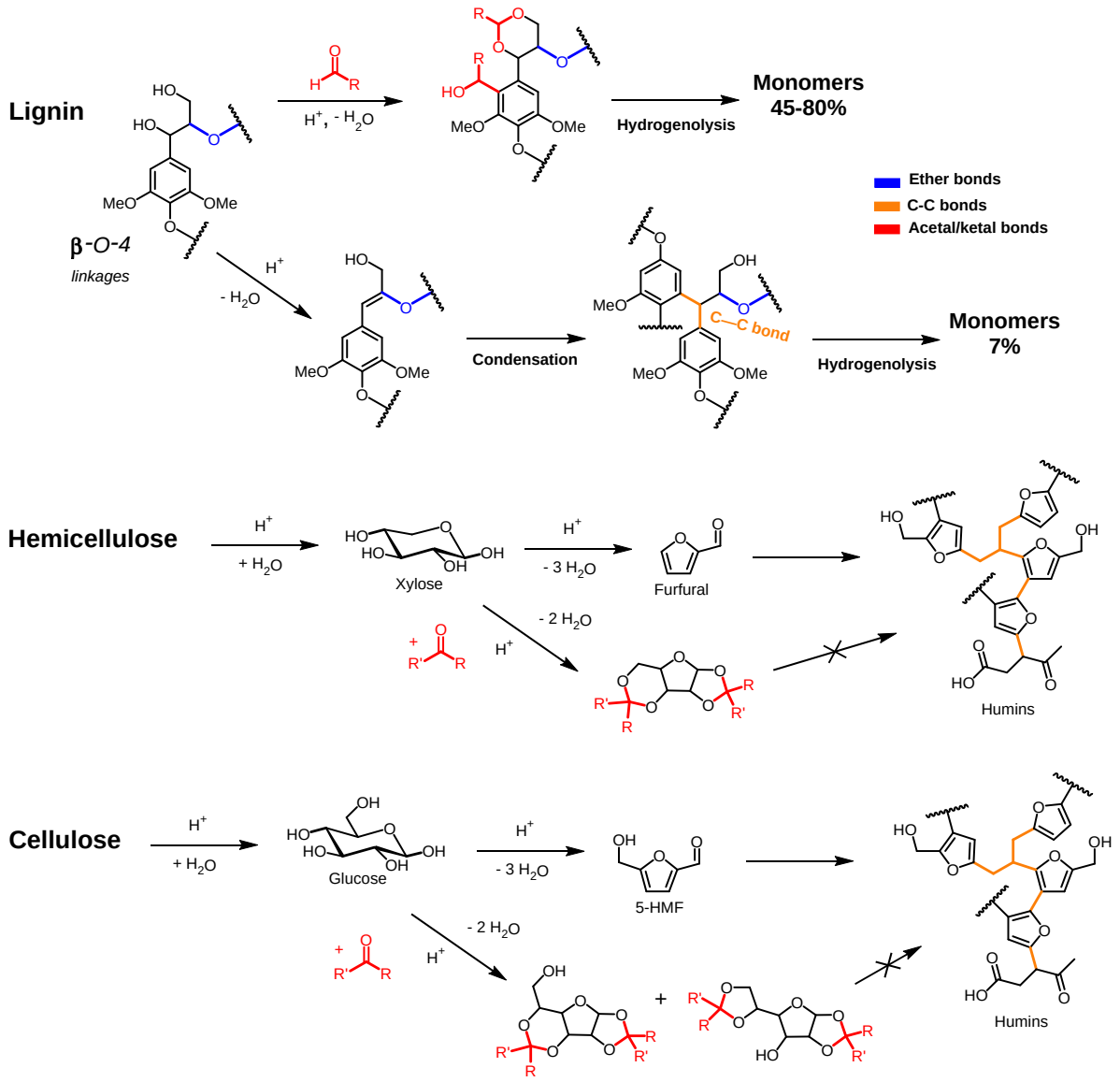

Figure 1.12 | Reactions scheme of the depolymerization of lignin, hemicellulose and cellulose in acid conditions with and without the use of protecting groups chemistry. Ether, C-C and acetal/ketal bonds are highlighted in blue, orange and red, respectively. 5-HMF stands for 5-hydroxymethylfurfural.

Chapter 2: Objectives

In line with this discussion, the overall goal of my thesis is to use protecting group chemistry in lignocellulosic biomass organosolv processes to push back the kinetic limitations of polysaccharide depolymerization reactions, and study new reaction mechanisms and upgrading routes that could result from these modified sugars. Based on this, I have defined four objectives in my thesis.

2.1 Objective 1. Stabilization of carbohydrates with formaldehyde during hemicellulose and cellulose depolymerization using conventional acid organosolv processes.

I plan to maximize the recovery of all three main fractions of lignocellulosic biomass in a two steps process by incorporating formaldehyde as a protective reagent for lignin fragments and carbohydrates. The first step consists in the pretreatment of beech wood to simultaneously extract and stabilize lignin and hemicellulose, leaving cellulose insoluble. In the second step, cellulose is depolymerized in a conventional flow-through reactor to control the retention time of soluble products such as glucose in the hot zone while varying product concentration. In both steps, formaldehyde could be added to the reaction mixture to avoid the formation of dehydration and degradation products.

2.2 Objective 2. Purify and characterize acetal-stabilized sugars found in the saccharification of hemicellulose and cellulose from beech wood.

In order to fully understand the acetal stabilization mechanism, I propose to synthesize and characterize acetal-stabilized sugars of all monosaccharides found in beech wood to identify those formed in the pretreatment and cellulose depolymerization. After identification, I intend to determine the structure of these molecules by Mass Spectra and NMR.

2.3 Objective 3. Mechanistic study of the deprotection and dehydration reaction of acetal-stabilized sugars.

I intend to study the mechanism pathway of the tandem hydrolysis-dehydration reaction of acetal-stabilized sugars into furans. Understanding the mechanism could allow us to identify unique reactivity properties of the acetal stabilized sugars. In order to minimize degradation products, the reaction will be carried out in a biphasic system to continuously extract the formed furans from the acidic media. The identification and role of highly reactive intermediates will be analyzed by *Operando* ^{13}C NMR using ^{13}C labeled sugars and acetal-stabilized sugars.

2.4 Objective 4. Preliminary techno-economic analysis of acetal-stabilized biomass-derived sugars for the production of ethanol.

In the context of biorefineries, the additional steps of protecting and deprotecting molecules could affect the process economy. Therefore, I plan to perform a preliminary techno-economic analysis (TEA) based on a previously studied organosolv process[148] and experimental data of formaldehyde recovery using flow sheeting software. Additional process implications resulting from the use of formaldehyde will be examined.

2.5 Objective 5. Direct upgrading of acetal-stabilized xylose for the production of xylitol.

The direct upgrading of acetal-stabilized sugars could be an interesting approach to open new routes in the valorization of biomass-derived sugars. In particular, the production of xylitol suffers from high operational cost due to high purity xylose requirements. In light of this, by using the volatility of acetal stabilized sugars, I propose to purify of acetal-stabilized xylose by distillation, a separation technique impossible to use with simple xylose, followed by the tandem hydrolysis-hydrogenation of acetal-stabilized xylose on a redox metal supported catalyst.

Chapter 3. Stabilization of biomass-derived carbohydrates by acetal formation

This chapter is part of a published article in *Nature Chemistry* as **Questell-Santiago, Y.M.,** Zambrano-Varela, R., Talebi Amiri, M. and Luterbacher, J.S. Carbohydrates stabilization extends the limits of chemical polysaccharides depolymerization, *Nature Chem.* **2018**, 10, 1222-1228. doi: 10.1038/s41557-018-0134-4.[68] Part of the manuscript and supplementary information are reproduced here with a few formatting changes with permission from Springer Nature.

The aim of this chapter is to chemically depolymerize and stabilize/protect biomass polysaccharides as simple sugars at conditions where degradation reactions outpace depolymerization reactions. The introduction of protection reactions in conventional organosolv polysaccharide depolymerization processes, leveraged the advantages of aforementioned solvent effects but also allowed trapping of carbohydrates, increasing yields and product concentration. Here, I used formaldehyde as a protecting reagent to produce acetal sugars (i.e. stabilized sugars). The formation of the acetal sugar is believed to occur through a hemiacetal intermediate followed by the formation of oxocarbenium ions.[195–197] The latter is considered the rate limiting step. Nevertheless, the protecting rate of sugars was shown in this work to be significantly faster than dehydration reactions, which successfully limited carbohydrate degradation. This was the case for the depolymerization of both hemicellulose and cellulose. However, given that cellulose requires high temperatures in acid organosolv process, the difference in rate between protection and dehydration reactions is narrower.

3.1 Biomass pretreatment

It was recently discovered that the addition of FA during pretreatment could stabilize lignin, preventing its condensation, and facilitate the conversion of extracted lignin to monomers at close to theoretical yields (47% for wild type beech and 78% for transgenic poplar).[190] In that work, we also noted that most of the xylose was recovered as a formylated molecule that we referred to as diformylxylose (DX). Here, we were interested in studying the ability of formaldehyde to act as stabilizing trap for carbohydrates including xylose. Using γ-valerolactone (GVL) as a pretreatment solvent, DX could be produced at yields above 90%, minimizing xylose degradation into furfural and other degradation products, (Figure 3.1 c). In comparison, biomass pretreatment without FA (Control) using either 1,4-dioxane or GVL led to significant xylose degradation with only 16% and 24% xylose recovery, respectively. This contrast in product yields is shown in the two-dimensional heteronuclear single-quantum coherence nuclear magnetic resonance (^{1}H-^{13}C HSQC NMR) spectra of beech wood pretreatment liquors produced without and with the addition of FA. When no FA was added, only the peaks corresponding to lignin methoxy groups and remaining xylose were observed (Figure 3.1 a). In contrast, when FA was used, we observed peaks corresponding to the 1,3-dioxane and 1,3-dioxolane structures in stabilized lignin and DX (Figure 3.1 b). All these structures were identified by comparison with spectra of authenticated standards including lignin model compounds,[190] pure xylose and pure DX (Chapter 4 Figure 4.1).

The stabilization of hemicellulose-derived sugars with FA was performed in various polar aprotic solvents showing comparable product distribution (Figure 3.1 c). Protic solvents such as ethanol led to poor yields with FA due to the propensity of the FA to react with the solvent (Fig. 3.2). After beech pretreatment using an ethanol-water system, no formation of diformylxylose was detected. Only 21% of FA was recovered in the liquor, whereas in polar

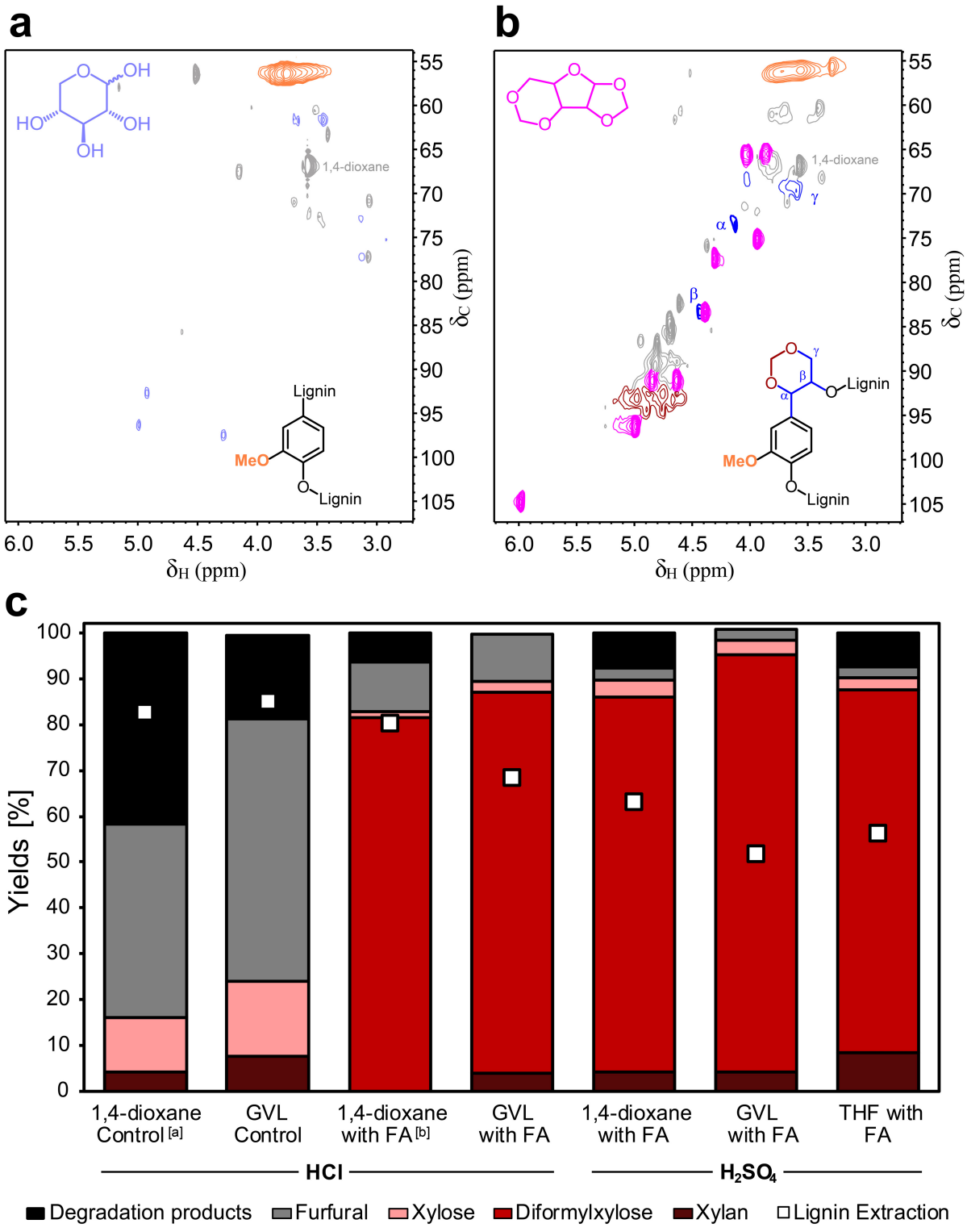

Figure 3.1 | Hemicellulose stabilization and lignin extraction during biomass pretreatment. (a) ^{1}H-^{13}C HSQC NMR spectrum of biomass pretreatment liquor without formaldehyde addition (Control). (b) ^{1}H-^{13}C HSQC NMR spectrum of biomass pretreatment liquor with formaldehyde addition, δ_H, proton NMR chemical shift (in parts per million); δ_C, carbon NMR chemical shift (in parts per million). (c) Product distribution resulting from biomass pretreatment in 90/10 v/v organic solvent-water mixture at 100°C for 2 h with 0.49 M of acid in the absence and presence of formaldehyde (~4 wt%). Unfilled squares represent lignin extraction at each pretreatment conditions. [a] Experiment used for the ^{1}H-^{13}C HSQC NMR spectrum showed in Figure 3.1 a. [b] Experiment used for the ^{1}H-^{13}C HSQC NMR spectrum showed in Figure 3.1 b.

aprotic solvent systems 56% FA is immediately recoverable (Table 3.5). This was due to the formation of diethoxymethane from FA and ethanol. After acid hydrolysis in aqueous solution, 55% of FA was recovered from the reversible conversion of diethoxymethane to ethanol. Similar to ethanol, THF was not stable at pretreatment conditions while using hydrochloric acid. THF-water system showed low formation of diformylxylose and high yields of xylo-oligomers (Figure 3.2) suggesting a lower reaction rate compared to other polar aprotic solvent systems. We also observed that THF underwent ring-opening to form 4-chlorobutanol due to chlorine in solution. This issue was overcome by substituting hydrochloric acid for sulfuric acid (Figure 3.2).

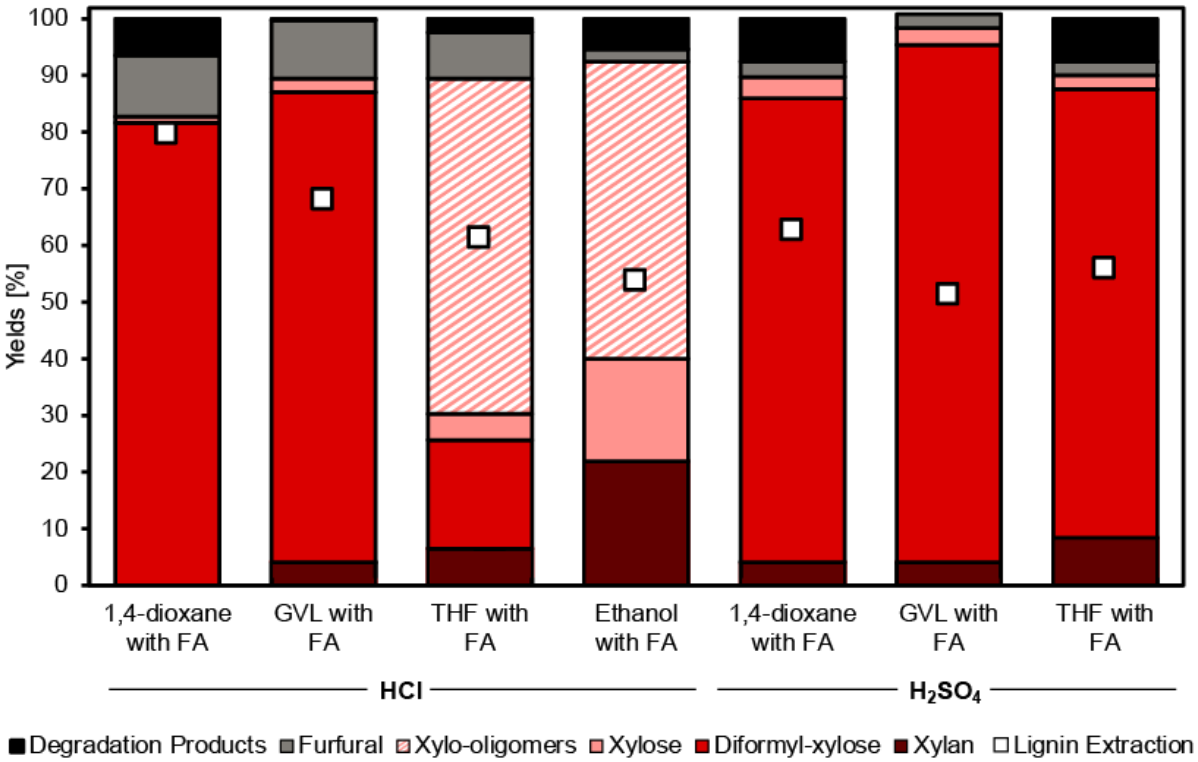

Figure 3.2 | Solvent and acid effects in hemicellulose product distribution during biomass pretreatment.

Hemicellulose stabilization was similar in GVL, 1,4-dioxane and THF solvent systems, although GVL led to the highest DX yield of 91% (Figure 3.1). Experiments with pure xylose confirmed that selectivity to DX was slightly better in GVL compared to 1,4-dioxane (Figure

3.3). The acidic proton has been shown to have a higher free energy in GVL-water compared to 1,4-dioxane-water systems, due to a decreased solvation free energy, leading to an increase in the acid-catalyzed reaction rate, which could explain the selectivity difference.[124,167]

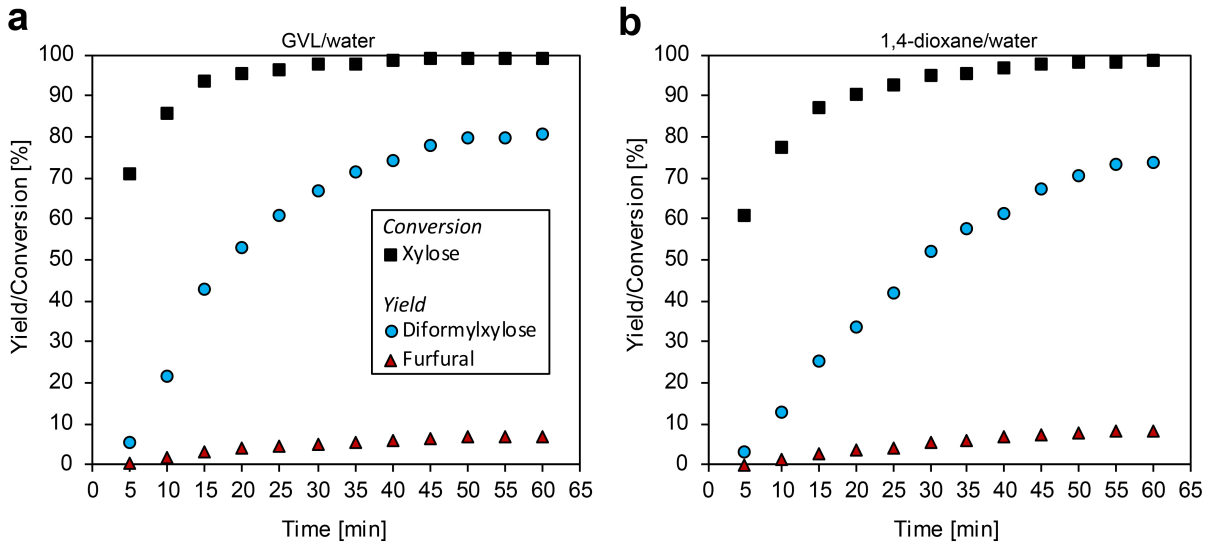

Figure 3.3 | Solvent effect in diformylxylose formation from xylose. Production of diformylxylose in 90/10 v/v organic solvent/water mixture at 80ºC with 0.49M HCl and 4 wt.% FA. (a)GVL/water. (b)1,4-dioxane/water.

Additionally, when increasing the solid loading to 18 wt% in the GVL-water mixture (i.e. decreasing the solvent usage by 60%), 80% of hemicellulose sugars could still be recovered as DX with a lignin extraction efficiency of 61% (Table 3.1). The experimental data showed an increased in degradation products from 1% to 9% with a 3% increase in solid loading. This points bring opportunities to optimize reaction conditions, e.g. temperature and reaction time, and extent the stabilization of sugars at high solid loadings.

Table 3.1 | Lignin extraction and product distribution of xylan and glucan at different biomass loading during pretreatment.

Entry	*Biomass loading [wt./wt.]*	*Acid*	*Yield [%]*										
			Xylan	*Xylose*	*Diformylxylose*	*Furfural*	*Lignin Extraction*	*Glucan*	*Glucose*	*Gluc-oligomers*	*Diformylglucose*	*5-HMF*	*Degradation Products*
1	8%	HCl	4	2	83	10	68						0
								77	5	0	5	2	11
2	15%	HCl	6	1	70	10	76						13
								86	0	3	5	2	4
3	8%	H_2SO_4	4	3	91	3	52						0
								88	0	10	0	1	1
4	15%	H_2SO_4	5	1	90	3	58						1
								85	0	10	0	1	4
5	18%	H_2SO_4	5	1	82	4	61						9
								81	0	10	0	1	7
6	18%*	H_2SO_4	12	1	73	2	53						12
								93	0	6	0	0	1

Notes: Reaction conditions are detailed in Appendix A.1.1. 5-HMF stands for 5-hydroxymethylfurfural. [*] 140 µL of 95-98wt% sulfuric acid.

Table 3.2 | Compositional analysis of beech wood and pretreatment solid residues.

Solid	*Glucan*	*Xylan*	*Mannose*	*Galactose*	*Arabinose*	*Klason Lignin*	*Moisture*	*Solvent*
Beech wood	37%	17%	2%	2%	2%	22%	5.7%	--
Pretreatment solid residues used in flow-through reactor	71%	2%	--	--	--	15%	1.8%	73%

Note: All percentages are on an air dried basis (aside from the solvent measure).

3.2 Cellulose depolymerization.

After pretreatment, up to 93% of the cellulose fraction was recovered in the remaining solids (Table 3.1). Our previous work has shown that solids extracted under similar conditions could undergo enzymatic hydrolysis.[190] However, for high glucose yields to be obtained, these pretreated solids had to be treated with a dilute acid solution (1 wt% H_2SO_4) prior to enzymatic treatment to remove grafted FA on the substrate's surface. Here, we instead attempted to depolymerize these pretreated solids using acid hydrolysis with GVL/water solvents, while again using the FA-stabilization strategy. Reactions were performed in a fixed bed flow-through reactor (Fig. 3.4), packed with rinsed pretreated solids (see composition in Table 3.2) using a progressive temperature increase from 160°C to 200°C and 50mM H_2SO_4 in GVL/water solutions as the solvent.

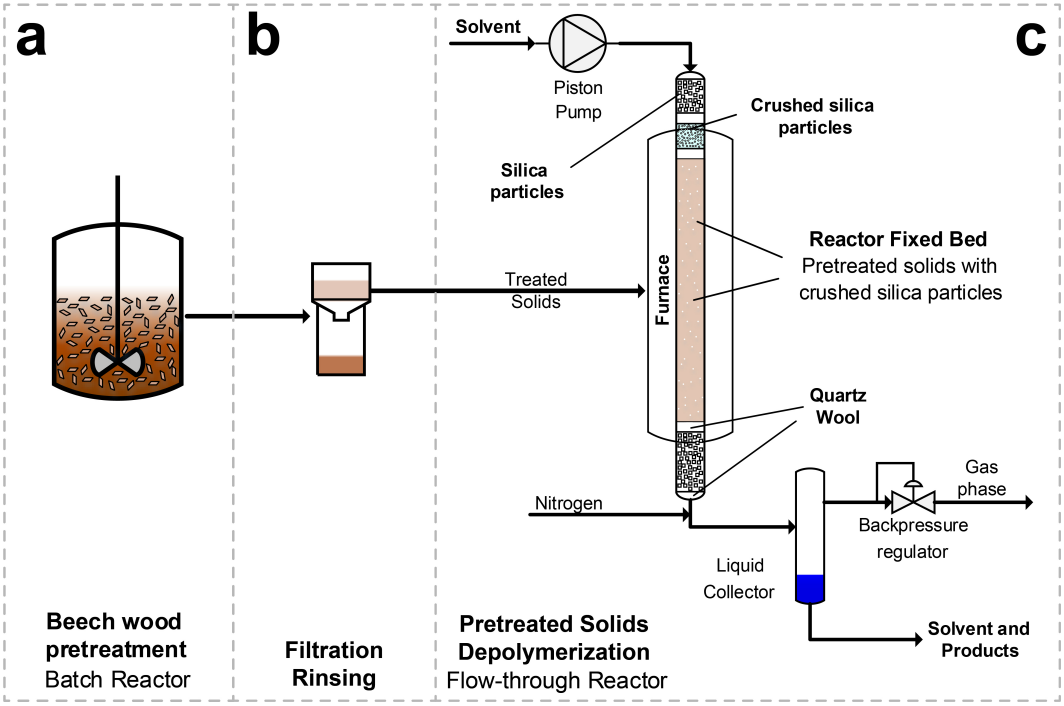

Figure 3.4 | Schematic representation of the overall process. (a) Biomass pretreatment in a batch reactor. (b) Filtration and rinsing of pretreated solids. (c) Pretreated solid depolymerization in a flow-through reactor.

Similar results to those with xylose were observed with glucose and FA during the depolymerization of the cellulose-rich pretreated solids. As glucose was produced, it rapidly formed stable

glucose-derived molecules (referred to hereafter as diformylglucose or DG). Specifically, the presence of FA led to the formation of two main DG isomers from glucose by creating 1,3-dioxolane (isomer 1) and 1,3-dioxane (isomer 2) structures (characterization given in Chapter 4 Figure 4.4 and 4.5). As with hemicellulose depolymerization, these structures stabilized the glucose that was formed at conditions that previously favored glucose dehydration and degradation. ^{1}H-^{13}C HSQC spectra of the cellulose hydrolysis liquor exiting the flow-through reactor when FA was used (Figure 3.5) revealed the presence of DG isomers with peak assignment confirmed by the spectra of purified species (Chapter 4 Figure 4.4 and 4.5). As expected, in the absence of FA, the ^{1}H-^{13}C HSQC spectra (Figure 3.5 a) showed chemical shifts that corresponded to pure glucose (Chapter 4 Figure 4.1 b) instead of DG isomers.

The total product yields exiting the reactor were difficult to quantify directly due to the presence of oligomers (8% to 25%). Therefore, we had the entire mixture undergo aqueous acid hydrolysis at 120°C, which is the preferred method to hydrolyze oligomers, and reversed the formation of DG isomers to yield glucose. The total soluble carbohydrate yield and the resulting total carbohydrate concentrations were measured for different solvent residence times (i.e., different quantities of solvents used) by varying the bed height in the reactor (represented in Figure 3.5 c as the final solvent-to-solid ratio).

Without the presence of FA, we observed that carbohydrates yields decreased as soluble carbohydrates underwent longer residence times in larger packed bed volumes. This decrease in yield eventually overtook the increase in concentration associated with a greater amount of biomass, such that we reached a maximum achievable concentration value at a solvent-to-solid ratio of 15 to 1 (in line with previous reports).[69,159]

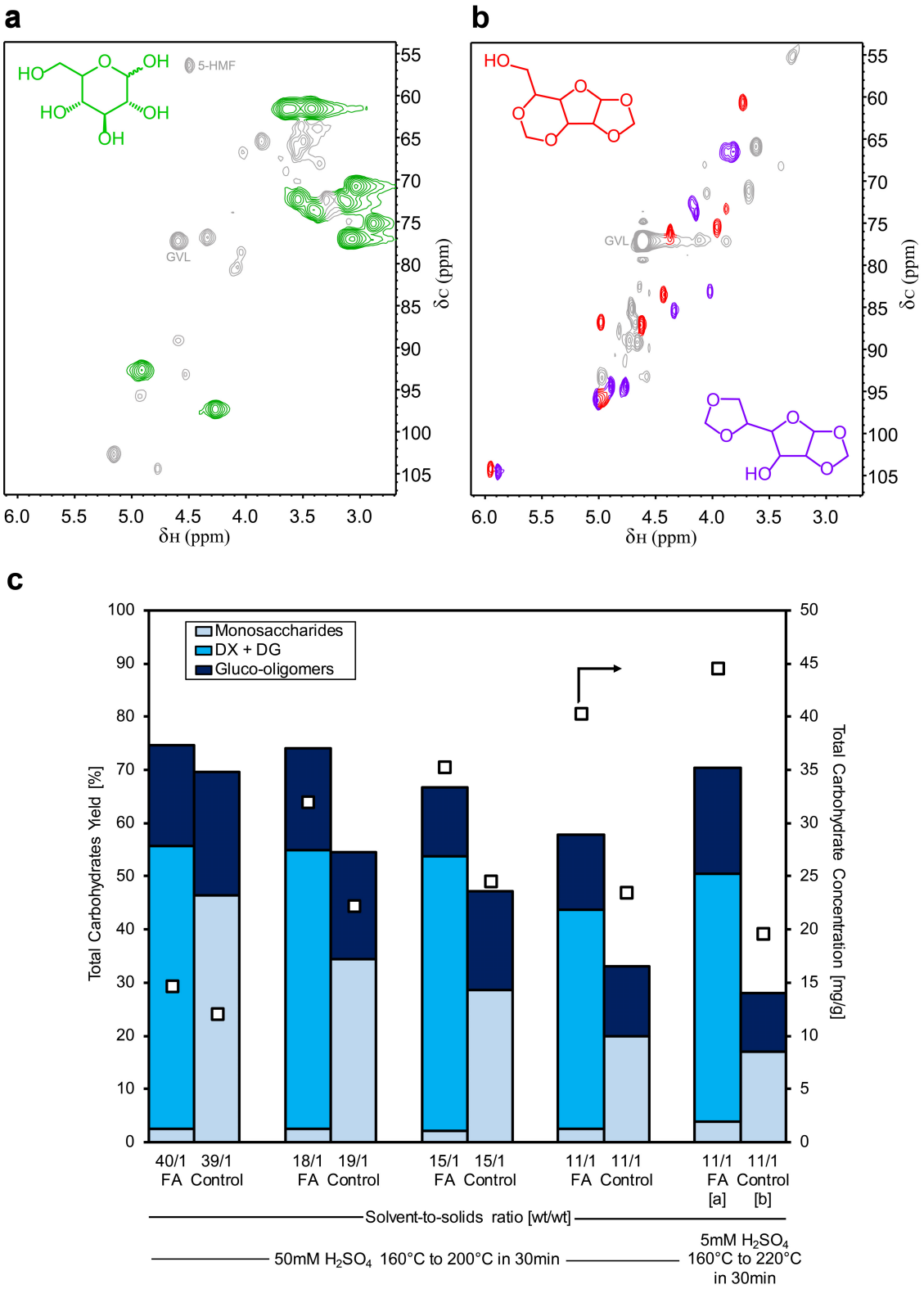

Figure 3.5 | Soluble carbohydrates produced from cellulose-rich pretreated solids using a flow-through reactor. (a) ^{1}H-^{13}C HSQC NMR spectrum of the liquor exiting the flow-through reactor without formaldehyde addition. (b) ^{1}H-^{13}C HSQC NMR spectrum of the liquor exiting the flow-through reactor with formaldehyde addition. (c) Total yield and concentration of soluble carbohydrates in the absence (Control) and presence of formaldehyde (FA, 7 wt%) as a function of the total amount of solvent used. [a] Experiment used to produce the liquor used for the ^{1}H-^{13}C HSQC NMR spectrum showed in Figure 3.5 a. [b] Experiment used to produce the liquor used for the ^{1}H-^{13}C HSQC NMR spectrum showed in Figure 3.5 b. The black arrow indicates the relevant axis to the associated data points.

When FA was used, the resulting stabilization of monosaccharides minimized the formation of furans and humins and led to significant yield increases at high solid loadings. The carbohydrate yield increased from 28 to 70% at a solvent-to-solid ratio of 11 to 1 (Figure 3.5 c). As a result, at the conditions we explored, we no longer hit a maximum carbohydrate concentration, reaching up to 45 mg/g carbohydrates (compared to 19 mg/g achieved without FA). Increasing concentrations in solvent-based processes is one of the most economically critical aspects of such technologies, due to the high cost of solvent recovery.[168] Interestingly, the effect of stabilization could be clearly observed by comparing the coloration of the stabilized and un-stabilized solutions after reaction. The un-stabilized solution was systematically significantly darker than the solution with formaldehyde which was indicative of increased humins formation (Figure 3.6).

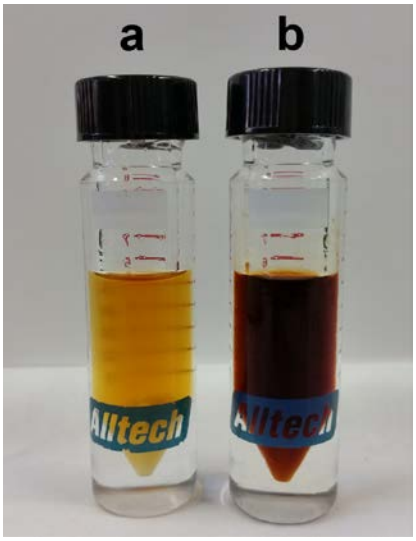

Figure 3.6 | Comparison of reaction mixtures after cellulose depolymerization. (a) Cellulose depolymerization with formaldehyde. (b) Cellulose depolymerization without formaldehyde. (Dark brown suggests a high degree of sugar degradation and humin formation).

The difference in yield and concentration was slightly less pronounced when pure dried cellulose was used (Avicel PH 101, Figure 3.7). This smaller difference could be attributed to the significantly lower surface area of Avicel[80] compared to non-dried pretreated solids due to pore

collapse during drying. However, in a biorefinery context, pretreated solids are a much more relevant substrate than Avicel, which has undergone extensive drying and compacting.

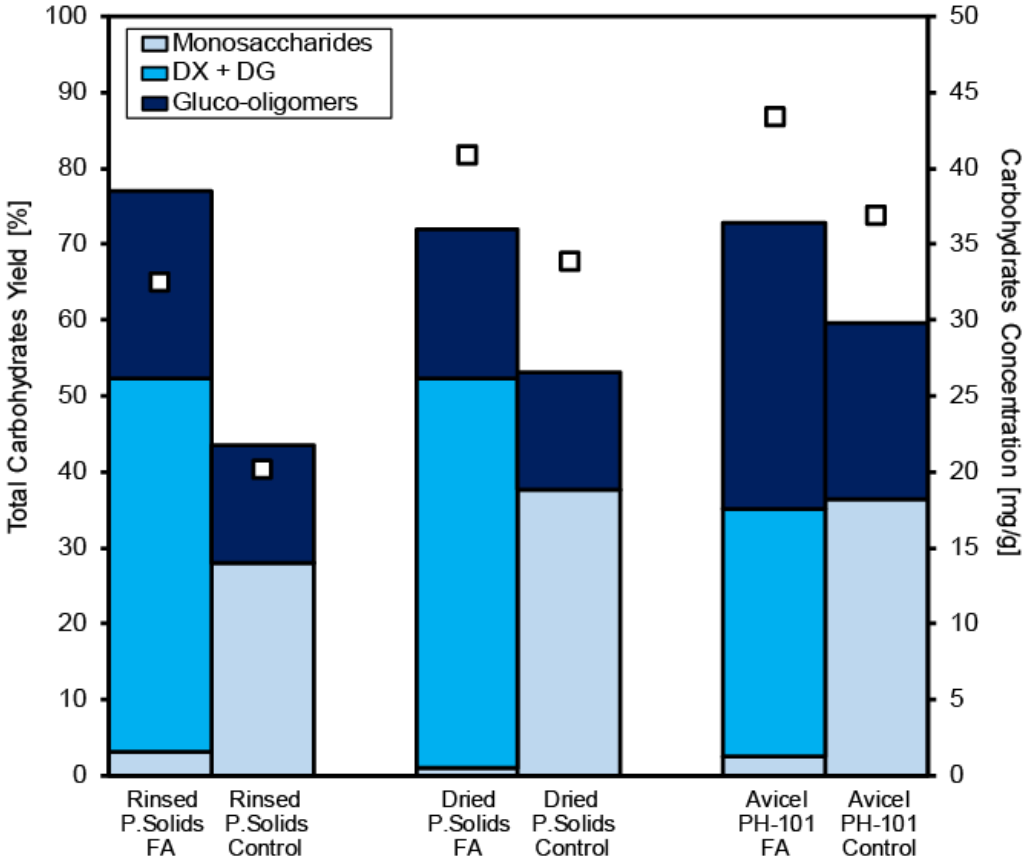

Figure 3.7 | Soluble carbohydrates after dilute-acid depolymerization. Effects of the substrate type on carbohydrates yield. Preparation of rinsed and dried pretreated solids (P. Solids) is detailed in Appendix A.1.2. For Avicel PH-101: the crystalline cellulose was used as purchased without further treatment.

These results demonstrate a shift in the typical kinetic trade-off seen for cellulose hydrolysis and glucose degradation when stabilization is used. The achieved yield of 70% carbohydrates with a concentration of 45 mg/g far exceeds what has been attained under aqueous conditions. Lee et al.[69] published an extensive review on the development and optimization of flow-through or "percolation" reactors featuring the hydrolysis of cellulose in aqueous conditions and reported that, for a yield of 70% glucose, the expected carbohydrate concentration was, depending on the acid concentration, between 1.1 and 1.4 g/100mL (ca. 11-14 mg/g) in a similar reactor—or 3-4 times lower than our result (Figure 3.8).

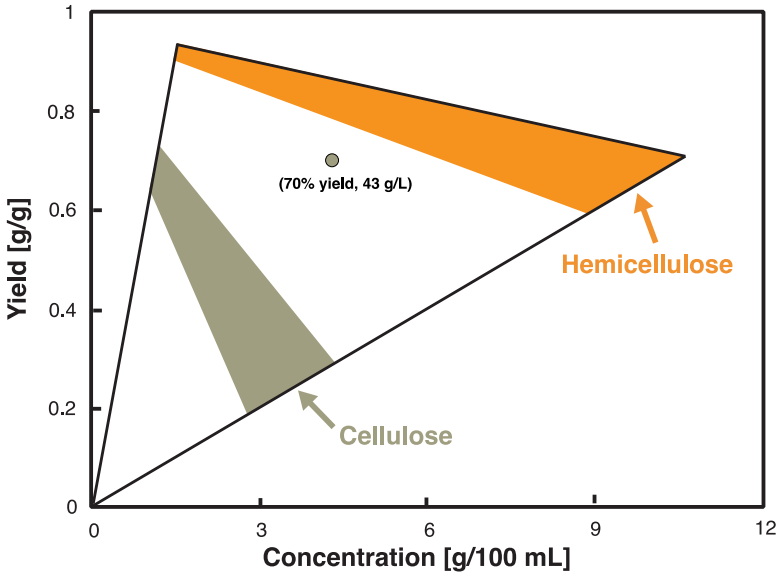

Figure 3.8 | Comparison of yields and concentration of carbohydrates in flow-through reactor setups. Colored zones were reported by Lee et al. as the achievable yields and concentrations attainable with aqueous flowthrough systems.[69] The data point is from this work and represents the glucose yield and concentration (the total yield and concentration of carbohydrates was 70% and 45 g/L, respectively, due to the presence of 2 g/L xylose)

Previous studies have shown that the optimal processing conditions are considered to be a two-step process because this led to lower solvent usage and higher product concentrations.[159,168] Experiments using raw biomass and the stabilization approach to perform a single-step process, reconfirm this statement with an overall carbohydrate yield (glucose + xylose) of 69% with a concentration of 26 g/L. In comparison, with a two-step process, total carbohydrate yields reached 86% with a concentration of 43 g/L (Table 3.3).

Table 3.3 | Comparison between a single-step and two-step process

Conversion process	*Carbohydrates yield/concentration during pretreatment [% / g/L]*	*Carbohydrates yield/concentration of treated solid depolymerizaton [% / g/L]*	*Total carbohydrates yield [%]*	*Carbohydrate concentration [g/L]*
Single step process	----	----	69	26
Two step process	83 / 43	70 / 45	86	43

Note: As expected from previous work[159], a single step process showed lower carbohydrates yields and concentrations compared to the two-step process.

Importantly, we also found that FA could be quantitatively recovered after de-protection in aqueous conditions (>98% recovery, which is within experimental error). After pretreatment about 20-56% of the original FA was recovered in the liquor (Table 3.4). This means that 44-80% of FA was bound to lignin and polysaccharides. Using purified model compounds or pre-treated cellulose, we demonstrated that the FA that has reacted with polysaccharides could be recovered quantitatively after de-protection in aqueous environments, while the FA bound to lignin ended up as methane or methyl groups in lignin monomers after hydrogenolysis.[190] During the depolymerization of pretreated solids, 73% of FA was recovered in the collected liquid (Table 3.5). Once the collected liquid was hydrolyzed to break all remaining oligomers and remove protective groups in carbohydrates, and any remaining solid underwent hydrolysis as well, >98% of the original FA was recovered. When performing a solvent blank run (without any biomass) at reaction conditions, we recovered >99% of FA in the resulting liquid after hydrolysis (Table 3.5). In the case of this control, about 4% FA was recovered in the form of dimethoxymethane and 1,3,5-trioxane prior to acid hydrolysis due to reversible self-condensation reactions of FA.

Table 3.4 | Mass balance of FA during biomass pretreatment

Biomass loading [wt.%]	*FA recovered in liquor [%]*
8	56
15	26
18	20

Note: Data points correspond to entries 1, 4 and 5 in Table 1, respectively.

Table 3.5 | Mass balance of FA after pretreated solid depolymerization

Pretreated solid loading [solvent/solids wt./wt.]	*Reaction solvent mixture*	*FA recovered in collected liquid, before / after acid hydrolysis [%]*	*FA recovered in gas phase [%]*
11/1	87/13 wt./wt. GVL/water 7 wt.% FA and 5mM H_2SO_4	73 / >95	>3
Blank		95 / >99	<0.01

3.3 Conclusion

It was shown that the use of protection group chemistry during biomass depolymerization could stabilize carbohydrates and enable their production at conditions that were previously unfavorable due to dehydration and degradation reactions. Specifically, formaldehyde, a cheap bulk chemical that can easily be produced renewably, was used to stabilize xylose during biomass pretreatment and glucose during cellulose depolymerization in a flow-through reactor by formation of acetal groups. Because these reactions can easily be reversed under aqueous conditions, we systematically and significantly increased sugar yields compared to un-stabilized controls. Using a flow-through reactor, we were able to produce a concentrated carbohydrates solution (ca. 5 wt% before solvent separation) at a yield of 70%, which was almost 3 times the yield of the un-stabilized control and 3-4 times more concentrated than the highly optimized aqueous system.

Chapter 4. Synthesis, purification and characterization of acetal-stabilized carbohydrates and intermediates.

This chapter is part of a published article in *Nature Chemistry* as **Questell-Santiago, Y.M.,** Zambrano-Varela, R., Talebi Amiri, M. and Luterbacher, J.S. Carbohydrates stabilization extends the limits of chemical polysaccharides depolymerization, *Nature Chem.* **2018**, 10, 1222-1228. Part of the manuscript and supplementary information are reproduced here with a few formatting changes with permission from Springer Nature.

The goal of this chapter is to synthesize, identify and characterize acetal-stabilized carbohydrates produced during the depolymerization of hemicellulose and cellulose. The characterization techniques used were: Nuclear Magnetic Resonance (NMR), Gas Chromatography – Flame Ionization Detector (GC-FID), Gas Chromatography – Mass Spectrometry (GC-MS), Liquid Chromatography – Mass Spectrometry (LC-MS).

All NMR spectra were obtained on a Bruker Avance III 400 MHz spectrometer.

All GC-FID chromatograms were obtained on an Agilent 789B series equipped with a HP5-column and a FID. The method used consisted of an injection and detection temperature of 300°C with a temperature program of: 40°C for 3 min, 30°C/min to 100°C, 40°C/min to 300°C and 300°C for 5 min.

All GC-MS spectra and chromatogram were obtained using an Agilent 7890B series equipped with a HP5-MS capillary column and an Agilent 5977A series Mass Spectroscopy detector. The method used consisted of an injection at 250°C with a temperature program of: 50°C for 1 min, 15°C/min to 300°C and 300°C for 7 min, and a detection temperature of 290°C.

4.1 Preparation and purification of diformylxylose

Approximately 15 grams of pure xylose, 31.5 mL of 37 wt.% HCl, and 75 mL of 37 wt.% FA were mixed in 675 mL of 1,4-dioxane and reacted at 80°C for 30 min. Then, the solution was neutralized with sodium bicarbonate and dried under reduced pressure with a rotary evaporator set at 60°C. The residue was extracted five times with 300mL of n-hexane or with 50mL of cyclopentyl methyl ether. All organic phases were combined and dried under reduced pressure with a rotary evaporator set at 60°C. The resultant residue was distilled at 120°C, under reduced pressure (0.1 mbar) to obtain a yellowish solid. The solid was recrystallized in ethanol three times. As result, a white solid crystal was obtained and used as the diformylxylose standard. The solid was analyzed by Heteronuclear Single Quantum Coherence Spectroscopy (HSQC) NMR to confirm its structure (Figure 4.1 c).

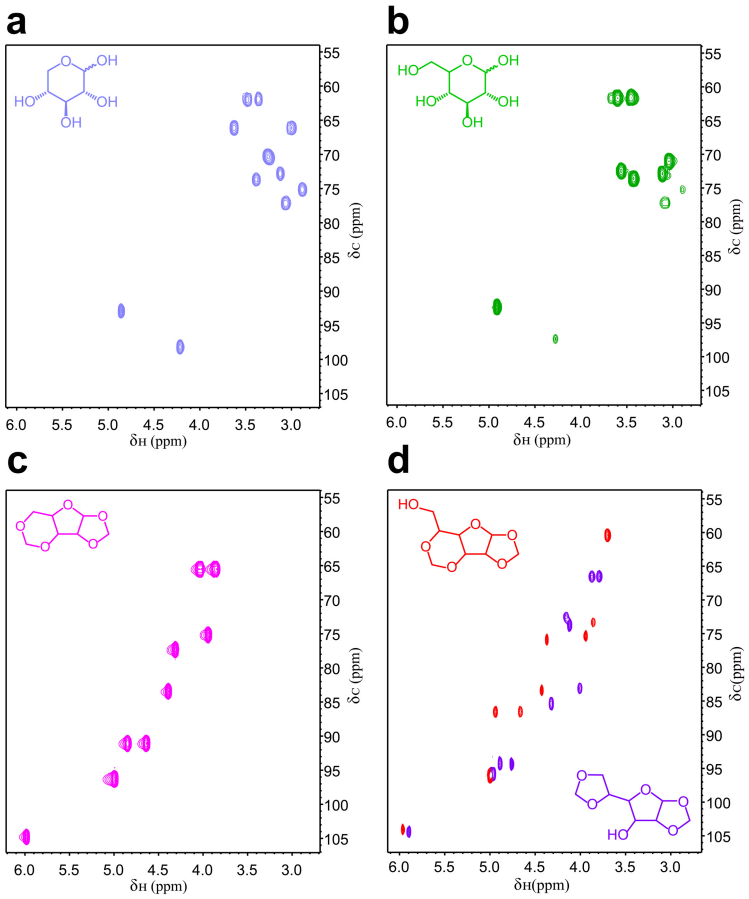

Figure 4.1 | ^{1}H-^{13}C HSQC NMR spectra of purified standards. (a) D-xylose (with peaks corresponding to α and β-D-xylose). (b) D-glucose (with peaks corresponding to α and β-D-glucose). (c) Purified diformylxylose (confirming our previously published data[32]). (d) Purified diformylglucose isomers (detailed characterization in Figure 4.4 and 4.5).

4.2 Preparation and separation of diformylglucose isomers

Both diformylglucose isomers were prepared by reacting approximately 15 g of pure glucose with 31.5 mL of 37 wt.% HCl and 75 mL of 37 wt.% FA in 675 mL of 1,4-dioxane at 80°C for 30 minutes. The resultant solution was sampled and analyzed by GC-MS and GC (Figure 4.2 and 4.7). Identification of diformylglucose peaks in the GC-FID chromatograms was performed initially by GC-MS. The peaks in the GC-MS chromatogram appear in the same orders as those in GC-FID chromatogram due to the use of a similar capillary column (Figure 4.2 and 4.3).

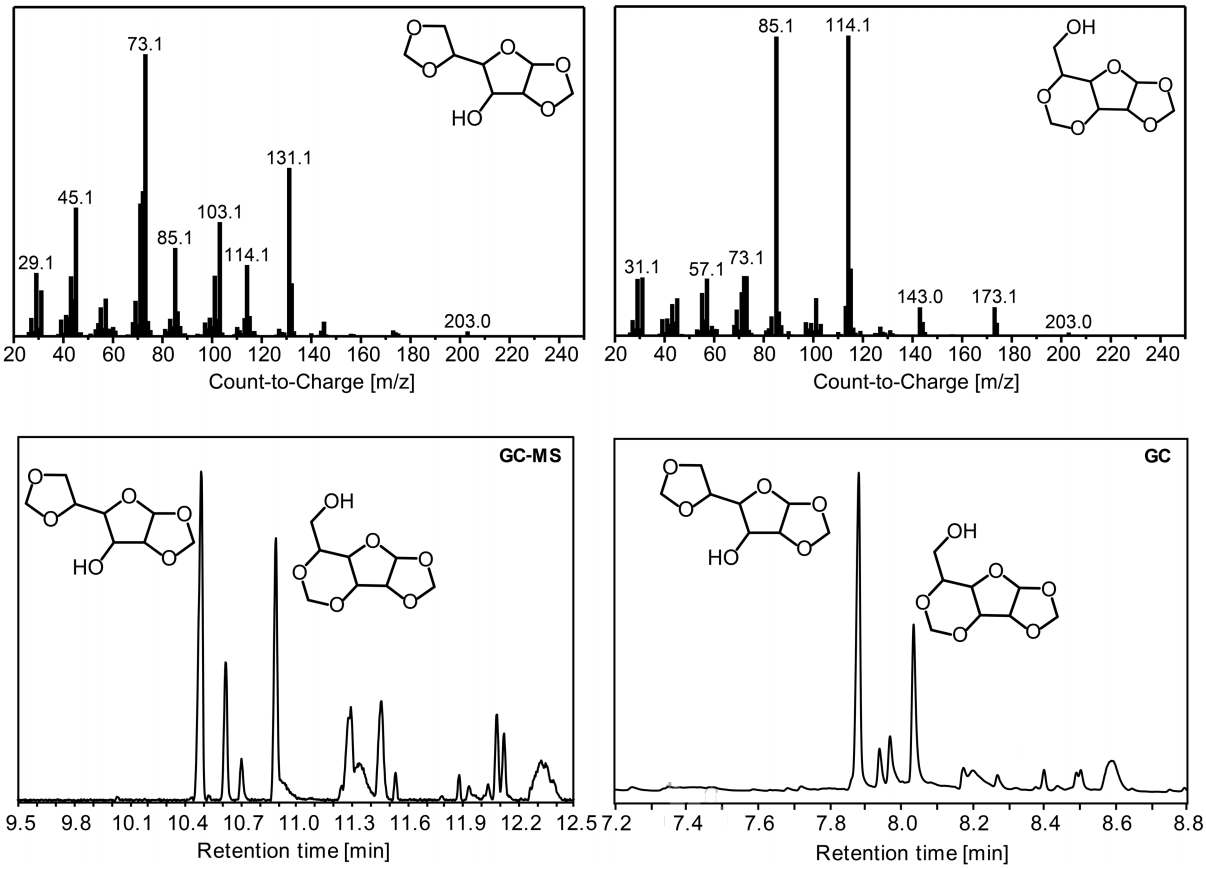

Figure 4.2 | GC-MS spectra of the two main diformylglucose isomers produced by the FA-treatment of glucose and comparison of the GC-MS and GC chromatograms.

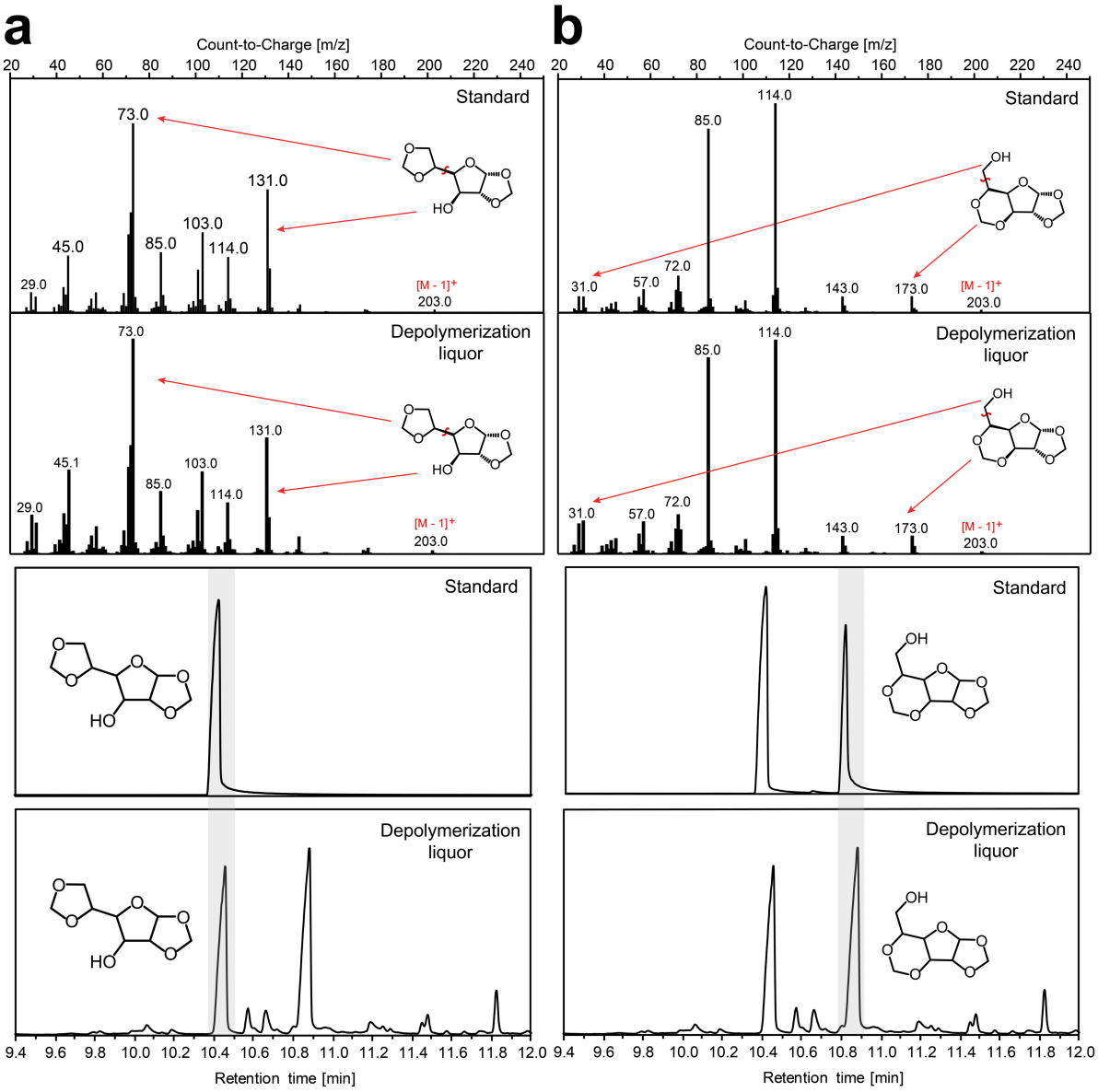

Figure 4.3 | Comparison of the authenticated diformylglucose isomers with the diformylglucose isomers derived from pretreated solids. (a) Diformylglucose isomer 1 standard from HPLC fraction collection. (b) Diformylglucose isomers standard from HPLC fraction collection with Diformylglucose isomer 2 highlighted.

Prior to separation, the solution was neutralized with sodium bicarbonate and dried under reduced pressure with a rotary evaporator at 60°C. The residue was extracted 5 times with 500 mL of ethyl acetate. All organic phases were combined and dried under reduced pressure with a rotary evaporator set at 40°C. The resultant residue was distilled at 125°C and ca. 0.06 mbar to obtain a yellowish paste. The paste was diluted with MQ-water and filtered with a 0.2µm PTFE filter. To obtain pure diformylglucose isomers to be used as standards, the solution was separated by HPLC and targeted peaks were collected using an automated fraction collector.

Isomer 1 was completely isolated from the mixture by this technique but isomer 2 always contained a certain amount of isomer 1, due to their similar retention times. However, these two spectra were sufficient for their conclusive identification. Collected fractions were neutralized with sodium bicarbonate and dried under reduced pressure in a rotary evaporator at 40°C. The solid residue was diluted with DMSO-d_6, filtered with a 0.2µm PTFE filter and used for GC-MS and NMR analyses (Figure 4.4, 4.5 and 4.3).

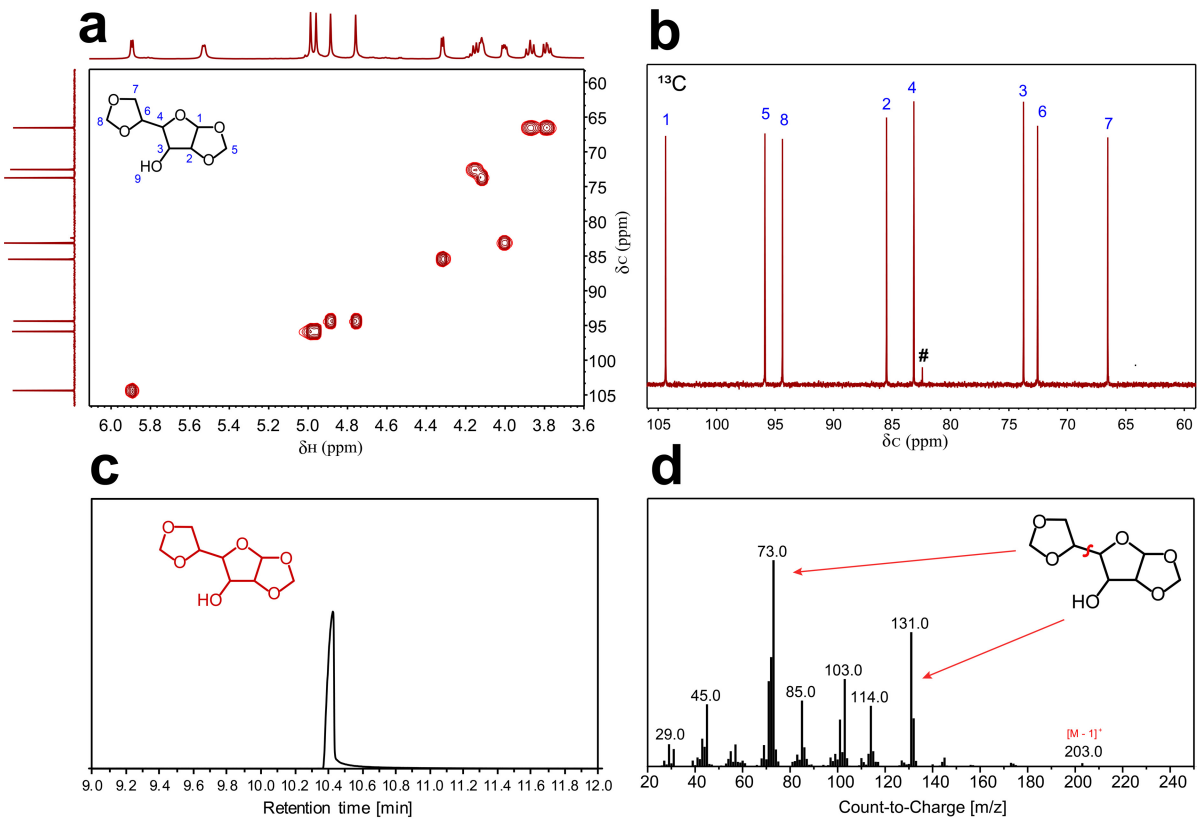

Figure 4.4 | Characterization and identification of diformylglucose isomer 1 (DG1). (a) ^{1}H-^{13}C HSQC NMR spectrum of DG1 in DMSO-d_6, (b) ^{13}C NMR spectrum of DG1 in DMSO-d_6, (c) GC-MS chromatogram of purified diformylglucose 1, and (d) mass spectrum of DG1. [#] formaldehyde-derived impurities.

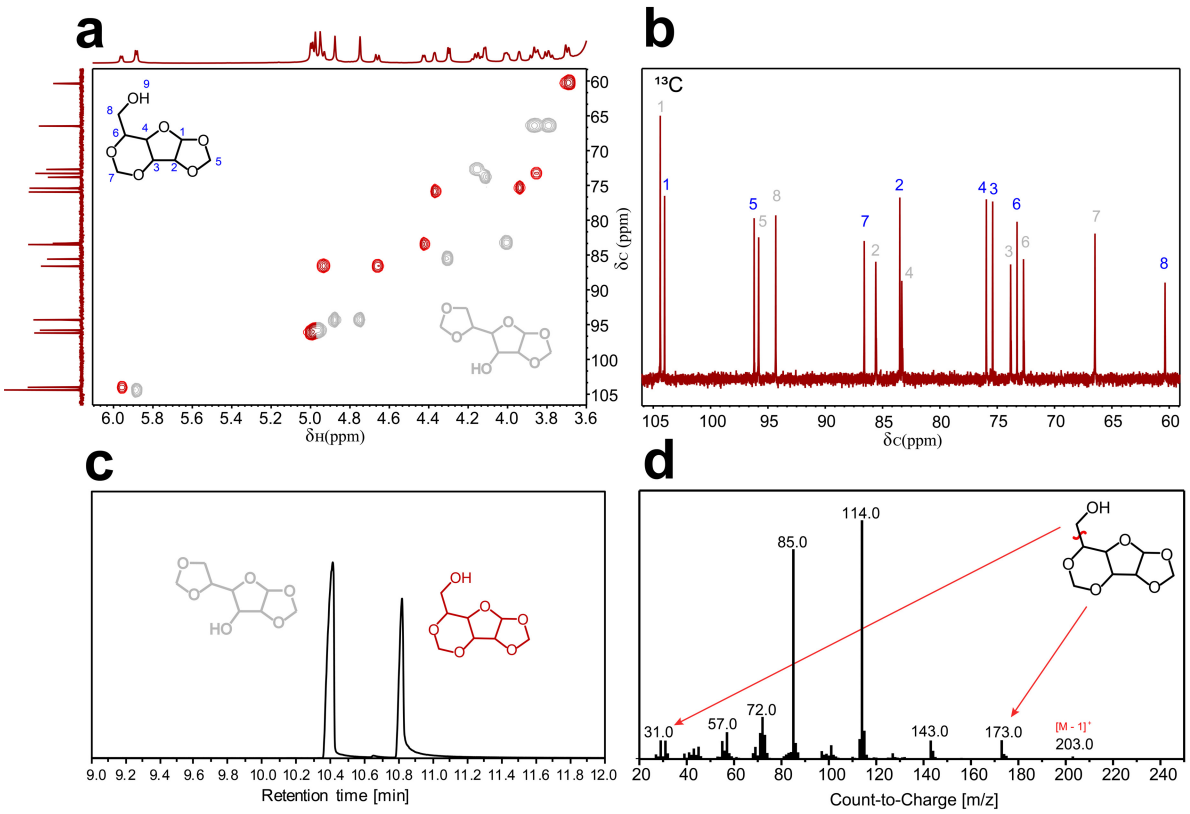

Figure 4.5 | Characterization and identification of diformylglucose isomer 2 (DG2). (a) ^{1}H-^{13}C HSQC NMR spectrum of DG2 in DMSO-d_6, (b) ^{13}C NMR spectrum of DG2 in DMSO-d_6, (c) GC-MS chromatogram of purified diformylglucose isomers, and (d) mass spectrum of DG2.

4.3 Synthesis of other acetal-stabilized sugars present in beech wood

In a 10 mL tick-walled reactor, 150 mg of hexose or 125 mg of pentose (glucose, galactose, mannose, fructose or arabinose) were mixed with 210 µL of 37 wt% HCl, 500 µL of 37 wt% FA and 4.5 mL of 1,4-dioxane. The FA-treatment was conducted in a silicon oil bath at 80°C for 30 min stirred at 600 rpm. The resultant solutions were analyzed by GC-MS (Figure 4.6). In the case of arabinose, two stabilized isomers were detected, while when fructose was used, no acetal formation was detected. In the case of galactose and mannose, three stabilized isomers of each sugar were identified by GC-MS. One of these stabilized galactose isomers had a similar retention time to a minor species formed after the FA-treatment of glucose. However, they resulted in different mass spectra (Figure 4.6). No detailed analysis was performed for arabinose and mannose due their low natural content in beech wood. On the other hand, there was a greater interest in analyzing fructose due to its highly selective conversion to 5-HMF.

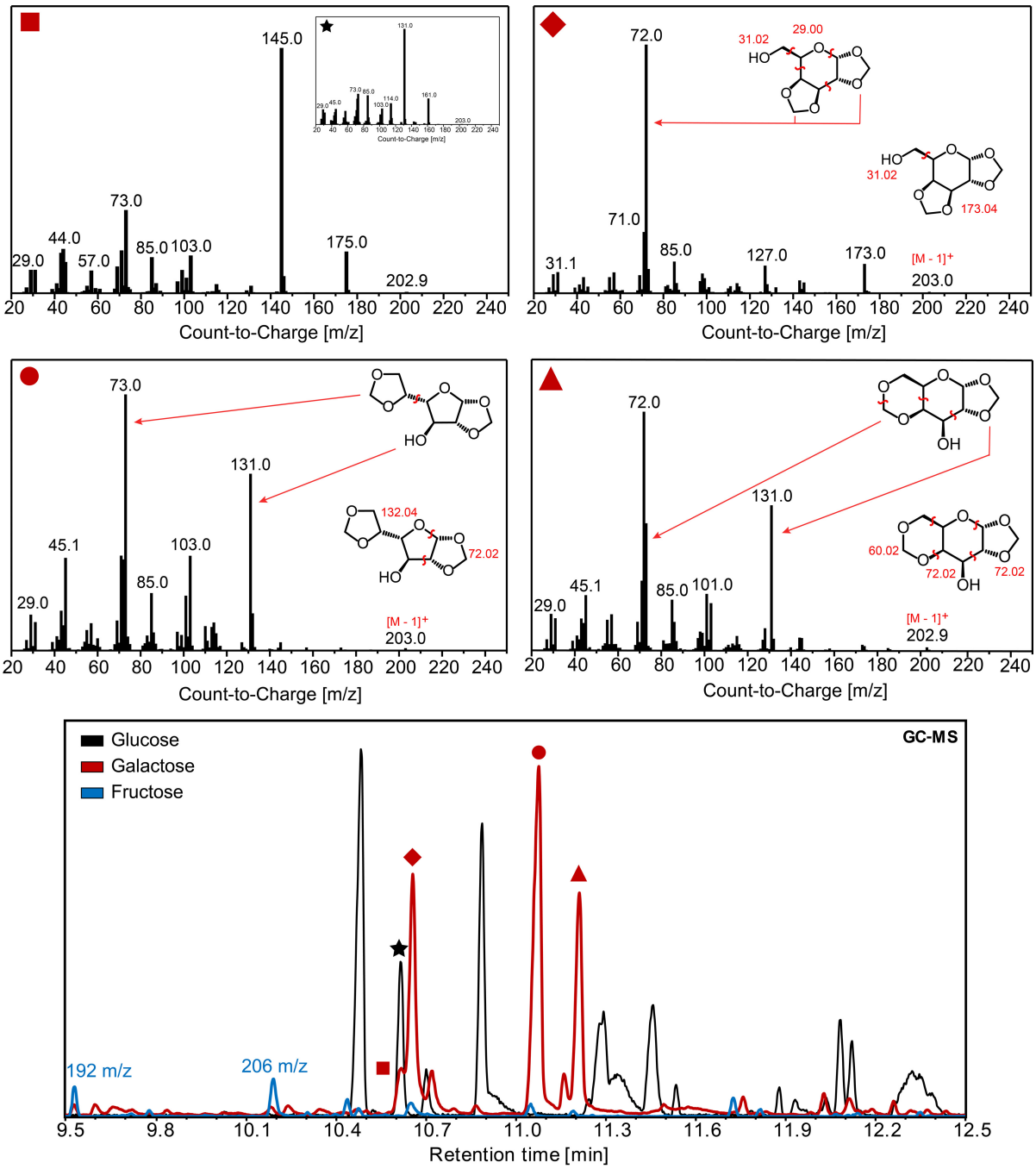

Figure 4.6 | GC-MS spectra of diformylgalactose isomers and comparison of the GC-MS chromatograms of FA treated hexoses (glucose, galactose and fructose). Glucose (★) and galactose (■) products overlapping with a retention time of 10.55min presented different mass spectra.

The minor species formed during the FA-treatment of glucose were not fully isolated and characterized due to their limited quantity. However, we could propose structures based on their MS spectra. Specifically, the peaks with retention times at 10.6 min and 10.7 min in the GC-MS (7.5-8.0min in the GC) are likely to be two additional diformylglucose isomers (Figure 4.7

and Table 4.1). Peaks with retention times of 11.35 min and 12.35 min in the GC-MS (8.2min and 8.6min in the GC) showed a m/z of 192 and 234 (Figure 4.7). Based on the fragments found on the mass spectra, these products probably correspond to a glucose with only one acetal ring and an additional hydroxymethyl group (Figure 4.7). All identified species in the FA-treatment of glucose sum to 88% of the total GC peak areas.

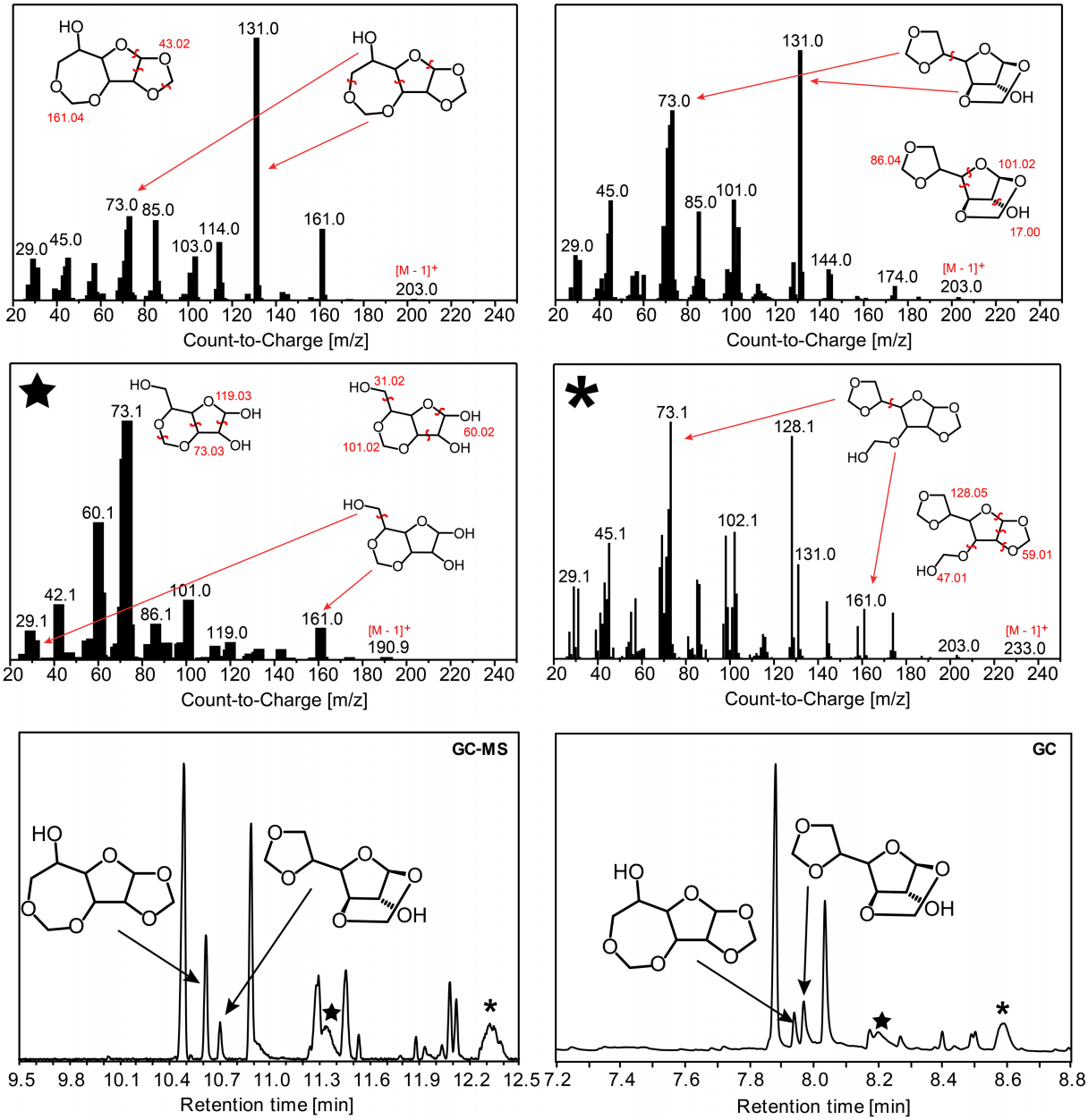

Figure 4.7 | GC-MS spectra of two minor diformylglucose isomers produced by the FA-treatment of glucose and comparison of the GC-MS and GC chromatograms.

Table 4.1 | Minor diformylglucose isomers and their reactive glucose configuration

Diformylglucose minor isomers	*Retention time in Figure 4.7 GC-MS / GC*	*Reactive glucose configuration*
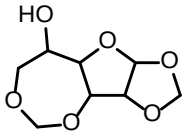	10.6 min / 7.5 min	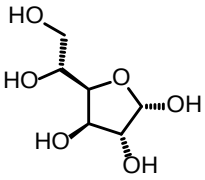 α-D-glucofuranose
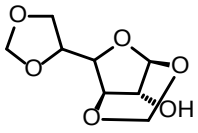	10.7 min / 8.0 min	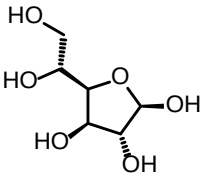 β-D-glucofuranose

4.4 Preparation and separation of 1-hydroxymethyl-xylofuranose (HMXF)

In a 60-mL glass reactor, 150 mg of DX were mixed with 15 grams of 3 wt.% of H_2SO_4 and reacted for 30 min at 120°C. Prior to separation, the solution was neutralized with sodium bicarbonate and dried under reduced pressure with a rotary evaporator at 40°C. The residue was extracted 6 times with 25 mL of ethyl acetate. All organic phases were combined and dried under reduced pressure with a rotary evaporator set at 40°C. The resultant residue was washed twice with 25 mL of hexane, dried under reduced pressure with a rotary evaporator set at 40°C, diluted with 2 mL of MQ-water and filtered with a 0.2µm PTFE filter. The obtained solution was separated by HPLC and the targeted peak was collected using an automated fraction collector. Collected fractions were neutralized with sodium bicarbonate and dried under reduced pressure in a rotary evaporator at 40°C. The solid residue was diluted with 150mM D_2SO_4 in D_2O, filtered with a 0.2µm PTFE filter and used for LC-MS and NMR analyses (Figure 4.8).

LC-MS analyses were conducted on a Xevo G2-S QTOF mass spectrometer coupled to the Acquity UPLC Class Binary Solvent manager and BTN sample manager (Waters, Corporation, Milford, MA). The separation was performed with a C18 column using an acetonitrile/water

gradient at 0.4 mL/min for 6 min. Mass spectrometer detection was operated in positive ionization using the ZSpray™ dual-orthogonal multimode ESI/APCI/ESCi® source. The TOF mass spectra were acquired in the sensitive mode over the range of m/z 50-1200 at an acquisition rate of 0.036 sec/spectra. The instrument was calibrated using a solution of sodium formate (0.01 mg/L in isopropanol/water 90:10). Data were processed using MassLynx™ 4.1 software.

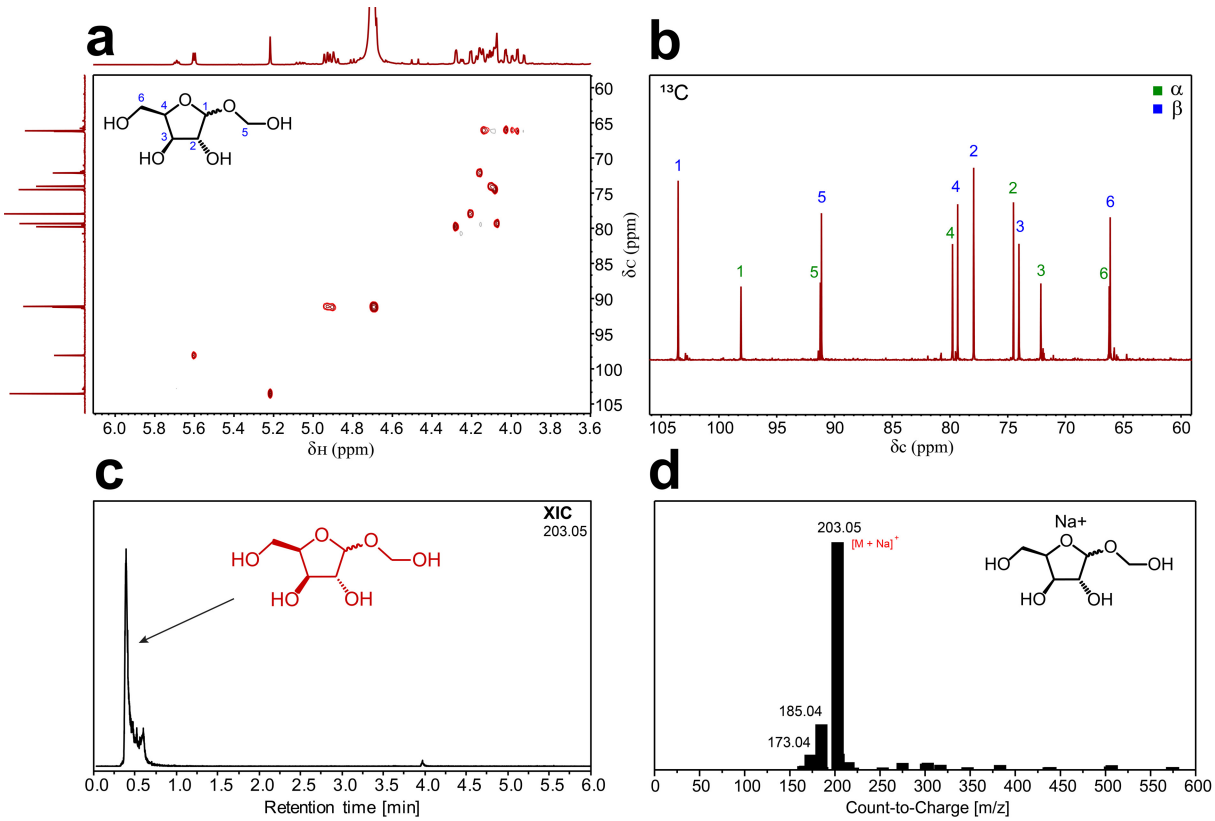

Figure 4.8 | Characterization and identification of 1-hydroxymethyl-xylosefuranose (HMXF). (a) ^{1}H-^{13}C HSQC NMR spectrum of HMXF in 150mM D_2SO_4 D_2O, (b) ^{13}C NMR spectrum of HMXF 150mM D_2SO_4 D_2O, (c) LC-MS extracted ion chromatogram (XIC) of the NMR sample, and (d) mass spectrum of HMXF (salt clusters present).

4.5 Conclusions

In summary, several methods were developed for the synthesis, purification and characterization of acetal-stabilized carbohydrates. Only the acetal-stabilized sugars found after depolymerizing beech wood and the intermediate found in the deprotection of diformylxylose by hydrolysis, were characterized by NMR, GC-MS and LC-MS. We found that out of all the treated sugars, only fructose did not possess the necessary spatial isomers to produce acetal sugars.

Chapter 5. Mechanistic study of the tandem hydrolysis-dehydration conversion of acetal-stabilized carbohydrates into furans

This chapter is part of a published article in *Nature Chemistry* as **Questell-Santiago, Y.M.,** Zambrano-Varela, R., Talebi Amiri, M. and Luterbacher, J.S. Carbohydrates stabilization extends the limits of chemical polysaccharides depolymerization, *Nature Chem.* **2018**, 10, 1222-1228. Part of the manuscript and supplementary information are reproduced here with a few formatting changes with permission from Springer Nature.

Given that acetal-stabilized biomass-derived carbohydrates can be produced quantitatively from raw biomass, a better understanding of their reactivity could lead to new catalytic upgrading routes. Here, I study the reaction mechanism of the deprotection and dehydration of diformylxylose to furfural. To do so, several reactions were carried out in biphasic media, where the deprotection was done by acid hydrolysis in the aqueous phase and the organic phase served to continuously extract the furans and isolate them from the reactive medium (aqueous phase). The aqueous phase was further characterized by *Operando* ^{13}C NMR where it was possible to identified a new intermediate during diformylxylose conversion that was not formed when compared to experiments with xylose.

5.1 Tandem hydrolysis-dehydration of acetal-stabilized carbohydrates

Diformylxylose is a versatile molecule that is volatile and soluble in hexane – properties that could make it an interesting bio-derived fuel or lubricant additive. DX can also be converted back to xylose in aqueous environments (71% xylose yield, Figure 5.1). Because of its modified structure, we hypothesized that diformylxylose might be a more favorable substrate for furfural production.

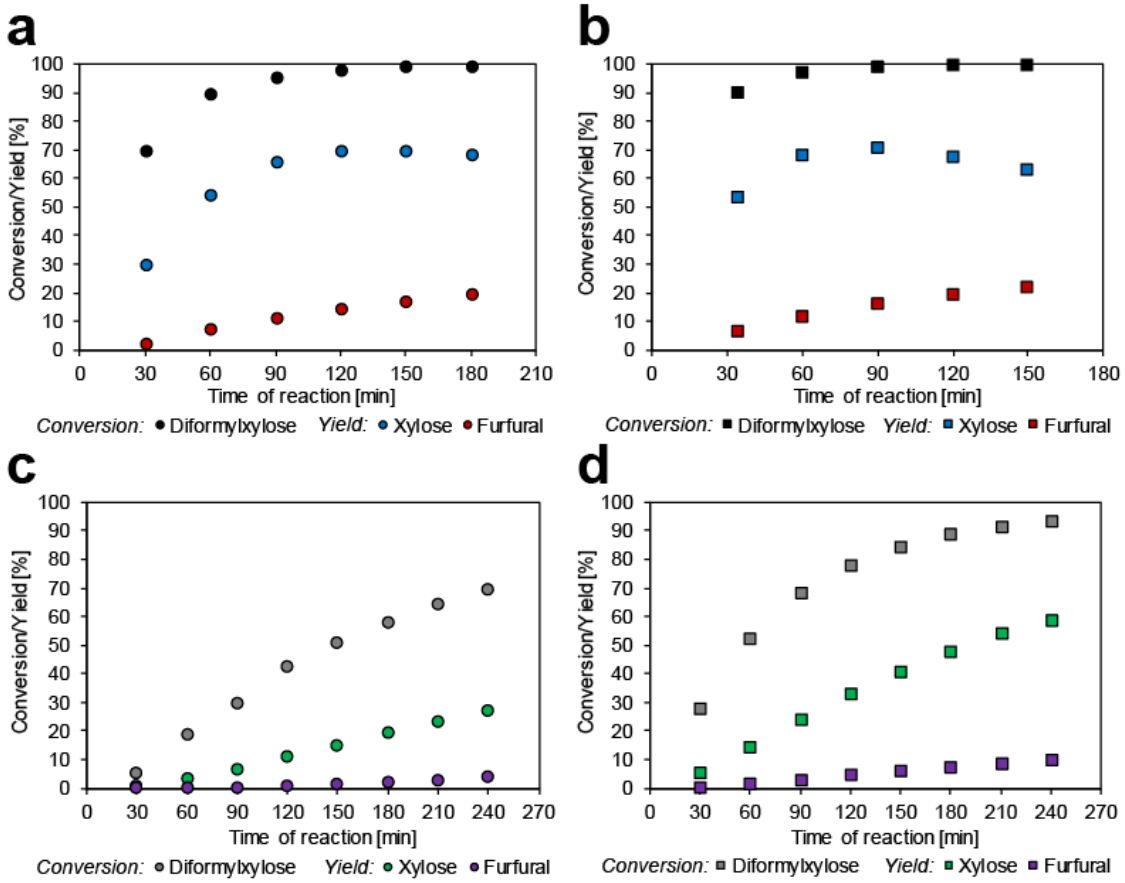

Figure 5.1 | Removal of protective groups from diformylxylose by acid hydrolysis. Recovery of xylose by the acid hydrolysis of diformylxylose in an aqueous environment at 120°C (a and b) and 100°C (c and d) with acid concentrations of 3 wt.% H_2SO_4 (a and c) and 6 wt.% H_2SO_4 (b and d).

Furfural is typically produced by the Brønsted acid-catalyzed dehydration of pentose, e.g., xylose, but this reaction can be further facilitated (especially at lower temperatures) by the combination of Brønsted and Lewis acids.[2,198,199] The rate is accelerated with Lewis acids because they catalyze the isomerization of xylose *via* a hydrogen transfer (1,2-hydride shift), which easily leads to the furanose configuration necessary for producing furfural (Figure 5.2 a).[200,201] This pathway has a lower activation energy compared to one-step xylose dehydration using only a Brønsted acids.[199] We verified this by comparing the xylose production in a two-phase system at 160°C in the presence 0.15 M H_2SO_4 with and without a Lewis Acid present (Figure 5.2 b). We observed significantly less xylose conversion and very low furfural production when no Lewis acid was present, whereas furfural yields around 70% could be achieved with a Lewis acid.

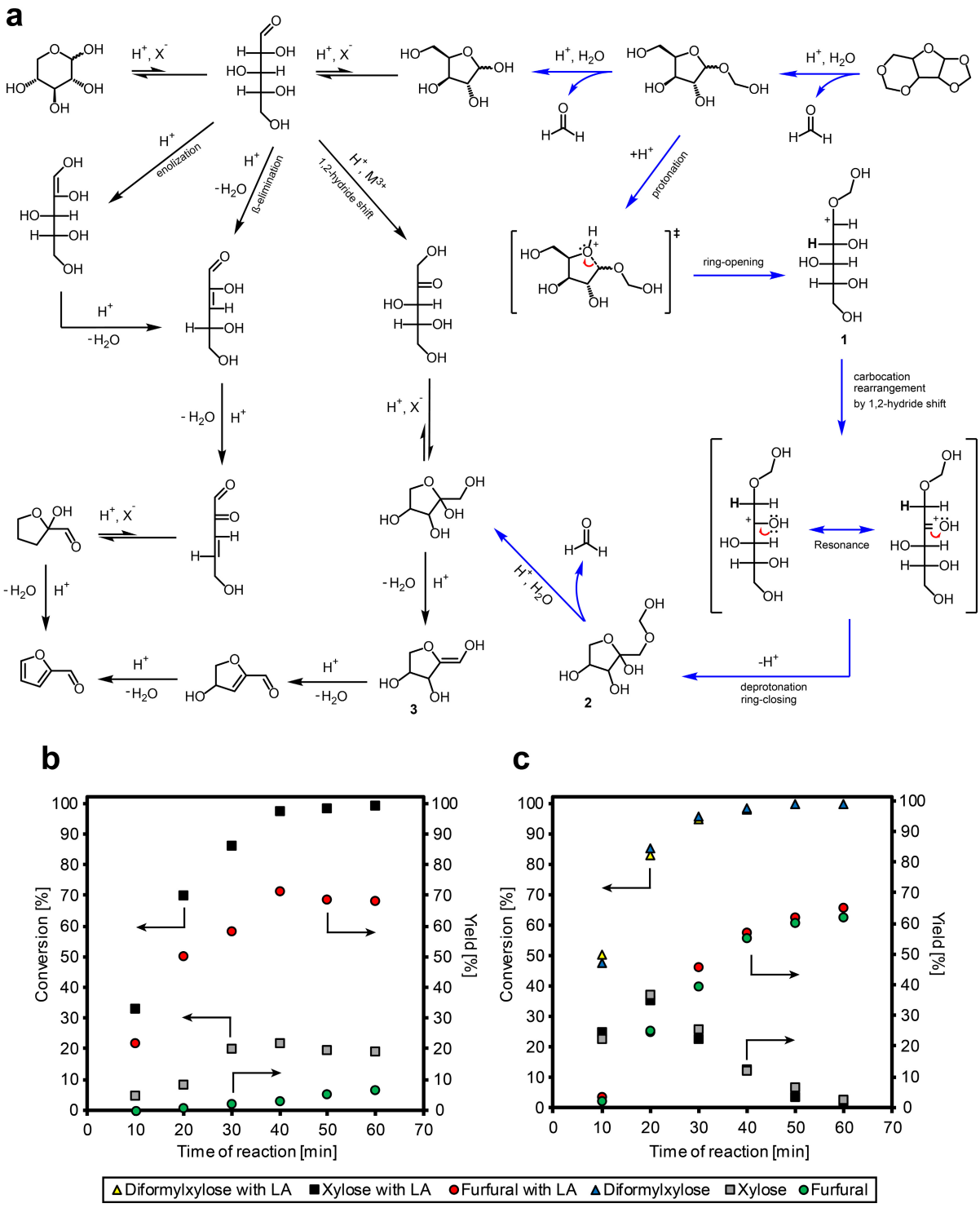

Figure 5.2 | Pentose dehydration to furfural in biphasic water-alkylphenol reaction systems. (a) Previously reported and proposed pentose dehydration mechanisms. Black arrows depict the conventional routes of xylose dehydration *via* the 1,2-hydride shift, enolization and β-elimination reactions.[202] Blue arrows highlight a proposed mechanism from diformylxylose *via* the tandem hydrolysis-dehydration of diformylxylose to furfural. (X^- represents halides ions, and M^{3+} metal cations). Brønsted acid-catalyzed production of furfural at 160°C in a biphasic aqueous alkylphenol reaction system from (b) xylose (with and without Lewis acid addition) and (c) diformylxylose (with and without Lewis acid addition). Black arrows indicate the relevant axis to the set(s) of associated data points.

When DX was used as a starting product, similar furfural yields (65%) were achieved without Lewis acid addition (Figure 5.2 c). Interestingly, no difference in the reaction kinetics was observed when a Lewis acid was added at these conditions (Figure 5.2 c), which suggested that DX proceeded to furfural through a new mechanism (proposed in Figure 5.2 a, blue arrows). In the aqueous environment in which DX was partially present within the two-phase reaction system, DX hydrolyzed, releasing one of its protective groups as FA and forming HMXF (characterization given in Chapter 4 Figure 4.8). Although HMXF was not quantified by HPLC, it was identified as the main intermediate during *operando* ^{13}C NMR studies of the aqueous phase with labelled 1-^{13}C-diformylxylose (Chapter 5.2 Figure 5.5 and 5.6). Product analyses of these labelled reactions also showed that the furfural produced by the dehydration of DX had its labelled carbon in the same position as that produced from xylose (aldehyde carbon). These observations led us to propose a new mechanism for the production of furfural where HMXF is protonated and undergoes ring-opening to form a carbocation in C1 (Figure 5.2 a), as is the case for unmodified xylose. Generally, the resulting hydroxyl group in C1 of unmodified xylose (or other carbohydrates) will rapidly deprotonate to form an aldehyde (aldose) that stabilizes the positive dipole induced by the ring-opening.[203]

The transition state was identified based on that of the analogous reaction of protonation of O5 in unmodified xylose.[204] In the case of HMXF, the aldehyde formation is blocked, and the ring-opening creates a carbocation in C1, forming **1** (Figure 5.2 for number reference). This carbocation likely rearranges to a more stable configuration *via* a similar 1,2-hydride shift to that observed for Lewis acid-catalyzed reactions (proton shown in bold in Figure 5.2 a, blue pathway). This intermediate is potentially more stable due its ability to resonate with the hydroxyl group in C2. We believe that this carbocation rearrangement occurs prior to any FA elimination

reaction, otherwise the reaction would lead to the formation of xylose. Afterwards, these resonance structures could deprotonate, creating an aldehyde in C2 which could rapidly undergo ring-closing by a nucleophilic attack of O5 to C2, forming **2**. O5 also could attack prior to deprotonation, also forming **2**. Whether **2** hydrolyzed first, releasing FA and forming xylulose before subsequently dehydrating (drawn route), or if dehydration occurs first followed by hydrolysis, is unknown. Nevertheless, both routes lead to **3**, which readily dehydrates to furfural.

The rate data suggest that this pathway's rate-determining step has a comparable activation energy to that of the tandem isomerization-dehydration of xylose-xylulose *via* the 1,2-hydride shift, which is catalyzed by the presence of Lewis acid (Figure 5.2 b and c), and could allow the production of furfural at lower temperatures without additional catalysts. Experiments using dipropylxylose (propionaldehyde-stabilized xylose, characterization given in Figure 5.3 a) featured the same Lewis acid independency as DX when forming furfural (Figure 5.3 b).

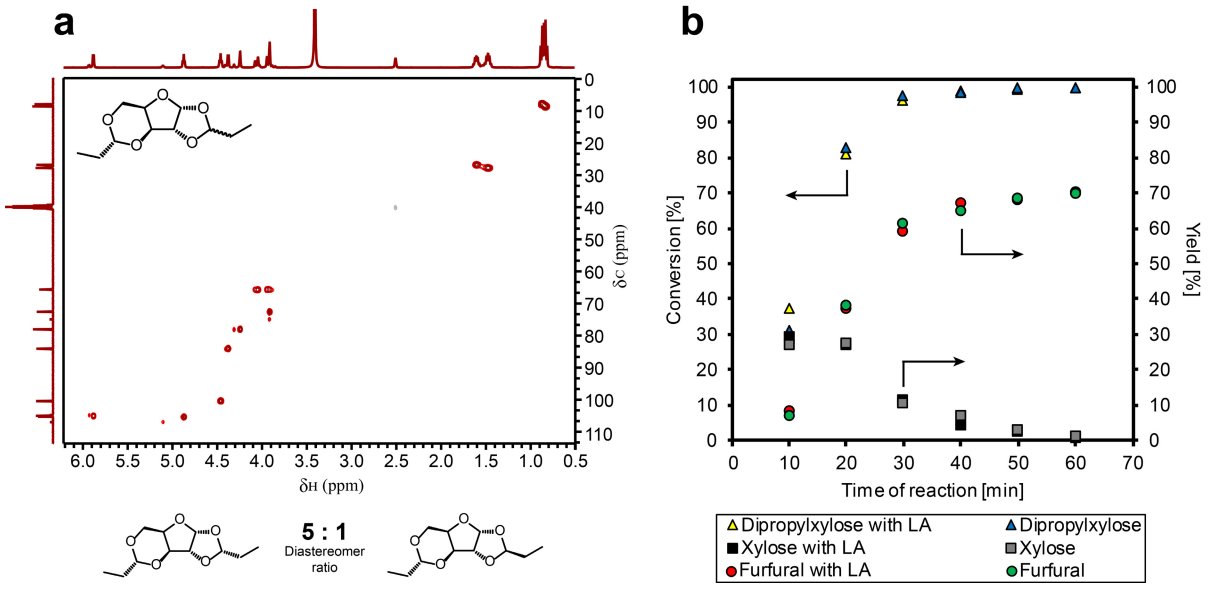

Figure 5.3 | ^{1}H-^{13}C HSQC NMR spectrum of dipropylxylose isomers and their dehydration to furfural in a biphasic reaction system. (a) ^{1}H-^{13}C HSQC NMR spectrum of dipropylxylose diastereomer in DMSO-d_6 (confirming our published data[188]) and the diastereomer ratio based on the integrated area of the ^{1}H NMR spectrum. (b) Brønsted acid-catalyzed production of furfural at 160°C in a biphasic aqueous alkylphenol reaction system from dipropylxylose (with and without Lewis acid addition). Black arrows indicate the relevant axis to the set(s) of associated data points.

This suggests that dipropylxylose forms a similar intermediate as that formed with DX and, thus, likely undergoes a similar pathway. Likely, other acetal-functionalities in xylose would also undergo similar transformations, which could potentially open new upgrading routes for biomass derived polysaccharides.

Preliminary results using a mixture of DG and glucose did not show significant differences in 5-hydroxymethylfurfural (5-HMF) yields compared to pure glucose with only a Brønsted acid as the catalyst (Figure 5.4). This could be explained by the absence of an intermediate that could promote a 1,2-hydride shift, commonly catalyzed by a Lewis acid, as in the case of the acetal-stabilized xyloses. In fact, LC-MS analyses revealed an exact mass of 241.1 m/z (50.00 ppm) during the acid hydrolysis deprotection of DG that could be attribute to the protonated dihydroxymethylglucofuranose $[M + H]^+$. Further characterization of this species is needed in order to understand its role during the formation of 5-HMF from DG.

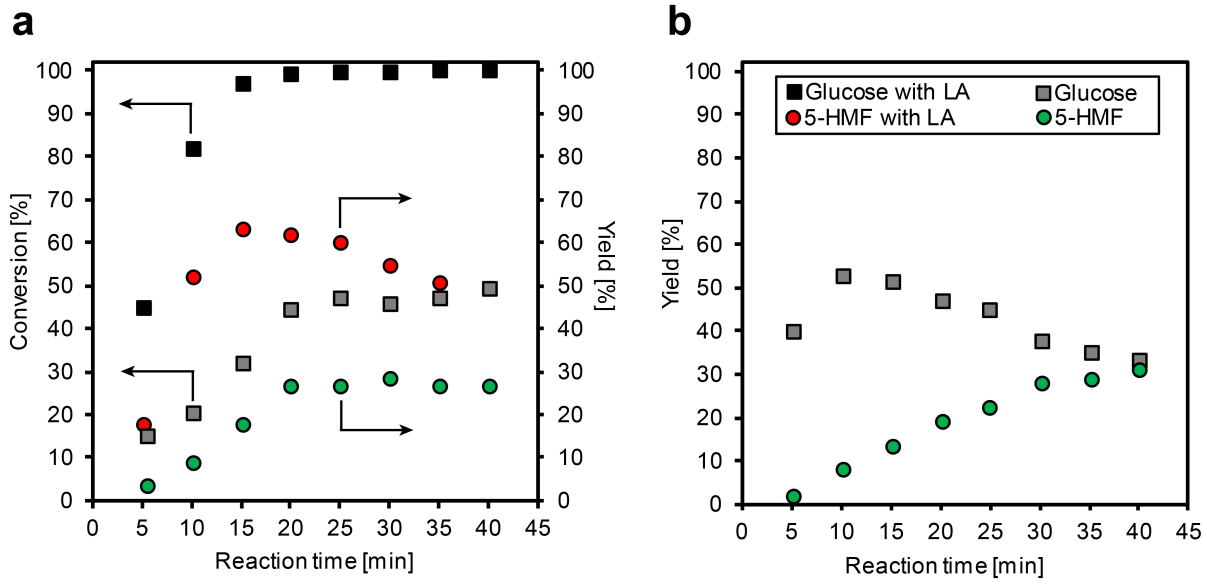

Figure 5.4 | Hexose dehydration to 5-HMF in biphasic water-alkylphenol reaction systems. Brønsted acid-catalyzed production of 5-HMF at 170°C in a biphasic aqueous alkylphenol reaction system from (a) glucose (with and without Lewis acid addition) and (b) a mixture containing ~60% diformylglucose (without Lewis acid addition). Black arrows indicate the relevant axis to the set(s) of associated data points.

5.2 *Operando* ^{13}C NMR studies

5.2.1 Dehydration of 1-^{13}C-xylose

Dehydration experiments with 1-^{13}C-xylose in 150mM D_2SO_4 D_2O showed the expected α- and β-xylo-pyranose configurations at chemical shifts of 92.11 ppm and 96.50 ppm (at 25°C), respectively (Figure 5.6 a spectrum 1). As temperature increased, we noticed that all chemical shifts slightly drifted to higher chemical shifts. At 148°C (maximum temperature of the probe) the chemical shifts corresponding to α- and β-xylo-pyranose forms were found at 93.66 ppm and 98.09 ppm, respectively (Figure 5.5 a spectrum 6). No formation of the xylo-furanose form or other intermediates were detected during the reaction. The 1-^{13}C-furfural signal appeared at 181.74 ppm after 38.7 min of heating (after the sample was at 148°C, Figure 5.6 a spectrum 7). After 68.9 min of heating another signal appeared at 165.81 ppm, which corresponds to ^{13}C-formic acid. Formic acid is assumed to form from furfural degradation *via* the hydrolytic fission of the aldehyde group.[202] After reaction completion, an extra ^{13}C NMR spectrum was taken at 25°C to confirm the chemical shifts of all these species (Figure 5.6 c).

5.2.2 Preparation of 1-^{13}C-diformylxylose

400 mg of D-1-^{13}C-xylose was mixed with 19.6 g of 90/10 v/v 1,4-dioxane/water containing ~4 wt.% of FA and 0.45 M of HCl, and reacted at 80°C for 1 hr. Then, the solution was neutralized with sodium hydroxide and dried under reduced pressure with a rotary evaporator set at 40°C. The residue was extracted five times with 40mL of n-hexane. All organic phases were combined and dried under reduced pressure with a rotary evaporator set at 30°C. The resultant residue was recrystallized twice in ethanol. The solid was analyzed by GC-MS and NMR to confirm its structure and isotopic abundance (Figure 5.5).

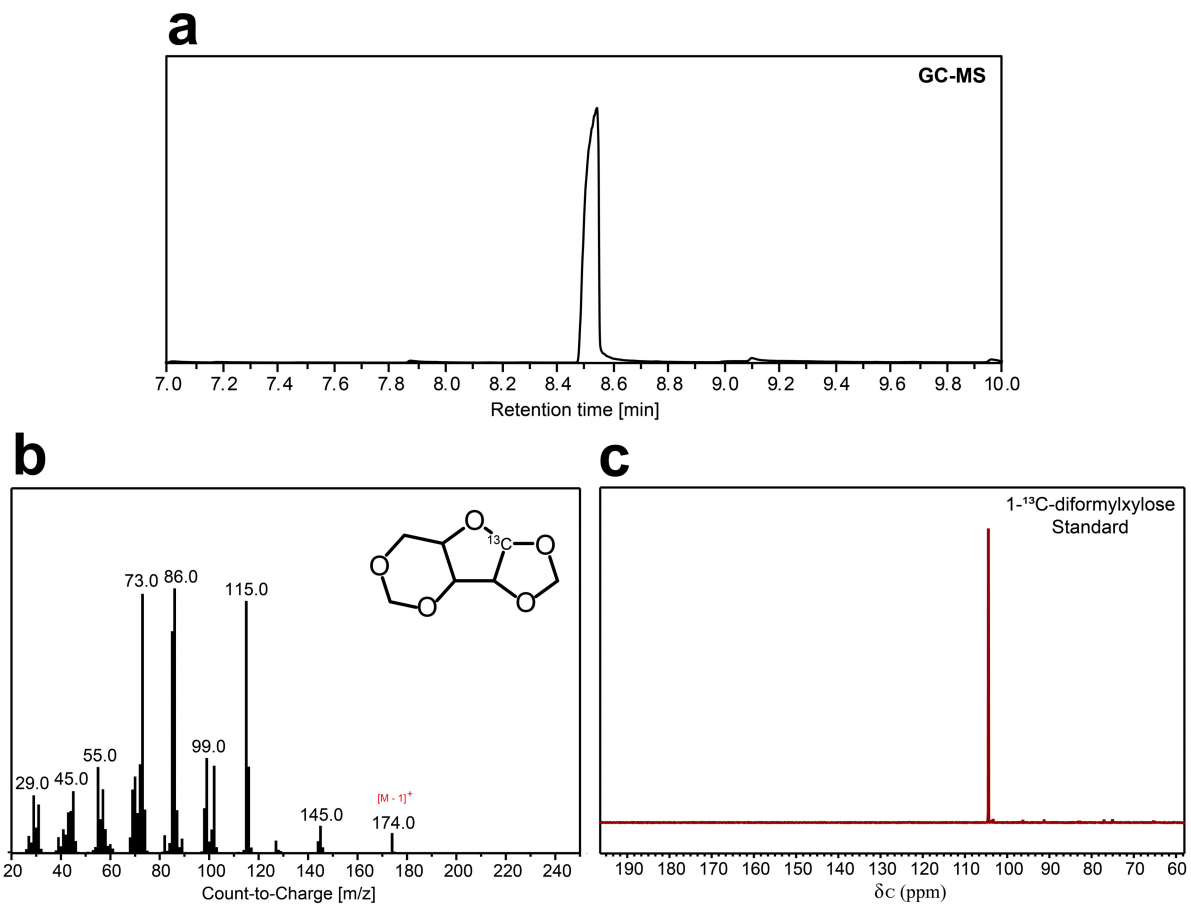

Figure 5.5 | Characterization of 1-^{13}C-diformylxylose. (a) GC-MS Chromatogram, (b) mass spectrum, (c) ^{13}C NMR spectrum of purified 1-^{13}C-diformylxylose in 150mM D_2SO_4 D_2O.

5.2.3 Hydrolysis-dehydration of 1-^{13}C-diformylxylose

When dehydration experiments were run with of 1-^{13}C-diformylxylose (1-^{13}C-DX) in 150mM D_2SO_4 D_2O, the initial spectra at 25°C showed a peak with a chemical shift at 104.46 ppm (Figure 5.6 b spectrum 1). As in 1-^{13}C-xylose, all chemical shifts were slightly shifted to higher values as the temperature increased. At 120°C, intermediate HMXF was detected at 104.79 ppm, whereas 1-^{13}C-DX was at 105.57 ppm (Figure 5.6 b spectrum 4). At 140°C, two additional peaks appeared at 93.57 ppm and 98.01 ppm corresponding to the α- and β-xylo-pyranose forms, respectively (Figure 5.6 b spectrum 5). The relative signals of these two species were significantly smaller compared those of 1-^{13}C-DX and HMXF until 1-^{13}C-DX was almost fully consumed. No formation of the xylo-furanose product was detected during the reaction.

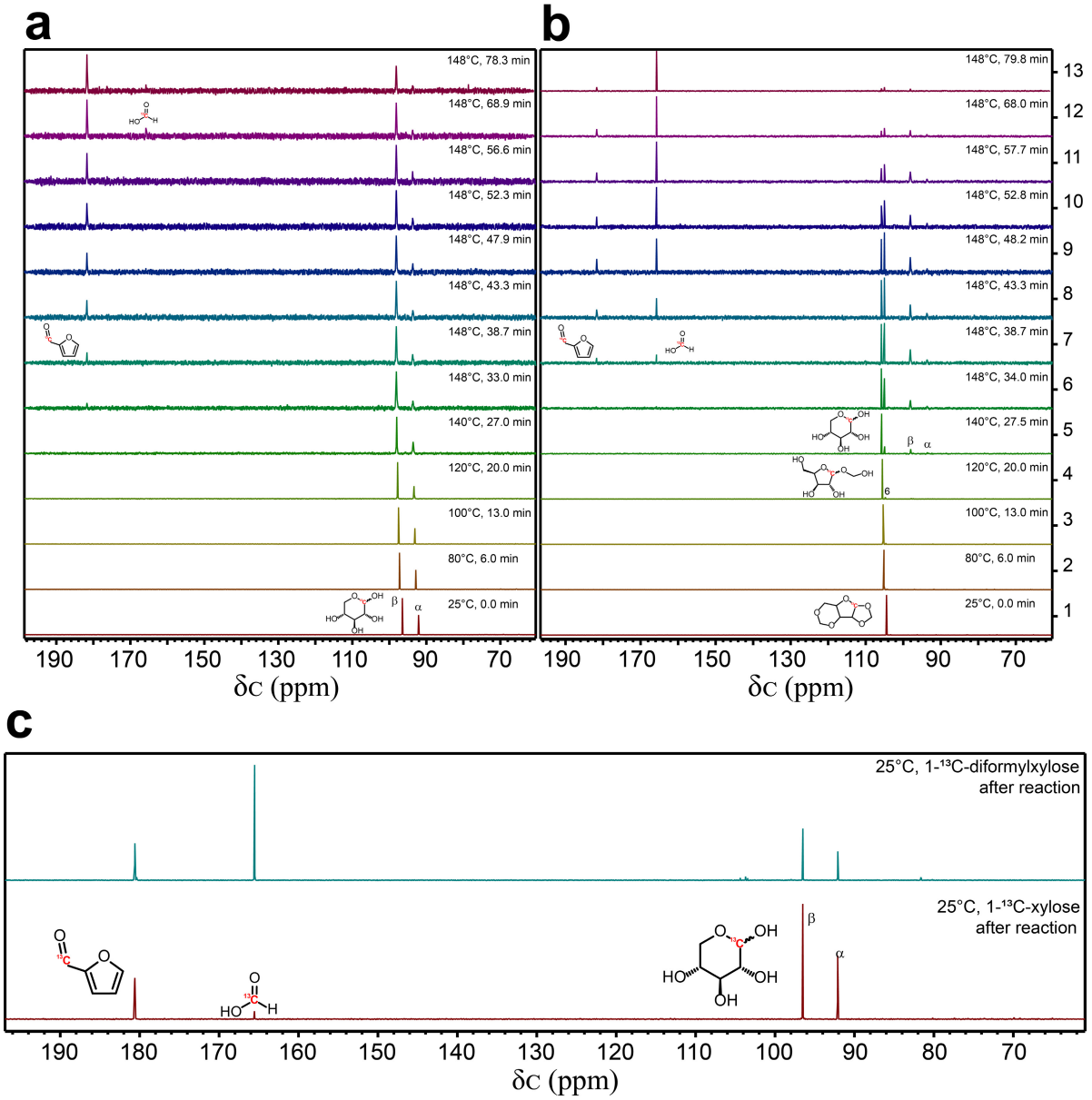

Figure 5.6 | *Operando* NMR of pentose dehydration to furfural. ^{13}C NMR spectra of (a) 1-^{13}C-xylose and (b) 1-^{13}C-diformylxylose dehydration in 150mM D_2SO_4 D_2O from 25°C to 148°C over time. (c) ^{13}C NMR spectra at 25°C after reaction.

In contrast to the experiment with 1-^{13}C-xylose, the formation of 1-^{13}C-furfural and ^{13}C-formic acid was noticed simultaneously after 38.7 min of heating (the sample was already at 148°C), at 181.72 ppm and 165.76 ppm, respectively (Figure 5.6 b spectrum 7). The relative amount of ^{13}C-formic acid formed was significantly higher compared to that obtained in the 1-^{13}C-xylose experiments, which was likely due to a higher production of furfural. As discussed in literature, the degradation rate of furfural does not only depend on the acid concentration and temperature,

but also on furfural concentration.[202] The absence of a signal at ca. 150.12 ppm (C5 of furfural in D_2O) suggested that the mechanism in which DX hydrolyzes and subsequently dehydrates to furfural, must undergo ring-opening. As the reaction progressed, no additional intermediate was detected. After reaction completion, an extra ^{13}C NMR spectrum was taken at 25°C to confirm the chemical shifts of all these species (Figure 5.6 c).

5.3 Conclusions

The use of diformylxylose as a reactant led to the formation of furfural in high yields at 160°C without the presence of Lewis acid as a co-catalyst. The partial deprotection of DX lead to the formation of an intermediate capable of performing the same isomerization that a Lewis acid catalyzes. This intermediate was not seen in experiments conducted with unmodified xylose. Moreover, the addition of Lewis acid, did not affected the reaction rate. Based on this observation a new reaction mechanism was proposed. This difference in reactivity demonstrates the potential of acetal-functionalized sugars to expand the number of upgrading routes available to biomass-derived carbohydrates.

Chapter 6. Preliminary techno-economic analysis for the production of ethanol from acetal-stabilized carbohydrates

This chapter is part of a published article in *Nature Chemistry* as **Questell-Santiago, Y.M.,** Zambrano-Varela, R., Talebi Amiri, M. and Luterbacher, J.S. Carbohydrates stabilization extends the limits of chemical polysaccharides depolymerization, *Nature Chem.* **2018**, 10, 1222-1228. Part of the manuscript and supplementary information are reproduced here with a few formatting changes with permission from Springer Nature.

The aim of this chapter was to evaluate the process economics of the non-enzymatic bio-ethanol production from acetal-stabilized sugars. This was done by performing a preliminary techno-economic analysis using a previously reported sensitivity analysis, experimental data and Aspen simulations. Finally, I discuss the production of high-quality lignin and important process consideration including the potential reactivity and toxicity issues linked to large-scale formaldehyde use.

6.1 Analysis approach

We performed a preliminary techno-economic analysis (TEA) based on a previously reported TEA of non-enzymatic ethanol production using GVL (our control scenario)[168]. A previously published sensitivity analysis[168] had already explored the effect of reducing solvent usage when using GVL-water mixtures (Figure 6.1 a). Therefore, we were able to use this analysis directly to calculate the effect of solvent reduction (leading to a price of $/gal of gasoline equivalent (GGE), 2014$ compared to $4.33 per GGE, 2014$, for the original solvent levels). Solvent reduction is the principle processing benefit brought on by using FA during cellulose depolymerization. We then qualitatively analyzed the effect of the two additional steps for FA recovery (hydrolysis and distillation), required by our process prior to the fermentation step. To do

so, we modelled the hydrolysis step and a simple distillation of a simplified water-FA mixture to represent FA recovery (highlighted in red Figure 6.2).

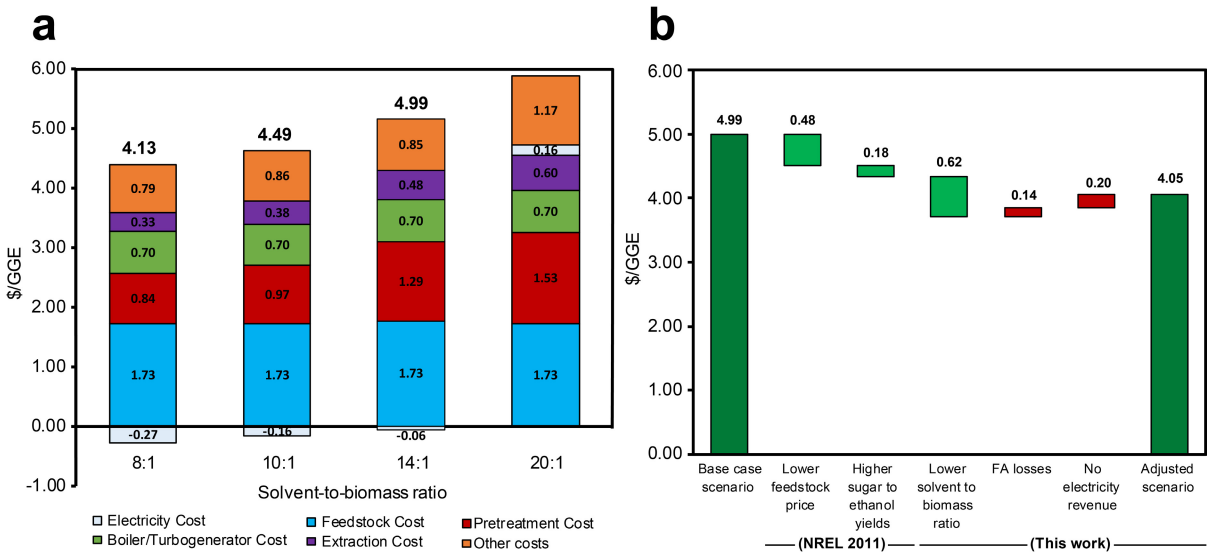

Figure 6.1 | Impact of solvent to biomass ratio on the minimum ethanol selling price (MSP). (a) Impact of solvent-to-biomass ratio on the MSP of ethanol (Modified from Han et. al.[168]). (b) Impact of adjusting key economic/process parameters to those of NREL (2011)[205] and this work (Modified from Han et. al)[168].

Despite FA's near-quantitative regeneration, its large-scale use will likely involve several challenges. Notably, several FA recovery steps would need to be implemented in a hypothetical process. The preliminary economic calculations here presented, show that FA use could be worthwhile despite additional recovery steps in the context of diminishing solvent-use in a GVL-based process for the non-enzymatic ethanol production (our control scenario). These additional steps also lead to costs within the range of those predicted for enzyme-based processes.[205] FA has been previously used in large-scale cellulose processing for increasing the stretch-ability of viscose fibers,[206,207] further demonstrating that its large-scale use is feasible. However, these past processes had to deal with the formation of insoluble FA side products in their spinning bath. Such possible side reactions, as well as regulatory and FA toxicity for subsequent biological sugar processing, are all aspects that remain unexplored and that will have to be addressed if FA is to be used in a biorefinery.

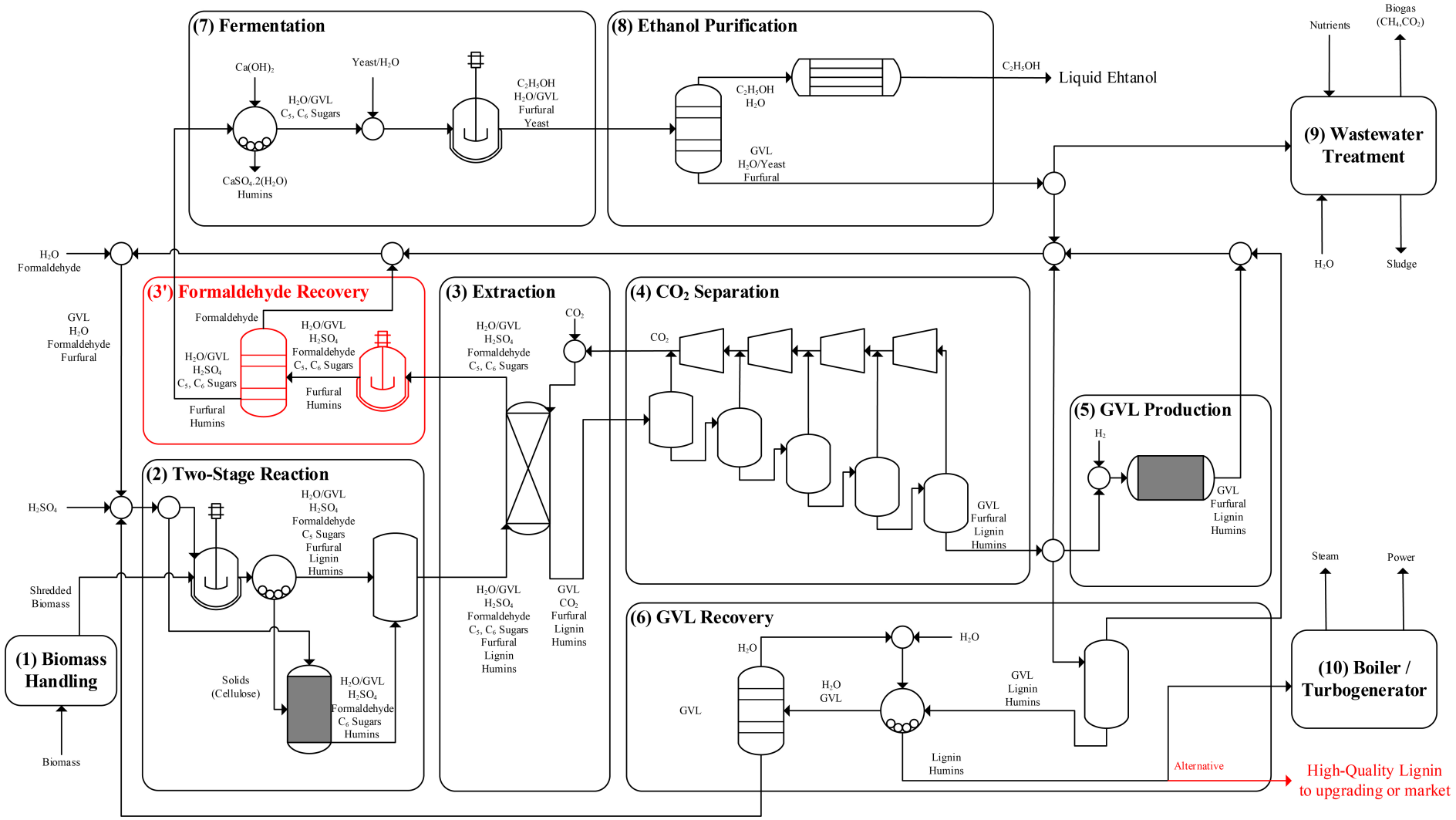

Figure 6.2 | Overall process flow diagram. Main modification to the base case scenario are highlighted in red; formaldehyde recovery section and the production of high-quality lignin. Note that the latter (production of high-quality lignin) was not included in our economic calculations.

The additional equipment was estimated to represent an increase of 1% compared to the original capital investment and was therefore considered negligible (Table 6.1). The additional energy requirement increased the original value by 28% (prior to heat integration). Heat integration reduced the energy requirement in our control scenario[168] by 77%. We expect a similar decrease for our additional heat requirement and thus assume that our heating needs will be increased by a third. Since more than 50% of the heat produced by the control process was a surplus and used for additional electricity production, we could reasonably estimate the economic effects of increased heat demand by eliminating any revenue that was obtained from the sale of surplus power (corresponding to $0.20 of revenue per GGE). We also account for a loss of 3% of FA per recycle based on the FA recovery after hydrolysis and distillation column (corresponding to a cost of $0.14 per GGE).

All these additional costs bring us to a minimum selling price (MSP) of ethanol of $4.05 per GGE (Figure 6.1 b), which is below that for a solvent-based process without FA use ($4.33 GGE, 2014$)[168] and within the range reported for enzyme processes by NREL in 2016 ($4.42 to $3.71 GGE (in 2014$) depending on process technology and process maturity assumptions)[205]. Moreover, the utilization of FA does not only enhances the conversion of carbohydrate but also leads to a much more upgradable lignin, which creates the possibility of generating a significant cash flow through the production of high-value lignin monomer (not included in the current analysis).[190]

6.2 Solvent to biomass ratio calculations

The following discussion refers to the process depicted in Figure 6.3. The overall solvent to biomass ratio used on the base case scenario is 14:1. (69.2 ton/h of biomass requires 968.8 ton/h of solvent). In the pretreatment reactor (R-1), we have:

Biomass = 69.2 ton/hr, Incoming solvent stream = 277 ton/h ⇨ Ratio = 4:1

In the cellulose depolymerization reactor (R-2), we have:

Solids = 34.6 ton/hr, Incoming solvent stream = 692 ton/h ⇨ Ratio = 20:1

The work in the current study will reduce the solvent ratio (incoming solvent) in R-2. Based on a solvent to solids ratio of 11 in the cellulose depolymerization reactor (R2), we have:

Stream 2^{bp} = Solids * Ratio = 34.6 * 11 = 380.6 ton/hr Equation 6.1

Overall solvent Ratio = (Incoming solvent in R1 + Incoming solvent in R2) / Biomass = (277 + 381) / 69.2 = 9.5 Equation 6.2

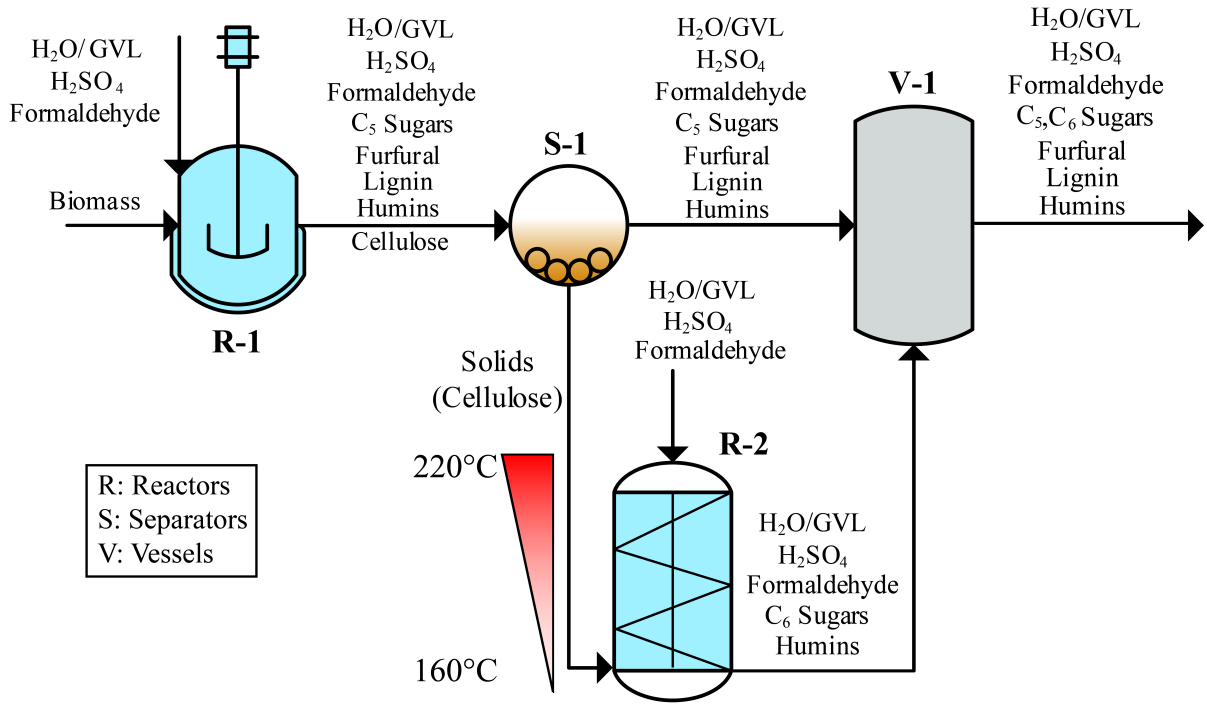

Figure 6.3 | Two-step biomass pretreatment process. Modified from Han et al.[168].

6.3 Correlation of ethanol price with solvent to biomass ratio

The following calculations are based on the data in S Fig. 20-a. We first performed a simple linear correlation between the product price (MSP) and solvent to solids ratio, which, based on the available data range was assumed to be reasonably accurate:

Product Price = 0.14 Ratio + 3 Equation 6.3

We then used this correlation to calculate our adjusted price based on our solvent to solids ratio:

Adjusted product price (APP) = 0.144 * 9.5 + 3.0024 = 4.37 $/GGE Equation 6.4

Contribution of lower solvent-to-biomass usage in the MSP = $APP - MSP_{14:1}$ Equation 6.5

$= 4.37 - 4.99$

= - 0.62 $/GGE

APP based on mass (PP) = $APP * \left(\frac{\$}{GGE}\right) * \frac{\text{Gasoline GGE}}{\text{Ethanol GGE}} * \frac{1}{3.78541}\left(\frac{\text{Gallon}}{\text{Liter}}\right) * \frac{1}{\text{Ethanol density}}\left(\frac{\text{Liter}}{kg}\right)$

Equation 6.6

$= 4.37 * \frac{1}{1.5} * \frac{1}{3.78541} * \frac{1}{0.789}$

$= 0.98$ $/kg

The total income required to cover the adjusted product price, can be calculated as:

Product flow (PF) = 18 ton/h = 18’000 kg/hr

Income (I) = PF * PP = 18’000 * 0.975 = 17’557 $/hr Equation 6.7

6.4 Final product price due to formaldehyde losses:

We used the following calculations to calculate the expense of unrecovered formaldehyde:

Required formaldehyde (FF) = (Incoming solvent in R1) * 4% + (Incoming solvent in R2) * 7%

Equation 6.8

$$= 276.8 * 4\% + 380.6 * 7\%$$

$$= 37.714 \text{ ton/h}$$

$$= 37'714 \text{ kg/h}$$

Formaldehyde recovery (FR) = 97% [Table 3.5 and distillation efficiency]

Formaldehyde Price (FP)^2 = 0.5 $/kg

Formaldehyde Expense (FE) = FF * (1-FR) * FP Equation 6.9

$$= 37'714 * (1-0.97) * 0.5 = 566 \text{ \$/h}$$

This lead to the following adjustment to cover the additional income required to cover FA losses:

Adjusted income (AI) = (I) + (FE) = 17'557.2 + 565.71 = 18'122.91 $/h Equation 6.10

The minimum selling price with 3% FA losses becomes:

$$MSP_{3\%FA} = (\text{AI}) \left(\frac{\$}{\text{hr}}\right) * \frac{1}{\text{PF}} \left(\frac{\text{hr}}{\text{kg}}\right) * \text{Ethanol density} \left(\frac{\text{kg}}{\text{Liter}}\right) * 3.79 \left(\frac{\text{Liter}}{\text{Gallon}}\right) * \frac{\text{Ethanol GGE}}{\text{Gasoline GGE}}$$

Equation 6.11

$$= 18'123 * \frac{1}{18'000} * 0.789 * 3.79 * \frac{1.5}{1}$$

$$= 4.51 \text{ \$/GGE}$$

Contribution of 3% FA losses in MSP of ethanol = $MSP_{3\%FA}$ – APP Equation 6.12

= 4.51 – 4.37

= 0.14 $/GGE

6.5 Further considerations

6.5.1 Formaldehyde recovery unit.

As mentioned before, a FA recovery section is required with respect to the base case scenario. The FA recovery section consists of a hydrolysis step (for de-protection of stabilized carbohydrates) and a distillation column to separate FA from the aqueous solution. The stream to the hydrolysis reactor is heated up to 120ºC with a residence time of 1 hr. After the hydrolysis, the product mixture is sent to the distillation column. For simplicity at this stage, we modelled the incoming stream as a clean FA-water mixture. The distillation column had 13 trays with a Murphree efficiency of 75%, a total condenser and a kettle reboiler. This distillation column was modelled in Aspen Plus V8.6. There was a 2% formaldehyde loss during the hydrolysis step (based on the experimental results) and 99.4% of FA in solution was recovered after distillation (based on this simulation). Therefore, the total FA recovery (FR) was calculated to be 97%.

6.5.2 Additional equipment cost

The additional direct equipment cost of distillation column and heat exchanger was calculated with the Economics analysis package of Aspen Plus V8.6. A summary of all additional equipment cost is presented in Table 6.1. The cost of the reactor is approximately 374’400 $ per 30 m^3 reactor. The number of reactors needed in this unit was calculated as follow:

Volumetric flow of feed (VF) = 313 $\frac{m^3}{hr}$

Residence time (RT) = 1 hr

Reactor volume (RV) = 30 m^3

Number of reactors = VF * RT * $\frac{1}{RV}$ = 313 $\left(\frac{m^3}{hr}\right)$ * 1 (hr) * $\frac{1}{30}$ $\left(\frac{1}{m^3}\right)$ = 10.4 Equation 6.13

= 11

The base case scenario reported a total project cost of $517.2 million. By adding a FA recovery section, this becomes $522.4 million. This represents an increase of 1% in the initial total project cost. This cost was considered negligible for calculating the ethanol final price (changes in the operating cost are discussed in the next section, 6.5.3).

Table 6.1 | Direct equipment cost of the formaldehyde recovery unit

Equipment	*Direct Equipment cost / unit ($)*	*Number of units*	*Direct Equipment cost ($)*
Heat exchanger	183'000	1	183'000
Reactor	374'400	11	4'118'400
Distillation column	908'400	1	908'400
Total			5'209'800

6.5.3 Additional utilities required for formaldehyde recovery.

The base case scenario has an energy requirement of 242.3 MW for the hot utility and 195.0 MW for the cold utility before heat integration. The FA recovery section requires 50.4 MW for the hot utility and 17.1 MW for the cold utility before integration (Table 6.2). This represents an increase of 20% and 8.8% to the hot and cold utilities, respectively. However, these numbers were calculated prior to heat integration and might drop dramatically as reported for the base case scenario, where heat integration led to a 77% drop in heating requirements.[168] We estimated, without accounting for the FA recovery section, that the total energy requirements of our process after heat integration should be around 68.2 MW (23% less than the base case scenario, 88.3 MW). This decrease leads to a heat surplus of 20.1 MW, which should be largely

sufficient to cover the heating requirements of the FA recovery section after heat integration. However, covering this requirement would prevent the use of this excess heat for generating surplus electricity. Therefore, the effects of increased heat demand due to FA recovery could be estimated by simply eliminating any revenue that could be obtained from the sale of surplus electricity. The detailed estimate of the heating surplus is given below.

Total energy requirements correlation = 4.782 Ratio + 22.797 Equation 6.14

Total energy requirements = 4.782 * 9.5 + 22.797 = 68.2 MW Equation 6.15

Heat surplus = Base scenario – this process Equation 6.16

=88.3 – 68.2 = **20.1 MW**

In order to calculate this loss in electricity revenue, we again used linear correlations between the total energy requirements or electricity revenue and solvent usage based on the sensitivity analysis available in the prior work (based on data in Figure 6.1 a and Han et al.[168]):

Electricity revenue correlation = 0.034 Ratio – 0.530 Equation 6.17

Electricity revenue = 0.034 * 9.5 – 0.530 = **- 0.20 $/GGE** Equation 6.18

Table 6.2 | Required utility for the formaldehyde recovery unit

Utility	*Initial temperature (°C)*	*Final temperature (°C)*	*Duty (MW)*
Heat exchanger	25	120	30.3
Reboiler	147.3	148.3	20.2
Condenser	65.6	24.4	-17.1
Total hot utility			50.4
Total cold utility			-17.1

6.5.4 High-quality lignin production

The utilization of FA does not only impact the yield and concentration of carbohydrates, but it also leads to the production high-quality lignin (i.e. lignin that can be upgraded to monomers at near theoretical yields)[190]. In the base case scenario, 15 tons/h of this high quality lignin was separated and used for power generation. It can be considered an alternative scenario where this lignin is upgraded to monomers to generate further revenue. Given their structure, these monomers can be considered as phenol replacements and, as a result, the price of phenol was considered to be a reasonable estimate of their potential value. Based on the price of phenol (ca. 1.1$/kg) and the reported monomer yield of 45%, a potential additional revenue of 7'425 $/h could be envisioned (without considering extra processing or energy costs). This number is considerable compared to 18'478 $/h of revenue achievable for ethanol and could potentially further improve process economics. However, given all these assumptions, our initial economic calculations did not include the effects of producing a high-quality lignin as a side product.

6.6 Potential challenges and limitation of the process

At this early stage, it is difficult to foresee all the limitations and additional complexities that FA would bring to a pilot-plant scale process. However, analogies can be made with more established processes. Specifically, matters regarding GVL recovery and water treatment have already been explored in several previous studies[49,159,163,168] and shown to be economically interesting due to the fast kinetics and high value products that result from solvent use. Due to the similarities in the proposed process scheme, it is expected that the process will follow similar trends for solvent recovery. A new and critical aspect to consider in the process is the use and recovery of FA, previously discussed. Potential reactivity or toxicity issues linked to FA use, have not yet considered or included the analysis, which are difficult to foresee at this stage but analogies with existing processes can be helpful. The use of FA in large scale cellulose

processing is not unheard of or impossible as it has been used in several commercial plants by Courtauld and Enka (Germany). In these processes (that have since been abandoned), FA was used as a modifier to extend the stretchability of viscose fibers but also led to the formation of problematic insoluble FA side products in the spinning bath circuit.[206,207] The process discussed here could face similar issues as well as additional regulations linked to large scale FA use.[208] Moreover, FA could create toxicity issues if our carbohydrates are used in biological processes such as fermentation. Currently, this TEA modelled a FA recovery of 99.4%, leaving a FA concentration of 30 mM in the stream, which is likely to be toxic to yeast.[209] Several methods exist to detoxify FA contaminated stream including using sodium dithionite, which is a relatively low cost reagent (<1000$/to).[209] In summary, scale up of FA use will likely generate side reactions and toxicity issues that might negate some of the benefits that come from its stabilization effects. These issues will have to be carefully considered in more advanced implementation studies.

6.7 Conclusions

In conclusion, the calculated ethanol MSP should not be interpreted as the result of a rigorous TEA. Instead, we found that this price qualitatively indicates that considering FA use is reasonable. These calculations indicate that FA use could pay for itself in the context of a solvent-based process due to its ability to reduce solvent use during cellulose depolymerization, and leads to costs that are within the range that are expected for enzyme use indicating that further research is worthwhile.

Chapter 7. Upgrading of acetal-stabilized xylose into polyols

In this chapter, the aim is to use acetal-functionalized xylose, diformylxylose (DX), as a new platform chemical to produce xylitol. To demonstrate the potential of this molecule as an intermediate for high value chemical production, the production and purification of DX from biomass was scaled-up. The direct conversion of DX into xylitol has multiple process advantages compared to the current chemical xylitol processes that start from xylose. These advantages are linked to the properties of DX and the incorporation of protecting group chemistry during beech wood pretreatment. These advantages include: the elimination of xylose purification steps and compatibility of acetal stabilization with the valorization of the three main biomass fractions (notably through the production of high-quality lignin).

7.1 Production, separation and purification of diformylxylose

7.1.1 Pretreatment

To obtain significant quantities of purified biomass-derived diformylxylose we needed to scale up the pretreatment of beech-wood using the previously listed reaction conditions (see Table 3.1 entry 5 and Appendix A.1.1) and applying them in a 1L Parr reactor equipped with a custom impeller.[210] The custom impeller facilitated the stirring of biomass at a high solid loading while allowing us to use a bigger particle size (<0.45 mm). The reaction time was decreased by 15 min (total time 1 h 45 min instead of 2 h) to compensate for the longer heating and cooling time of the large volume. These modifications actually led to an increase in DX yield and concentration (96% yield at 3.5 wt%, Table 7.1). Cellulose was separated from the liquor by filtration and washed first with GVL and then, water. More details concerning these steps in Appendix A.1.1 and A.1.2.

7.1.2 Recovery of high-quality lignin

Because the use of FA produces high-quality lignin (which can be depolymerized to monomers at high yield),[190] its recovery should be considered. To do so, one part liquor was slowly added to three parts of water while stirring to precipitate the stabilized lignin. The lignin was then separated by filtration, washed with water and dried at 45°C under reduce vacuum. Importantly, the liquor was added dropwise (not *vice versa*) using vigorous stirring to prevent the condensation of lignin or agglomeration of DX with the precipitates. The neutralization of the liquor prior to the dilution did not improve lignin precipitation. This facilitates the recovery of sulfuric acid. The hydrogenolysis of the precipitated lignin let to 30% monomer yield (72% compared to the direct hydrogenolysis of raw biomass, reaction details in Appendix A.1.10). Interestingly, the monomer product distribution showed 58% selectivity towards propylsyringol.

Table 7.1. Product distribution after the pretreatment of beech wood in a 1L reactor.

Fraction of biomass	*Xylan/ Glucan*	*Xylose/ Glucose*	*Diformylxylose/Diformylglucose*	*Gluc-oligomers*	*Furfural/ 5-HMF*	*Extraction/Monomer yield [% / %]*
Lignin						72 / 30
Hemicellulose	9	2	82	--	7	
Cellulose	93	0	0	6	1	

7.1.3 Recovery of GVL and purification of DX

Once the lignin was removed, GVL and DX were extracted from water using liquid CO_2 (pressurized CO_2). The extraction unit was previously constructed for GVL recovery and is detailed elsewhere.[163] The extraction was performed by adding a volume of solution that corresponded to 2/3 of the total volume of the extraction vessel. Then, the system was pressurized at 75 bar of CO_2 and left to stabilize overnight. The liquid CO_2 was then added at a rate of 15 mL/min from the bottom of the vessel. The pressure was kept constant using a back pressure regulator at the top end of the extraction vessel. The CO_2-rich phase was collected and depressurized in

a second vessel. The flow of liquid CO_2 was stopped when no liquid was collected after de-pressurizing the extracted CO_2-rich phase. Up to 98% and 99% of the original GVL and DX were recovered, respectively. The resulting extracted solution contained 92 wt% GVL and 4 wt% DX. A simplified overall process diagram is shown in Figure 7.1.

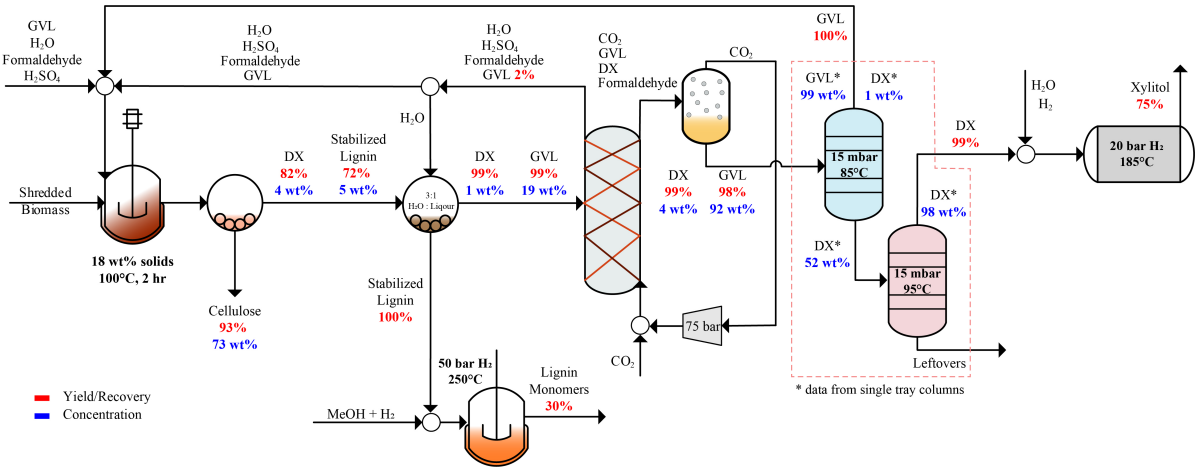

Figure 7.1 | Process diagram of xylitol production from beech wood by the upgrading of diformylxylose.

The separation of DX from GVL can be done by DX extraction with hexanes. However, due to the preferable miscibility of DX with GVL, this approach requires very large quantities of hexanes. Instead, we propose to use distillation due to the volatility of both components. GVL distills first, followed by DX. The distillation was done using two temperature steps, 230°C and 250°C. After distillation, >99% of GVL was recovered. Because most of the sulfuric acid was left in the aqueous phase after the CO_2 extraction, DX only was degraded by 9% after being at 250°C for 8 hr. A more efficient industrial set up (as opposed to lab scale distillation) could probably significantly reduce this degradation by reducing the residence time at high temperature in a continuous distillation. However, to limit degradation, the distillation could also be carried out under reduced pressure (15 mbar). This pressure was chosen based on commonly used conditions in oil refining vacuum distillation.[211] In this case, 99% of DX was recovered using a two-step (80°C and 95°C) distillation process (Figure 7.1). The distillate from the first step had a DX concentration of 1 wt%, which was then redistilled to mimick a multi-stage

column. The bottoms were combined and sent to the second step where DX was recovered with a purity of 98%.

7.2 Reaction network of the tandem hydrolysis-hydrogenation of diformylxylose to xylitol

The hydrogenation of xylose requires a hydrogen pressure around 20 to 50 bar to enhance the dissociation of hydrogen on the catalyst (redox-active metals) surface and avoid the scarcity of hydrogen on the catalyst surface.[53] The surface reaction between absorbed atomic hydrogen and the absorbed xylose, is the rate limiting step. However, at temperature above 100°C, xylose is not absorbed but reacts directly with the adsorbed hydrogen on the surface through an Eley-Rideal mechanism.[212] Technically, the hydrogenation of xylose could be done at temperature slightly above 100°C to eliminate the adsorption competition between xylose and hydrogen. In our case, the conversion of DX to xylitol was carried out at 185-200°C to ensure that the water had the required amount of protons to remove the acetal functionalities of DX.

The most common metals used for xylose hydrogenation are ruthenium (Ru), rhodium, nickel (Ni) and palladium. A limited amount of work has been done with platinum (Pt), but in 2013, it was found that Pt on carbon has a higher activity for the hydrogenation of xylose compared to Ru on carbon and Raney Nickel.[213] Therefore, we decided to use Pt on carbon (Pt/C) as our catalyst. The catalyst preparation and characterization are detailed in Appendix A.1.12 and A.1.13. After preparation, the catalyst had a Brunauer–Emmett–Teller (BET) surface area of 1002 m^2/g, a total metal loading 2.6 wt% and a metal dispersion of 35% (Table A.3).

Catalytic tests were done using DX synthesized and purified from pure xylose following the detailed procedure in Chapter 4. The reaction was performed using a flow reactor at 185°C with a catalyst bed of 0.50 grams of Pt/C and a hydrogen pressure of 20 bar at a flow rate of

50 mL/min. At a weight hour space velocity (WHSV) of 0.38 h^{-1}, DX reached a stable conversion of 89% after an induction period of 20 h (Figure 7.2).

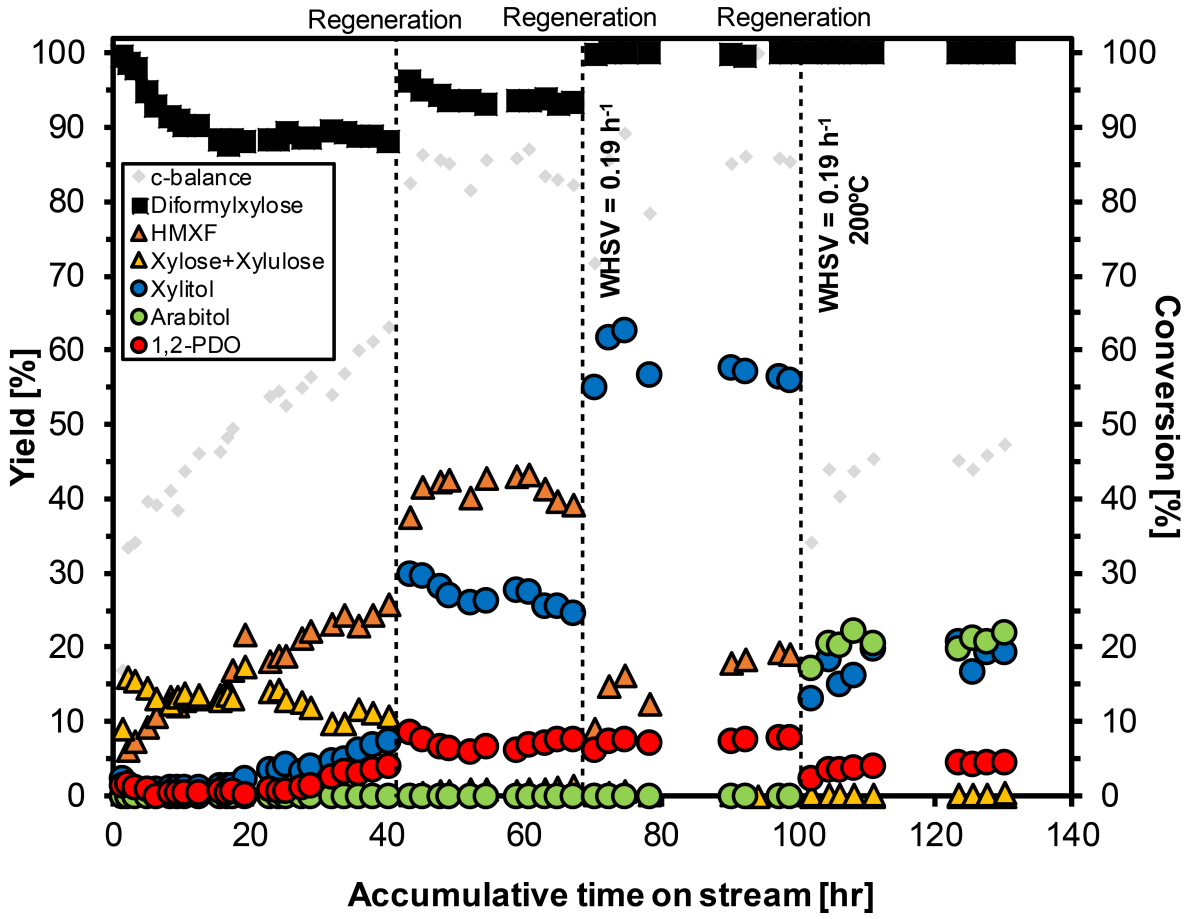

Figure 7.2 | Upgrading of diformylxylose by tandem hydrolysis-hydrogenation over Pt/C in the presence of hydrogen. (WHSV = 0.38 h^{-1}, H_2 flow = 50 mL/min, P_{H2} = 20 bar, T = 185˚C and feed = 2 wt% of DX in water). WHSV was calculated based on diformylxylose mass flow and the total catalyst weight).

The main identified intermediates were xylose and xylulose with a mole ratio of 0.82 xylose/xylulose. HMXF was also detected (characterization in Figure 4.8). Although it appeared to be the main intermediate after the 20h induction time, the quantification was not necessarily precise as the HMXF concentration was estimated assuming the same response factor as DX. Therefore, in the case of HMXF, we could only conclude that its formation was increasing over time. In general, the hydrolysis of DX appeared to occur rapidly compared to the hydrolysis of HMXF and hydrogenation of xylose and xylulose. Based on these observations and the detection of other compounds such as 2-methylfuran (2-MF), 2-methyltetrahydrofuran (2-MTHF),

pentane and others in trace quantities, we proposed a reaction network of the conversion of DX to polyols (Figure 7.3).

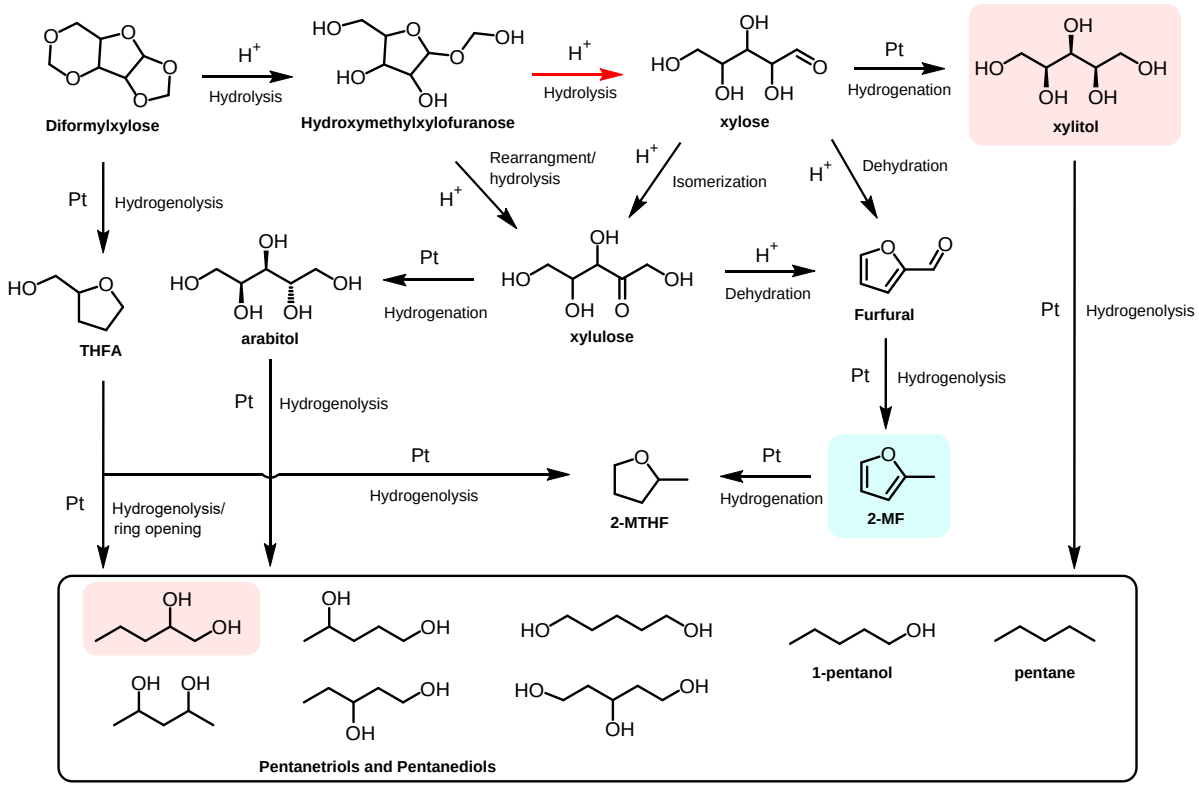

Figure 7.3 | Proposed reaction network for the conversion of diformylxylose to xylitol in an aqueous media. The compounds were identified in either the liquid or gas phase. The main products found in the aqueous phase are highlighted in pink. The main product found in the gas phase is highlighted in light green. Neither CO nor CO_2 were detected in the GC using a TCD. The red arrow highlights the suggested rate limiting step. For simplicity, several intermediate steps are omitted (example: the equilibrium between the open chain and pyranose form of xylose). THFA stands for tetrahydrofurfuryl alcohol.

Although the carbon balance increased overtime suggesting a decrease in coke formation, the main products were non-hydrogenated molecules. This could be due to the blockage of Pt active sites by coke deposition. After 40 h on stream, the catalyst was regenerated by reduction under H_2 (details in Appendix A.1.11). Interestingly, after regeneration, we observed an increase in HMXF, hydrogenation products and DX conversion (Figure 7.2). Xylose and xylulose were fully consumed, which led us to conclude that, in this reaction system, the rate limiting step is the hydrolysis of HMXF and not the hydrogenation of pentoses. Therefore, after a second regeneration, the WHSV was decreased to 0.19 h^{-1} in order to increase the retention

time of intermediates (in this case principally HMXF). This led to a maximum yield of xylitol of 61% (an increase of 2-fold) and a decrease in HMXF of 25%. Although HMXF yields should be interpreted qualitatively, its percentage decrease was independent of the quantification assumptions that were made and could be used for result interpretation.

The reaction was also carried out at a higher temperature in order to increase the equilibrium concentration of protons in the water and thus, increase the hydrolysis of HMXF. At 200°C, there was no HMXF (Figure 7.2). However, the increase in temperature could also promote the reversible isomerization of xylose to xylulose leading to the formation of arabitol. Alternatively, the ring opening of HMXF detailed in Figure 5.2 can also form xylulose. In any of these cases, the selectivity of the process decreases, which is what we observed.

7.3 Changes in the catalyst active sites

In order to understand the phenomenon that led to a boost in the hydrogenation products after the catalyst regeneration, we studied the product distribution at the conditions with the highest xylitol yields (185°C, 0.19 h^{-1}, 20 bar H_2). The study was carried out over a fresh catalyst bed reduced *in situ*, i.e. after two thermal treatments. The highest hydrogenation activity of pentoses was observed after a forth catalyst reduction (Figure 7.4): the first reduction was after catalyst preparation (followed by passivation), the second reduction was performed *in situ* prior to the reaction, and the third reduction and forth were performed during regenerations. At the beginning of the reaction, the reaction was at full conversion and only negligible amounts of pentoses were detected. For over 20 h of reaction the main product was 1,2-PDO which then was slowly overtaken by xylitol. This suggested that during the induction period, the hydrogenolysis of DX was more favorable than hydrolysis. Arabitol was detected at about 5% yield, implying that there was limited formation of xylulose.

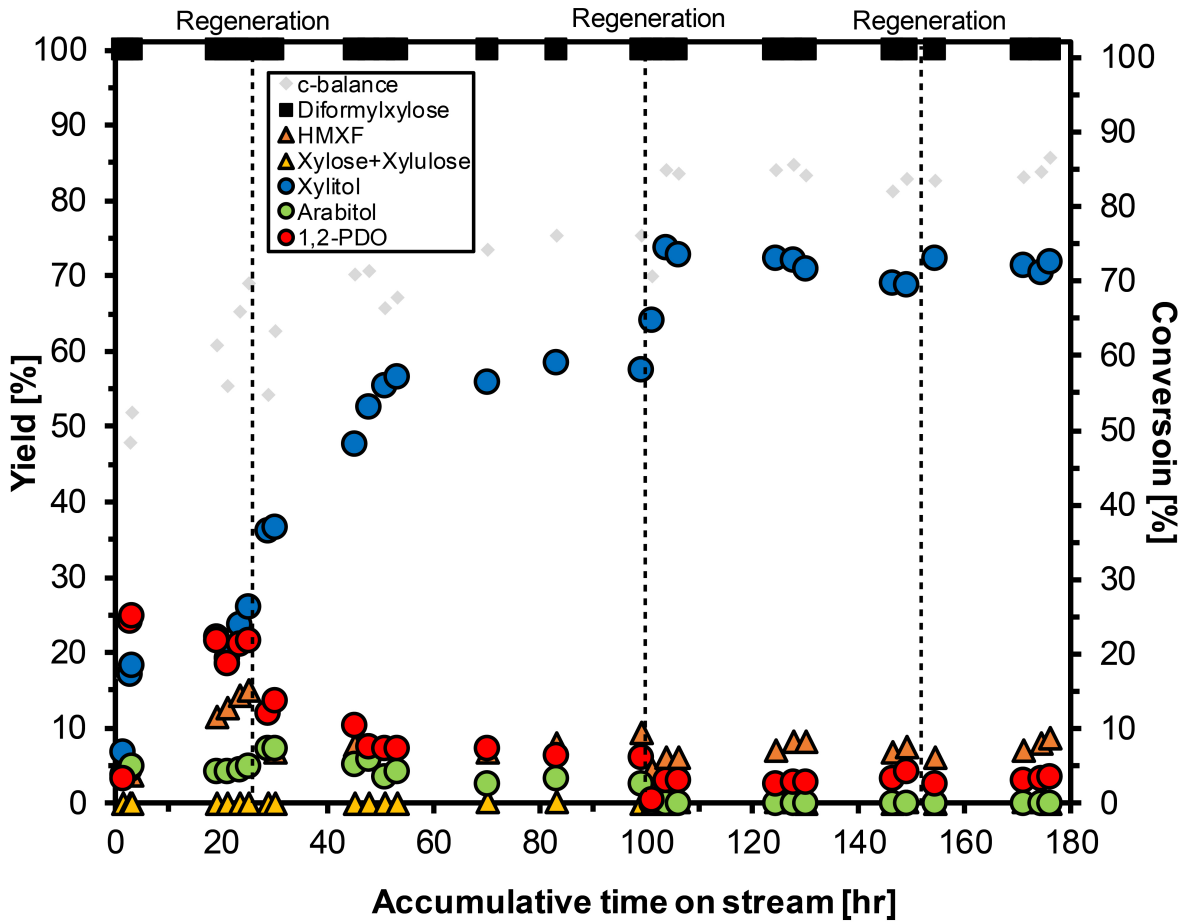

Figure 7.4 | Changes in the catalyst activity after multiple regeneration of the catalyst bed at 20 bar of H_2. (WHSV = 0.19 h^{-1}, H_2 flow = 50 mL/min, T = 185°C and feed = 2 wt% of DX in water). WHSV was calculated based on diformylxylose mass flow and the total catalyst weight).

After the first regeneration, the yield of xylitol increased rapidly for over 25 h and stabilized at 60% yield for about 50 h. As the yield of xylitol increased, the formation of 1,2-PDO decreased, suggesting that the changes in catalytic activity favored the tandem hydrolysis-hydrogenation of DX instead of the hydrogenolysis of DX or the over hydrogenation of xylitol. A second regeneration led to a further xylitol yield increase of 15%. The catalyst was reasonably stable for 50 h with only a small decrease in xylitol yield of 5%. A third regeneration was done, but no significant change in yield was observed. The yield of xylitol was maintained around 72% and remained stable for 25 h.

The same study was done at 50 bar of hydrogen pressure (Figure A.1). The evolution of xylitol and 1,2-PDO was different at the beginning of the reaction. However, after the first regeneration the performance was almost identical to the run at 20 bar of H_2. The second regeneration increased xylitol yield by 10%, but the yield then rapidly decreased. This insensitivity to pressure in combination with the observation of HMXF being the main intermediate (Figure 7.2), pointed out that the rate limiting step is the hydrolysis of HMXF (highlighted in red in Figure 7.3). In addition, this provides opportunities to further lower the operational H_2 pressure but this would not guarantee that water remains liquid. Nevertheless, the effect of hydrogen content could be studied by changing the partial pressure of the gas.

In light of these observations, we hypothesized that the changes in the catalyst activity could be explained by changes in nanoparticles size (rearrangement of surface atoms), the formation of coke or changes in the oxidation state of Pt.[214–217] The changes in the catalyst dispersion were measured by comparing the dispersion prior to reaction (after reduction *in situ*) with measurements after a second regeneration (details in Appendix A.1.14). The dispersion decreased by 6% (32% vs. 26%), suggesting minor changes in Pt nanoparticle size. However, it was unclear whether the crystal structure of Pt evolved with these thermal treatments.[215]

Alternatively, coke formation could induce changes in catalytic effects by covering certain nefarious active sites. To investigate this, a fresh catalyst was reduced *in situ* for 9 h prior to reaction (originally 3 h). This long reduction was done to mimic the four thermal treatments that were done prior to the point when the highest yield of xylitol (74%) was obtained but without the influence of coke deposition. However, these thermal treatments by themselves did not appear to be responsible for the increase in the catalyst activity. In fact, the catalyst was less active and selective compared to the catalyst bed reduced for only 3 h. For over 30 h, the

yield of xylitol was less than 6% while the 1,2-PDO yield slightly increased to 13% and then decreased to 6% (Figure 7.5).

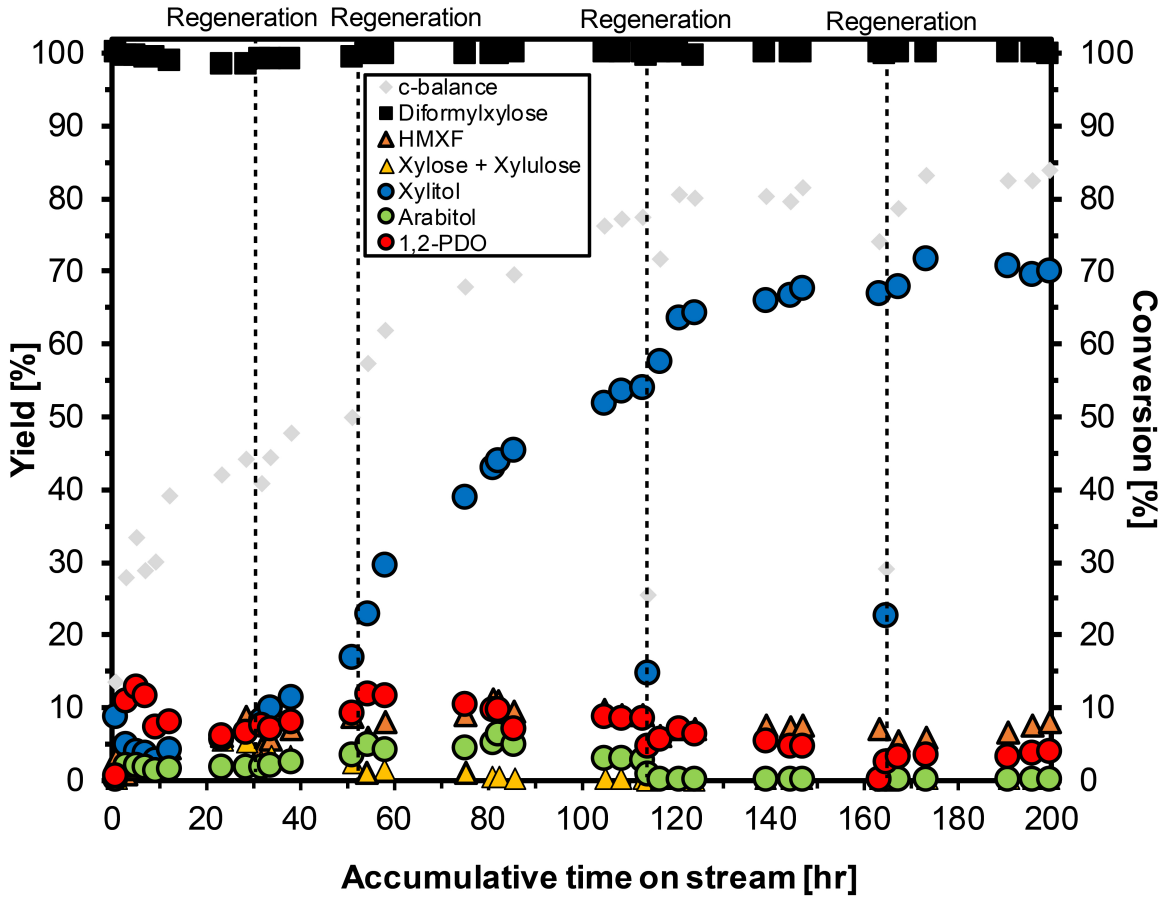

Figure 7.5 | Upgrading of diformylxylose over a catalyst bed reduced *in situ* for 9 h. (WHSV = 0.19 h^{-1}, H_2 flow = 50 mL/min, P_{H2} = 20 bar, T = 185°C and feed = 2 wt% of DX in water). WHSV was calculated based on diformylxylose and the total catalyst weight).

The gas phase data showed a maximum yield of 9% of 2-MF and trace quantities of 2-MTHF. No other compounds were detected. Further regenerations led to similar changes in the catalyst activity with a delay of about 30 h featuring the same phenomenon as in Figure 7.4. This led us to conclude that the changes in active sites are somehow linked to the formation of coke on the support or Pt nanoparticles.

In order to address these interrogatives, the spent catalyst from Figure 7.4 was characterized and showed a BET surface area and metal dispersion of 377 m^2/g and 6%, respectively (Table

A.3). The decrease in BET surface area, pore volume, pore area and dispersion (without significant changes in particles size, Figure A.2) reconfirmed coke deposition. The formation of coke has been known to change the activity of catalyst by chemically or physically adsorbing as monolayer or multilayer on metal surface sites, encapsulating metal particles and plug micro- and mesopores, which can block the access of actives sites within these pores and reduce total surface area.[218] For these reasons, coke formation generally leads to catalyst deactivation by blocking active sites. In our system, it seems that apart from this, another phenomenon is taking place. X-ray powder diffraction (XRD) of a fresh catalyst and the spent catalyst did not show significant differences in their crystalline structure nor mean crystallite size (Figure A.3). On the other hand, X-ray photoelectron spectroscopy (XPS) revealed a substantial amount of $Pt(OH)_2$ in the spent catalyst compared to the fresh catalyst (Figure 7.6). Both catalysts were analyzed without being exposed to air after being reduced under H_2 flow at 300°C.

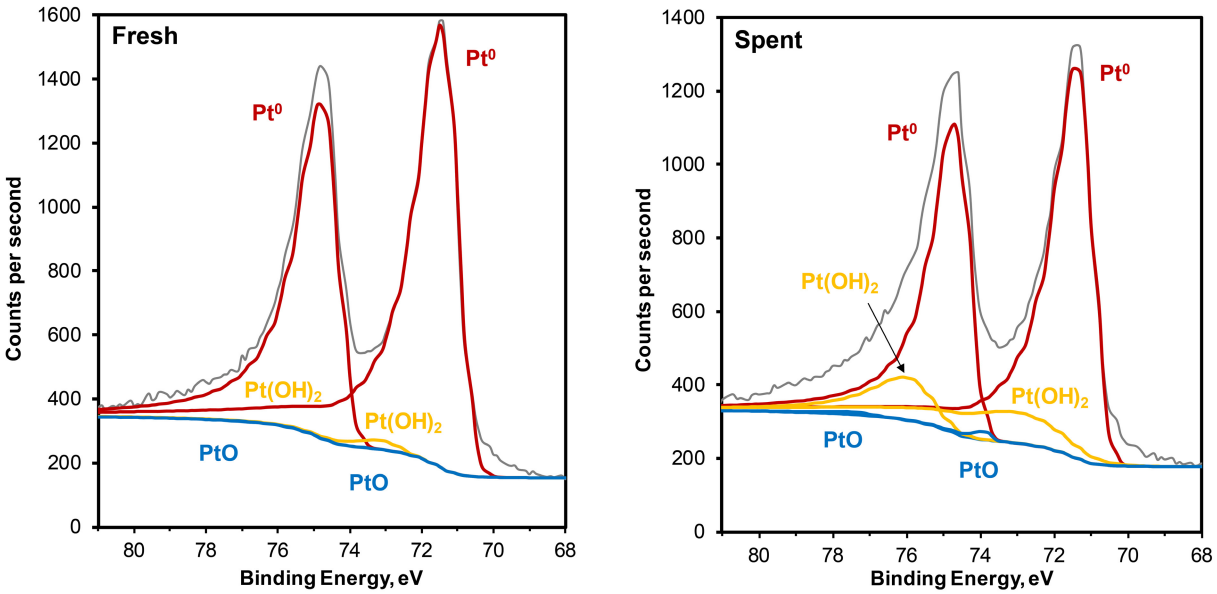

Figure 7.6 | X-ray photoelectron spectroscopy (XPS) of the fresh and spent catalyst. (The spent catalyst was used at WHSV = 0.19 h^{-1}, 20 bar H_2 and 185°C for 180 h (time on stream), Figure 7.4.) The deconvolution was performed in CasaXPS v.2.3.19PR1.0. using asymmetric line shape defined by LA (1,50,70) and the peak position with a constrained doublet separation of 3.33eV. More details in Table A.4.

This analysis suggested that $Pt(OH)_2$ is the active site responsible for the increases in xylitol yield. Given that HMXF is the main intermediate and no pentoses were detected, we propose that these OH groups could increase the hydrolysis of HMXF and, because this takes place near Pt atoms, the open chain of xylose could rapidly react minimizing its chance to isomerize to xylopyranose (Figure 7.7 b). Current efforts are focused on studying the formation of this Pt species and understanding its stability under H_2 at 300°C.

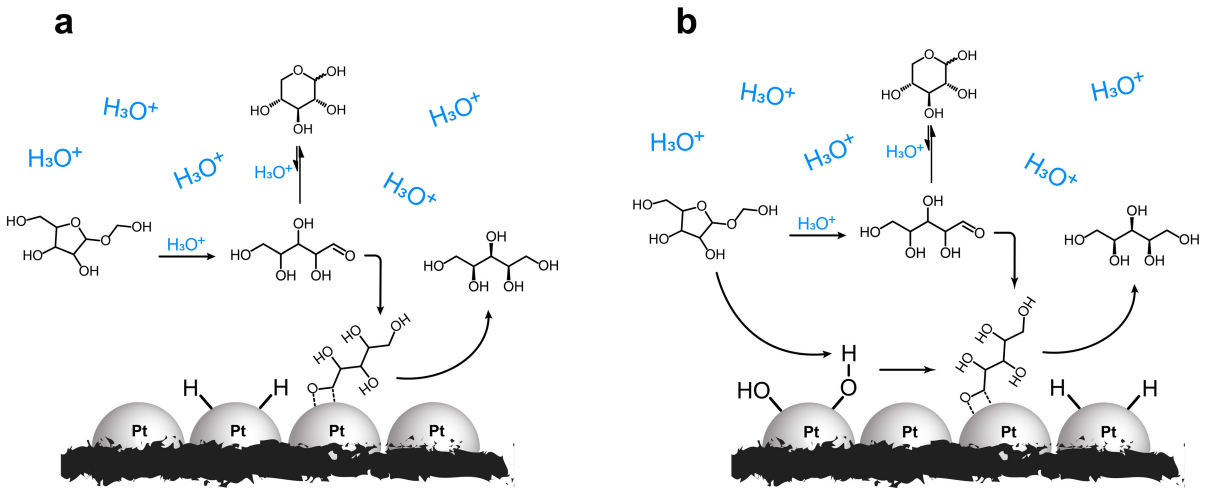

Figure 7.7 | Schematic representation of the role of $Pt(OH)_2$ in the enhanced production of xylitol from diformylxylose. Reaction pathway of HMXF to xylitol using (a) a fresh Pt/C catalyst and (b) a spent Pt/C catalyst.

7.4 Conclusions

We proposed an alternative process to produce xylitol from raw beech wood using diformylxylose as a starting material. Due to the properties of DX, it could be purified by distillation, which avoids costly processes like the use of activated carbon, ion exchange chromatography or other sophisticated purification methods. In addition, the process is compatible with the valorization of the three main lignocellulosic biomass fractions. The upgrading of DX to xylitol could be performed through a tandem hydrolysis-hydrogenation reaction where the hydrolysis of HMXF (produced by the partial deprotection of DX) seems to be the rate-limiting step. These reactions allowed us to run xylitol production at lower H_2 pressures than those that are

typically used for xylose. Finally, we found that, over the course of the reaction, the active sites of the catalyst changed, which lead to increases in catalyst activity and selectivity to xylitol. XPS studies on the spent catalyst suggested that this is due to the formation of $Pt(OH)_2$. It is believed that this Pt specie accelerates the rate-limiting step by hydrolyzing HMXF and due to its proximity to Pt^0 the open chain xylose could rapidly hydrogenate minimizing its isomerization into xylopyranose.

Chapter 8: Conclusions and Outlook

8.1 Conclusions

We showed that that the use of protection group chemistry during biomass depolymerization could stabilize carbohydrates and enable their production at conditions that were previously unfavourable due to dehydration and degradation reactions. Specifically, formaldehyde, a cheap bulk chemical that can easily be produced renewably, was used to stabilize xylose during biomass pretreatment and glucose during cellulose depolymerization in a flow-through reactor by formation of acetal groups. Because these reactions can easily be reversed under aqueous conditions, we systematically and significantly increased sugar yields compared to un-stabilized controls. Using a flow-through reactor, we were able to produce a concentrated carbohydrates solution (ca. 5 wt% before solvent separation) at a yield of 70%, which was almost 3 times the yield of the un-stabilized control and 3-4 times more concentrated than the highly optimized aqueous system. Furthermore, this stabilization strategy has the advantage of being fully compatible with lignin stabilization, which could facilitate the integrated chemical depolymerization of the three major biopolymers in biomass.

To characterize these functionalized carbohydrates, several methods were developed to synthesize, identify and purify acetal-stabilized sugars found after depolymerizing beech wood using formaldehyde as a protecting agent. By studying the reverse reaction, we found that up to 99% of the formaldehyde used for sugar protection was recovered upon deprotection by acid hydrolysis.

Moreover, diformylxylose was shown to be an advantageous platform chemical for the production of furfural due to the formation of a new intermediate that did not occur when unmodified xylose was used. This intermediate was identified during *Operando* ^{13}C NMR studies and

was shown to enable a favourable 1,2-hydride shift. In other cases, this 1,2-hydride shift requires a Lewis acid catalyst. However, we found that the reaction rate of DX to furfural was not affected by the presence of Lewis acid confirming that the structure, rather than a catalyst, induced this shift. These observations allowed us to propose a new tandem hydrolysis-dehydration mechanism for DX conversion to furfural.

The calculations of a preliminary TEA for the non-enzymatic production of bioethanol showed that the utilization of FA as protecting agent during the depolymerization of biomass polysaccharides could be worthwhile despite the additional recovery steps. The saving in solvent usage and the additional recovery steps led to an ethanol MSP of $4.05 GGE (in 2014 $). This calculation should not be interpreted as a rigorous price analysis, but instead as an indication that FA use could pay for itself due to its ability to reduce solvent use during cellulose depolymerization.

Lastly, the direct conversion of DX was investigated for the catalytic production of xylitol. Due to the volatility of DX, this molecule was purified by distillation, which can be far more economical than existing methods for xylose purification. Contrary to xylose hydrogenation where the limiting step is dependent on the amount of adsorbed hydrogen, the production of xylitol from DX was limited by the hydrolysis of HMXF. This provided an opportunity for xylitol production at reduced hydrogen pressures. Moreover, the active sites responsible for the hydrolysis-hydrogenation of DX to xylitol evolve while the reaction proceeds leading to a maximum yield of 74%. We have identified that the phenomenon that enhances the xylitol yield is due to the formation of a new active site in Pt, $Pt(OH)_2$. It was proposed that this species improves the production of xylitol by accelerating the rate limiting step and limiting the isomeri-

zation of the open chain of xylose to xylopyranose. Overall, the proposed process has the potential to improve the global yield and process economics of biomass to xylitol, but a further understanding of the active site formation could greatly facilitate process development.

8.2 Outlook

Acetal functionalized sugars are interesting molecules with versatile properties that have been shown to be beneficial when upgraded to important bio-based chemicals. However, the upgrading these molecules at an industrial scale must examine the following aspects: the formation of formaldehyde side-products at large volumes and potential toxicity to downstream microorganisms due to traces of formaldehyde. In the case of toxicity, the distillation step of formaldehyde and the detoxification of the sugar streams are key factors to investigate for the preservation of downstream microorganisms.

On the other hand, the purification of diformylxylose from raw biomass could be improved in terms of recovery and energy efficiency. This process should be studied in continuous mode to minimize the retention time of diformylxylose at the distillation temperature. A detailed TEA along with sensitivity analyses could be worthwhile to bring insight into the most critical steps of the overall production of xylitol from diformylxylose. Moreover, both of the upgrading processes proposed here produce high-quality lignin along with valuable biomass-based chemicals. This compatibility with lignin has been one of the most challenging features to achieve in lignocellulosic biomass depolymerization. Therefore, the recovery and downstream upgrading of this high-quality lignin could be profitable for the overall process.

Finally, the studied reactivity was mostly focused on formaldehyde-stabilized carbohydrates. There is a large amount of aldehydes that could assist the depolymerization of polysaccharides

as was the case when propionaldehyde was tested. The use of any aldehyde could produce other acetal-stabilized sugars with interesting properties and beneficial reactivity. As in the case of formaldehyde, the incorporation of an extra reagent into the process will require the optimization of additional recovery steps and further process aspects.

Appendix

A.1 Experimental methods

A.1.1 Biomass pretreatment

In a 60-mL glass reactor, 1.0 to 2.5 grams of air-dried beech wood particles (< 0.45-mm) were mixed with 9 mL of solvent (GVL, 1,4-dioxane, THF or EtOH), 420 µL of 37 wt.% HCl solution and 1 mL of 37 wt.% FA solution. When sulfuric acid was used, 280 µL of 95-97 wt.% sulfuric acid and 340µL of water were added instead of the HCl solution. For control experiments (without FA), 690 µL of water was added instead of 1 mL of the 37 wt.% FA solution. The reaction was conducted in a silicone oil bath set at 100°C and stirred by a stir bar at 600 rpm. After reaction, the slurry was filtered and washed with 10 mL of the same organic solvent used for the reaction and then with 50 mL of water. Both resulting solutions (liquor and water wash) were analyzed by HPLC to quantify xylan and glucan–derived products. Carbohydrate yield determination is detailed in below (A.2.2). The amount of extracted lignin was determined by subtracting the amount of Klason lignin in the filtered pretreated solids from the amount of Klason lignin in untreated wood particles.

A.1.2 Cellulose (pretreated solids) depolymerization

A schematic representation of the flow-through reactor setup is given in Figure 3.2 c. From 1.0 to 5.0 grams of pretreated solids (dry basis, but loaded as rinsed pretreated solids, dried pretreated solids or Avicel) were mixed with 8 grams of crushed silicon dioxide fused granules and placed in the heated zone of the flow-through reactor between two beds of silica granules separated by quartz wool plugs. Rinsed pretreated solids were prepared by substituting the 50 mL water wash during filtration by a wash with 10 mL of the solvent mixture to be used in the flow-through reactor per gram of pretreated solids. Dried pretreated solids were prepared by

drying the water-washed pretreated solids at 120°C in an oven overnight. The composition of pretreated solids is given in Table 3.2

The flow-through reactor was a 38 cm long stainless steel tube with a ½ inch diameter (OD), connected with the corresponding stainless steel valves and fittings. The heated zone of the reactor was fitted between two aluminum blocks placed within an insulated furnace. Two type-K thermocouples were placed at the reactor wall to monitor and control the reactor temperature using a custom made controller. The solvent mixture was flowed through the system using a piston pump (Eldex). Pressure was maintained constant at 15 bar by flowing nitrogen through the headspace of the liquid collector connected to a back-pressure regulator (Tescom). At the beginning of the reaction, the packed reactor was heated to 150°C under nitrogen flow with a 20 min ramp. The temperature was allowed to stabilize from 150°C to 160°C for 3 min. Right after, the solvent was flowed through the reactor at 2 mL/min for 5 min, then changed to 1.5 mL/min, while a 30 min linear temperature ramp was applied from 160°C to 200°C or 160°C to 220°C, depending on the experiment. The resulting flow-through liquor was sampled every 5 min by draining the liquid collector.

A.1.3 Biomass depolymerization in a single-step process (flow-through)

The treatment of raw beech wood was performed using the exact set-up used for cellulose (pretreated solids) depolymerization. The reactor was filled with the maximum amount of biomass that could fit within the heated zones of a 38 cm long ½ inch diameter stainless steel tube (7.0 grams). At the beginning of the reaction, the packed reactor was heated to 150°C under flowing nitrogen (15 bar) with a 20 min ramp. The temperature was allowed to stabilize from 150°C to 160°C for 3 min. Right after, while an 80 min linear temperature ramp was applied from 160°C to 200°C, a solvent mixture composed of 87/13 wt/wt GVL/water, 7 wt% FA and

50 mM H_2SO_4 was flowed through the reactor at 2 mL/min for the first 40 min, then changed to 1.5 mL/min with a 5 mM H_2SO_4 concentration for the final 40 min. The resulting flow-through liquor was sampled every 10 min by draining the liquid collector.

A.1.4 Aqueous phase separation using CO_2 for NMR studies

Approximately 40 g of the collected liquid from flow-through experiments using rinsed pre-treated solids and a solution of 87/13 wt./wt. GVL/water, 5 mM sulfuric acid without FA was loaded into a 60 mL vessel. The CO_2-extraction setup is given in Figure A.4, based on a design described by Luterbacher et al.[159] The vessel was made with a ½ in stainless steel tube, with corresponding valves and fittings. Once closed, the vessel was pressurized to 90 bar using a high-pressure syringe pump (Teledyne ISCO Model 260D) connected to a CO_2 siphon gas cylinder. The reactor was allowed to stabilized overnight, re-pressurized to 75 bar and let to equilibrate for 20 min. The aqueous phase was collected by opening the ball valve and then the needle valve at the bottom of the vessel until no foam was observed. If the pressure dropped below 65 bar, the system was closed, re-pressurized to 75 bar and left to equilibrate for 20 min. This procedure was repeated until no foam was observed during sampling. A second CO_2 extraction was then performed on the collected aqueous phase using the same procedure. The resultant solution was neutralized with sodium bicarbonate and dried under reduced pressure with a rotary evaporator at 60°C. The residue was diluted with DMSO-d_6, filtered with a 2µm PTFE filter and transferred to a NMR tube.

A.1.5 Diformylxylose production

In a 10 mL thick wall glass reactor, 100 mg of pure xylose was mixed with 4.5 mL of GVL or dioxane, 0.5 mL of 37 wt% FA and 210 µL of 37 wt% HCl. The reaction was conducted in a silicon oil bath at 80°C and stirred with a stir bar at 600 rpm. The reactors were removed from

the oil bath at specific times to analyzed the reaction progress using the method for carbohydrate analysis by HPLC described in Section A.2.2. One reactor was prepared for each data point in Figure 3.3.

A.1.6 Diformylxylose hydrolysis

In a 10 mL thick-wall glass reactor, 50 mg of pure diformylxylose was mixed with 4.95 g of MQ-water containing 3 wt.% to 6 wt.% of sulfuric acid. The reaction was conducted in a silicon oil bath at 100°C or 120°C and stirred with a stir bar at 600 rpm. Aliquots of 300 µL of the reaction mixture were sampled at specific times to analyze the reaction progress using the method for carbohydrate analysis by HPLC described in Section A.2.2.

A.1.7 Pentose dehydration to furfural

In a 10 mL tick-walled glass reactor, 0.12 mmol of substrate (xylose, diformylxylose or dipropylxylose), 1.5 g of 0.15 M sulfuric acid in MQ-water and 3 g of 2-SBP were reacted by placing the reactor in a silicone oil bath at 160°C and stirred at 600 rpm. For reactions with $AlCl_3$, 0.015 mol $AlCl_3$ per mol substrate was added. Reactors were cooled at specific reaction times by placing them in a water bath at room temperature. For a better phase separation, the reactor was centrifuged for 3 min at 4000 rpm by placing it inside a 50 mL centrifuge tube. The aqueous phase was collected with a glass pipe and analyzed by HPLC. The organic phase was analyzed by GC. Analysis methods are detailed in Section A.2.1 and A.2.2.

A.1.8 Preparation and purification of dipropylxylose

Approximately 15 grams of pure xylose, 31.5 mL of 37 wt.% HCl, and 71.25 mL of propionaldehyde were mixed in 675 mL of 1,4-dioxane and reacted at 80°C for 15-20 min. Then, the

solution was neutralized with sodium bicarbonate and dried under reduced pressure with a rotary evaporator set at 45°C. The residue was extracted five times with 40mL of n-hexane. All organic phases were combined and dried under reduced pressure with a rotary evaporator set at 45°C. The resultant residue was distilled at 75°C, under reduced pressure (0.02 mbar) to obtain a yellowish solid. The solid was recrystallized in n-hexane until a white solid crystal was obtained and used as the dipropylxylose standard. The solid was analyzed by ^{1}H ^{13}C HSQC NMR to confirm its structure (Figure 5.3 a).

A.1.9 Hexose dehydration to 5-HMF

In a 10 mL tick-walled glass reactor, 0.40 mmol of substrate (glucose or a mixture of diformylglucose and glucose), 1.5 g of 3mM HCl (pH 2.5) NaCl saturated MQ-water and 3 g of 2-SBP were reacted by placing the reactor in a silicone oil bath at 170°C and stirred at 600 rpm. For reactions with $AlCl_3$, 0.015 mol $AlCl_3$ per mol substrate was added. Reactors were cooled at specific reaction times by blowing compressed air and then placing them in a water bath at room temperature. For a better phase separation, the reactor was centrifuged for 3 min at 4000 rpm by placing it inside a 50 mL centrifuge tube. Both phases were collected with a glass pipe and analyzed by HPLC. Analysis methods are detailed in Section A.2.2.

Note: in all cases, the temperature of the oil bath was set 3°C higher than the specified reaction temperature to compensate for differences between the wall and interior of the reactor.

A.1.10 Hydrogenolysis of stabilized lignin

In a 25 mL Parr reactor, 100 mg of stabilized lignin were mixed with 50 mg of 5% Ru/C in 10 mL of methanol. The reactor was purged three times with H_2 and then, pressurized up to 50 bar of H_2. The reaction was carried out at 250°C for 4 h at 600 rpm. The monomers quantification

was done by GC-FID and ECN using decane as internal standard following the procedure detailed elsewhere[32]. Prior to injection the sample was filtered with a 2µm PTFE filter.

A.1.11 Tandem hydrolysis-hydrogenation of diformylxylose

The reaction was carried out in a fixed bed tubular reactor with a OD = 0.25 inch in an up flow configuration. Around 0.50 grams of catalyst were loaded into the heated zone of the reactor and maintained in place by crushed fused silica (inert) beds with quartz wool plugs at both ends of the bed. The catalyst (0.50g = ca. 1.5 mL) was diluted to a volume of 3.4 mL with crushed fused silica (ca. 2.8 grams). The height of the catalyst bed was 17 cm. The catalyst was reduced *in situ* under 100 mL/min of H_2 at 300°C using a ramp of 1 °C/min for 3 h, then cooled to the desired temperature of 185°C or 200°C. The regeneration step followed the same procedure after drying the bed with 100 mL/min of H_2 at the reaction temperature for 2 h. The feed was prepared by diluting pure diformylxylose in water to 2 wt%. A SSI LS-class HPLC pump was used to deliver the feed. The pressure in the reactor was set using a Tescom back-pressure regulator. The H_2 flowrate was controlled with a Brooks mass flow controller but the final flow rate was measured after the back-pressure regulator at 1 bar. The liquid samples were collected using a gas-liquid separator.

A.1.12 Catalyst preparation

Pt supported on activated carbon (Pt/C) was prepared by wet impregnation. The targeted amount of $PtCl_4$ was dissolved in water and HCl with a Cl:Pt molar ratio of 3:1 to facilitate the dissolution of $PtCl_4$. The solution was slowly added to the activated carbon while stirring at 600 rpm. The resulting slurry let to stir for 4h and then dried at 105°C overnight. Subsequently, the catalyst was reduced by two methods. First, the catalyst was reduced using a 0.125 M solution of $NaBH_4$ at a Na:Pt molar ratio of 10:1 for 3 h at 600 rpm. The solid was then washed

until the pH was neutral and dried at 105°C overnight. The second reduction was performed at 300°C for 3h under a hydrogen flow of ca. 100 mL/min using a heating ramp of 1 °C/min.

A.1.13 Catalyst Characterization

The total metal loading was determined by treating 50 mg of catalyst with 5 mL of fresh aqua regia at 45°C for 3h with vigorous stirring. The solution was then diluted with MQ-water, filtered and analyzed by Inductive Couple Plasma Mass Spectrometry (ICP-MS).

The total number of acid sites on the catalyst and the metal dispersion were determined by ammonia temperature-programmed desorption (NH_3-TPD) and by injecting CO pulses using a Micrometrics Autochem II 2920 connected to a MKS Cirrus 2 Quadrupole mass spectrometer (MS). For each analysis, ca. 150 mg of fresh or spent catalyst were loaded into the cell. The carrier gas was He flowing at 50 ml/min.

The NH_3-TPD was performed after the catalyst was dried at 300°C under He for 30 min. The adsorption of NH_3 on the catalyst surfaces was done by flowing 1% NH_3 in He at 120°C and 50 mL/min for 30 min followed by purging with He for 1 h. The desorption was quantified by integrating the mass 16 signal on the MS with a temperature ramp of 5 °C/min from 120°C to 800°C. The mass 16 was calibrated in the MS after each analysis using 1% NH_3 in He.

The metal dispersion was calculated by injecting CO pulses at 42°C. Prior to the injection of CO pulses, the catalyst was reduced in-situ via H_2 temperature-programmed reduction (TPR) at 300°C for 30 min with 10% H_2 in Argon flown at 50 ml/min and a heating ramp of 5 °C/min. The CO pulses were sent over the catalyst until no consumption was observed as determined by monitoring the mass 28 signal on the MS.

Electron microscopy imaging. High-angle annular dark-field scanning transmission electron microscopy (HAADF-STEM) imaging was performed on a FEI Talos with 200 keV acceleration voltage. The fresh and spent catalyst were dry impregnated on Lacey carbon grids. The particle size distribution was done by counting 300 particles for each catalyst.

X-ray diffraction (XRD) was done using a Bunker D8 advance with CuKα radiation (λ = 1.5406 Å) and 2θ scanning from 10° to 130° (step = 0.035° and step time = 3 sec).

X-ray photon spectroscopy (XPS) measurements were carried out using a PHI Versa Probe II scanning XPS microprobe (Physical Instruments AG, Germany) and a monochromatic Al Kα X-ray source of 24.8 W (1490 eV) power with a beam size of 100 μm. The spherical capacitor analyser was set at 45° take-off angle with respect to the sample surface. The pass energy was 46.95 eV yielding a full width at half maximum of 0.91 eV for the Ag 3d 5/2 peak.

The spent catalyst was recovered by collecting the catalyst bed and suspending it in acetone. After taking the solution containing the suspended catalyst (the crushed fused silica sunk to the bottom,) the acetone was removed under reduced pressure with a rotary evaporator at 45°C and then, dried at 120°C for 2 hr.

A.1.14 Dispersion test

In order to determine whether changes in metal dispersion occurred after subsequent *in situ* catalyst regenerations, 133 mg of fresh catalyst were loaded in the Autochem cell for characterization. First, the catalyst was purged with a carrier gas (He) for 15 min and then, H_2 was flowed at 50 mL/min for 5 min. Second, the catalyst was heated up to 300°C with a heating ramp of 5 °C/min for 3 h. After the catalyst was cooled to 42°C and purged with He, CO pulses were sent over the catalyst until no consumption was observed as determined by monitoring

the mass 28 signal on the MS. Then, the catalyst was purged and reduced a second time following the same conditions as the first reduction but for 6 h instead of 3 h to mimic two regenerations in the flow reactor. Finally, the catalyst was cooled to 42°C, purged with He and exposed to pulses of CO following the same procedure as described above.

A.2 Analytical methods

A.2.1 GC quantification

GC-FID chromatograms were obtained on an Agilent 789B series equipped with a HP5-column and a flame ionization detector (FID). The method used consisted of an injection and detection temperature of 300°C with a temperature program of: 40°C for 3 min, 30°C/min to 100°C, 40°C/min to 300°C and 300°C for 5 min.

A.2.2 HPLC quantification

All HPLC quantifications were made by creating a calibration curve between the area below the peak and the standard concentration. The standards were made with commercially available chemicals. All aqueous HPLC chromatograms were obtained using an Agilent Infinity 1260 HPLC system equipped with an RI Detector, a UV-Vis Detector, an automatic fraction collector and an Aminex HPX-87H column at 60°C using 5mM H_2SO_4 in water at a flow rate of 0.6 mL/min as the mobile phase. All organic HPLC chromatograms were obtained using an Agilent Infinity 1260 HPLC system equipped with a UV-Vis Detector and a Phenomenex Luna® 5µm C18(2) 100Å column at 25°C, using an acetonitrile/water gradient at a flow rate of 0.7 mL/min.

A.2.3 Analysis of biomass pretreatment liquor and flow-through reactor liquid

After biomass pretreatment the slurry was filtered and washed, first with 10 mL of the organic solvent used during the pretreatment and then 50 mL of MQ-water. Both washes were analyzed

by HPLC. To hydrolyze possible oligomers into monomeric sugars, we adapted the National Renewable Energy Laboratory's (NREL's) protocol for oligomer quantification[123]. The organic wash was diluted ten times with 3.3 wt.% of H_2SO_4 in water and heated to 120°C for 1h in an oil bath. For the aqueous wash, 20 μL of concentrated H_2SO_4 was added to 1 mL of the aqueous wash instead of dilution. After hydrolysis, both solutions were analyzed by HPLC.

For an accurate quantification of soluble sugars, protected carbohydrates, and/or oligomers in flow-through experiments, all collected liquid fractions exiting the reactor were autoclaved for 1h at 121°C after a 10x dilution with 3.3 wt% of H_2SO_4 in water, and analyzed by HPLC. HPLC analysis of carbohydrate, diformylxylose and furans were conducted following the details in Section A.2.2. The quantification of diformylglucose was done before hydrolysis following steps detailed in Section A.2.5.

A.2.4 Compositional analysis of biomass

The compositional analysis of untreated biomass and pretreated solids was performed according to the standard carbohydrate and Klason lignin procedures detailed by NREL[123].

A.2.5 Product quantification and yield calculation in cellulose depolymerization

The product distribution of the total soluble carbohydrate yield was determined by measuring the amount of glucose, xylose, diformylglucose and diformylxylose before and after acid hydrolysis by GC and HPLC. During acid hydrolysis not only protected carbohydrates are converted back to their respective monomers, but gluco-oligomers (and potentially protected gluco-oligomers) are also depolymerized to glucose. Therefore, the additional simple sugars measured after hydrolysis are assumed to come from oligomers.

Due to the difficulty of purifying a large enough quantity of diformylglucose isomers to be used as a standard, we used a quantification based on the effective carbon number (ECN) method and a similar reference compound (in this case diformylxylose) to predict relative response factors. Specifically, we used the response factor of diformylxylose based on a standard curve and modified it using the ECN method. These resulting modified response factors are based on the molecular structure of diformylglucose isomers. The ECN is calculated by the sum of contributions for each carbon atom in the molecule according to its surroundings (Table A.1 and A.2). Diformylglucose yields were then calculated based on the area of the isomer in the GC chromatogram and a relative response factor, calculated with respect to the diformylxylose response measured using standards. The detailed calculations are shown below:

$$F_{DG\ isomer} = \frac{MW_{DG\ isomer} \cdot ECN_{DX}}{MW_{DX} \cdot ECN_{DG\ isomer}} \cdot F_{DX} \quad \text{Equation A.1}$$

$$M_{DG\ isomer} = \frac{A_{DG\ isomer\ in\ injection}}{F_{DG\ isomer}} \quad \text{Equation A.2}$$

$$n_{DG\ isomer} = \frac{M_{DG\ isomer}}{MW_{DG\ isomer}} \quad \text{Equation A.3}$$

$$n_{i\ glucose} = \frac{M_{pretreated\ solids} \cdot x_{glucan} \cdot y_{glucose/glucan}}{MW_{glucose}} \quad \text{Equation A.4}$$

$$Y_{DG\ isomer} = \frac{n_{DG\ isomer} \cdot V_{sample}}{n_{i\ glucose}} \cdot 100\% \quad \text{Equation A.5}$$

In equations:

$F_{DG\ isomer}$ [pA min mg^{-1}]: response factor of the diformylglucose isomer;

F_{DX} [pA min mg^{-1}]: response factor of diformylxylose based on a calibration curve;

$MW_{DG\ isomer}$[mg mmol^{-1}]: molecular weight of the DG isomer (204.06 mg mmol^{-1});

ECN_{DX}: effective carbon number of diformylxylose (see Table 4);

MW_{DX}[mg mmol^{-1}]: molecular weight of diformylxylose (174.05 mg mmol^{-1});

$ECN_{DG\ isomer}$: effective carbon number of diformylglucose (see Table 4);

$M_{DG\ isomer}$ [mg]: mass (milligrams) of the diformylglucose isomer in GC injection (in 1 µL);

$A_{DG\ isomer\ in\ injection}$ [pA min]: peak area of the diformylglucose isomer in the GC-FID chromatogram;

$n_{DG\ isomer}$ [mmol]: millimoles of the diformylglucose isomer in GC injection (in 1 µL);

$n_{i\ glucose}$ [mmol]: initial millimoles of packed glucose- equivalents as pretreated solids in the reactor bed;

$M_{pretreated\ solids}$ [mg]: mass (milligrams) of packed pretreated solids in the reactor bed (air dried basis);

x_{glucan} [mg/mg]: glucan content in pretreated solids (air dried basis);

$y_{glucose/glucan}$ [mg/mg]: conversion factor of glucose to glucan (1/0.9);

$MW_{glucose}$[mg mmol^{-1}]: molecular weight of glucose (180.16 mg mmol^{-1});

$Y_{DG\ isomer}$ [%]: yield of diformylglucose isomers based on the packed pretreated solids in the reactor bed;

V_{sample} [mL]: total sample volume of collected liquid from flow-through reactor;

Table A.1 | Increments used to calculate the effective carbon number (ECN)[219]

Atom/group	*ECN contribution*
Carbon-aliphatic	1
Carbon-aromatic	1
Oxygen-primary alcohol	-0.25
Oxygen-secondary alcohol	-0.75
Oxygen-ether	-1

Table A.2 | Effective carbon number (ECN) for protected carbohydrates

Protected carbohydrate	*Effective carbon number calculated based on ECN contribution*
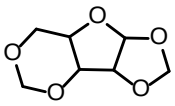	2
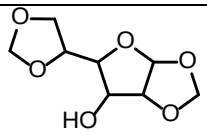	2.25
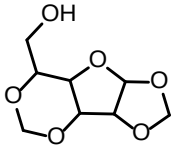	2.75

A.2.6 NMR analysis of pretreatment liquor and pretreated solids depolymerization.

NMR analyses of pretreatment liquors were done directly on the resulting liquors after removal of the 1,4-dioxane-water solvent mixture. Specifically, after biomass pretreatment with or without FA addition, 1 mL of liquor was neutralized with sodium bicarbonate and dried under reduced pressure with a rotary evaporator at 60°C. The dried sample was then dissolved in 1 mL of DMSO-d_6, filtered with a 0.2 µm PTFE filter and transferred into an NMR tube.

The collected liquid from the pretreated solids depolymerization without the addition of FA was prepared for NMR by extracting GVL with liquid CO_2 at 75 bar. The GVL extraction procedure is detailed in Section A.1.4. In the case of pretreated solids depolymerization with the addition of FA, the sample was directly neutralized with sodium bicarbonate and dried under reduced pressure in a rotary evaporator. The resulting solution was diluted with DMSO-d_6, filtered with a 2µm PTFE filter and transferred into an NMR tube.

A.2.7 Analysis of pentose dehydration to furfural

After aqueous/organic phase separation, the aqueous phase was diluted ten times with MQ-water, filtered with a 0.2 µm PFTE filter and analyzed using a HPLC using the procedure described in Section A.2.2. The organic phase was filtered with a 0.2 µm PFTE filter and analyzed using a GC-FID to quantify furfural following the procedure described in Section A.2.1.

A.2.8 Analysis of hexose dehydration to 5-HMF

After aqueous/organic phase separation, the aqueous phase was diluted ten times with MQ-water, filtered with a 0.2 µm PFTE filter and analyzed using an HPLC using the procedure described in Section A.2.2. The organic phase was filtered with a 0.2 µm PFTE filter and analyzed using the procedure in Section A.2.2.

A.2.9 Operando ^{13}C NMR analysis of 1-^{13}C-xylose and 1-^{13}C-diformylxylose

78 μmol of 1-^{13}C-xylose or purified 1-^{13}C-diformylxylose and 100 μL of 150 mM D_2SO_4 in D_2O were mixed and pressurized with 10 bar of He in a heavy-wall pressure NMR tube from Armar Isotopes. The temperature of the sample was increased from 25°C to 80°C in 6 min, then by increments of 20°C from 80°C to 140°C and a finally to 148°C (see time increments on Figure 5.5). All ^{13}C NMR spectra were obtained on a Bruker Avance III 400 MHz spectrometer within 3 to 5 min of a stable temperature being reached.

A.2.10 Analysis of the tandem hydrolysis-hydrogenation of diformylxylose

The liquid phase was analyzed by HPLC without dilution. The samples were filtered with an 0.2 μm PTFE filter before injection. All compounds in the liquid phase, except for HMXF, were quantified using commercial standards. The gas phase was analyzed with an online Agilent Technologies 7890A gas chromatography with a gas sampling valve equipped with a HP-PLOT Q column, a FID detector and a Thermal Conductivity Detector (TCD). All compounds in the gas phase were quantified based on the ECN method using methane as external standard.

A.2.11 Definition of conversion and yields

Conversion was defined as the final moles of reactant divided by the initial moles of reactant. Yields were defined as the final carbon moles of the product divided by the initial carbon moles of reactant.

A.3 Supplementary Figures

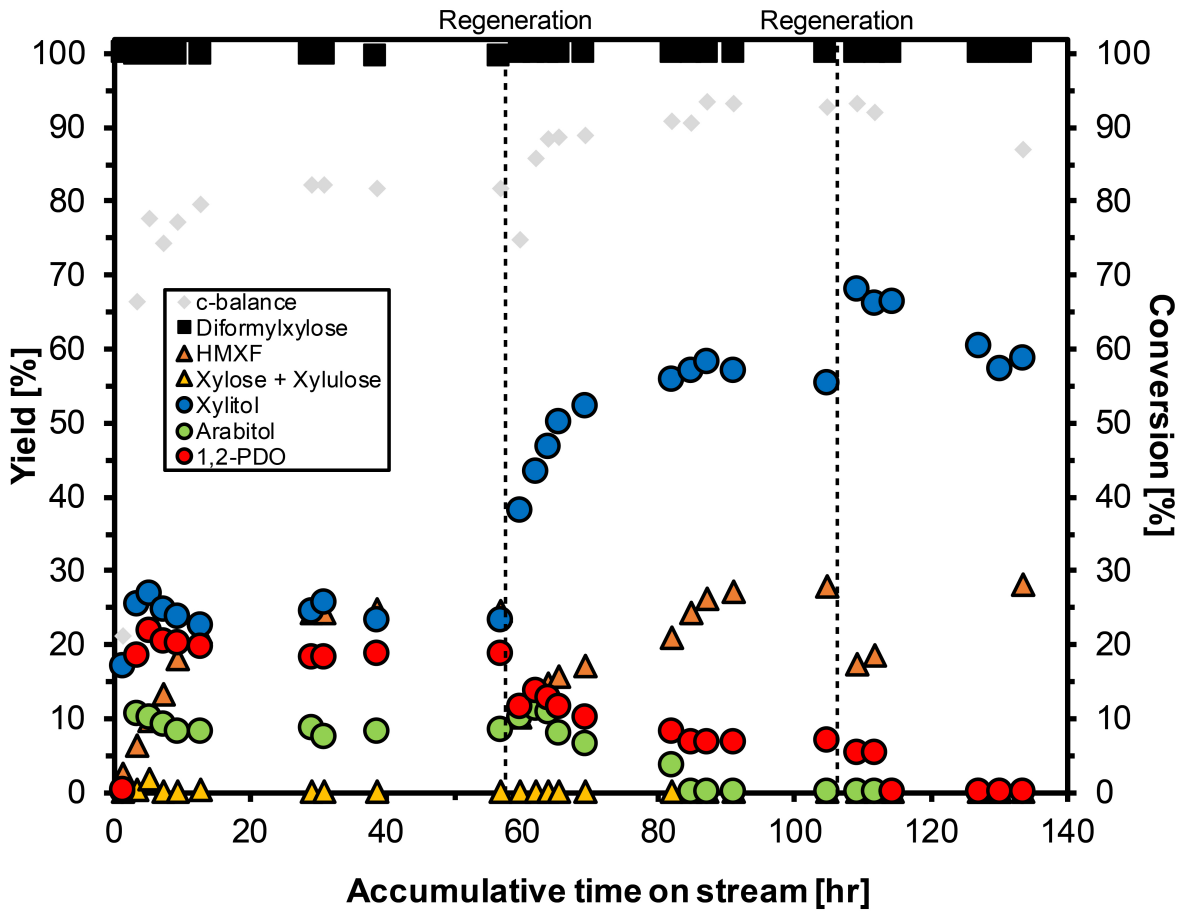

Figure A.1 | Changes in the catalyst activity after multiple regeneration of the catalyst bed under 50 bar of H_2. (WHSV = 0.19 h^{-1}, H_2 flow = 50 mL/min, T = 185°C and feed = 2 wt% of DX in water). WHSV was calculated based on the diformylxylose mass flow and the total catalyst weight).

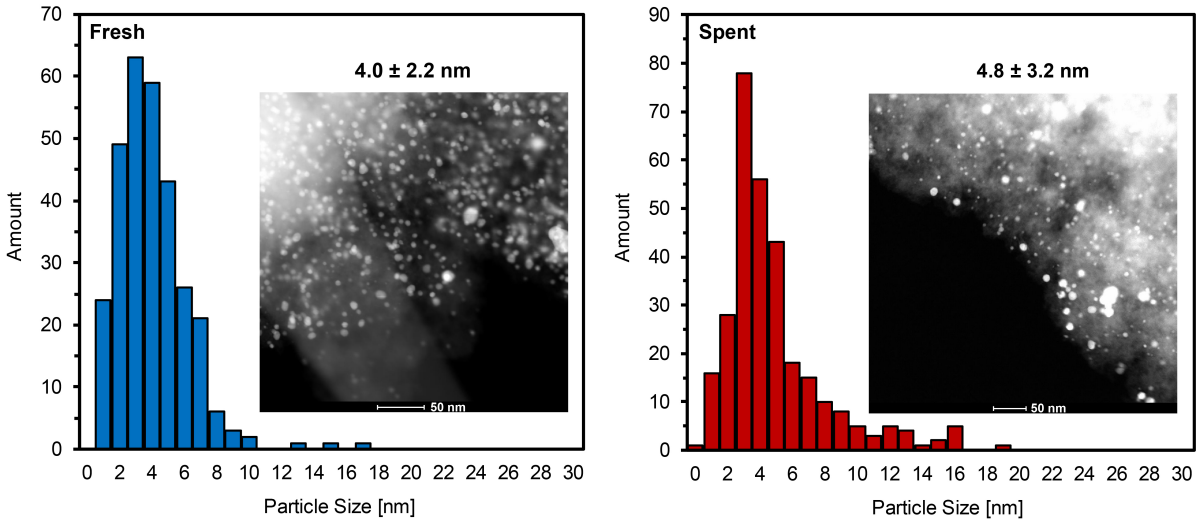

Figure A.2 | Transmission electron microscopy (TEM) images and particle size distribution of the fresh and spent catalyst. (The spent catalyst was used at WHSV = 0.19 h^{-1}, 20 bar H_2 and 185°C for 180 h (time on stream), Figure 7.4.)

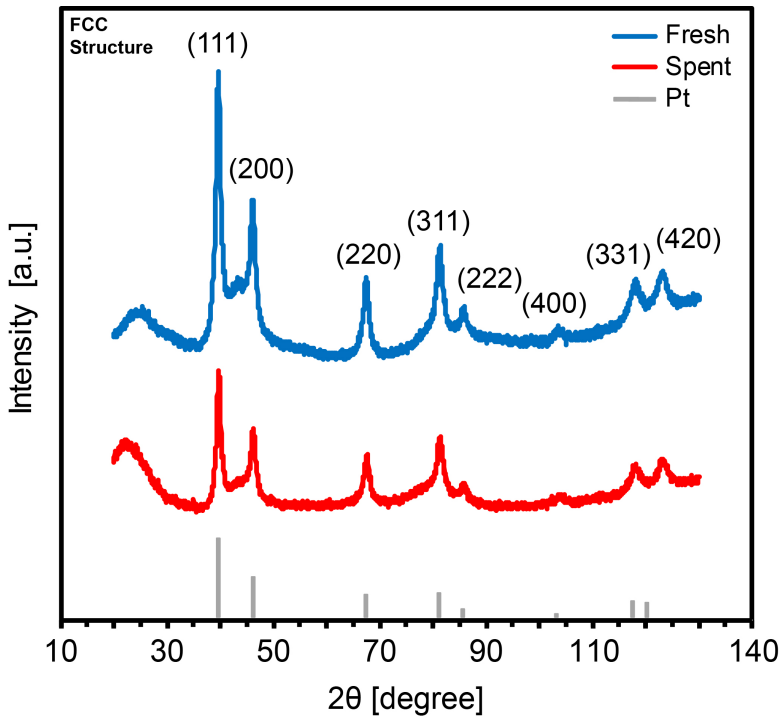

Figure A.3 | X-ray powder diffraction (XRD) of the fresh and spent catalyst. (The spent catalyst was used at WHSV = 0.19 h^{-1}, 20 bar H_2 and 185°C for 180 h (time on stream), Figure 7.4) Both samples had a lattice parameter of 3.921 for Pt and an isotropic domain size of 5 – 6 nm. Pt indices and relatives intensities taken from Swanson and Tatge.[220]

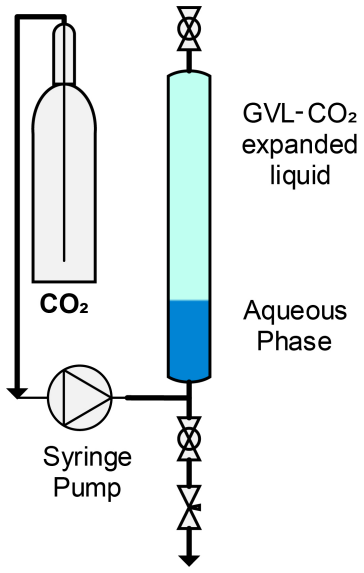

Figure A.4 | Schematic representation of the CO_2 extraction unit.

A.4 Supplementary Tables

Table A.3 | Summary of the characterization of fresh and spent catalyst.

Catalyst	*Metal loading [%]*	*Pt dispersion by CO [%]*	*BET surface area [m^2/g]*	*Pore Volume [cm^3/g]*	*Pore Area [m^2/g]*	*Particle size distribution by TEM [nm]*	*Total acid sites [μmole NH_3/g]*
Fresh	2.6	34.6	1001	0.522	356	4.0 ± 2.2	19
Spent	--	6.2*	375	0.242	152	4.8 ± 3.2	24

Note: spent catalyst was used at WHSV = 0.19 h^{-1}, 20 bar H_2 and 185°C for 180 h (time on stream).
* based on the metal loading of fresh catalyst.

Table A.4 | Results of the X-ray photoelectron spectroscopy (XPS) peak deconvolution of all detected platinum species.

Catalyst	*FWHM / % Area*					
	Pt metal 4f 7/2	*Pt metal 4f 5/2*	*PtO 4f 7/2*	*PtO 4f 5/2*	*$Pt(OH)_2$ 4f 7/2*	*$Pt(OH)_2$ 4f 5/2*
Fresh	1.12 / 51.00	1.10 / 38.24	2.11 / 0.04	0.50 / 0.03	1.17 / 6.11	8.73 / 4.58
Spent	1.04 / 25.22	0.98 / 18.91	0.50 / 0.26	1.10 / 0.19	3.00 / 31.67	1.63 / 23.75

Note: spent catalyst was used at WHSV = 0.19 h^{-1}, 20 bar H_2 and 185°C for 180 h (time on stream).

References

1. Questell-Santiago, Y. M. & Luterbacher, J. S. in *High Press. Technol. Biomass Convers.* 9–36 (2017).
2. Luterbacher, J. S., Alonso, D. M. & Dumesic, J. A. Targeted chemical upgrading of lignocellulosic biomass to platform molecules. *Green Chem.* **16,** 4816–4838 (2014).
3. Sorrell, S. Reducing energy demand: A review of issues, challenges and approaches. *Renew. Sustain. Energy Rev.* **47,** 74–82 (2015).
4. In *New Era Glob. Health* (ed. Rosa, W.) (Springer Publishing Company, 2017).
5. *BP Statistical Review of World Energy*. (2018).
6. *IEA Bioenergy - Annual Report 2017*. 144 (International Energy Agency - IEA Bioenergy, 2018).
7. Brown, A. & Le Feuvre, P. *Technology Roadmap: Delivering Sustainable Bioenergy*. 94 (International Energy Agency - IEA, 2017).
8. Morais, A. R. C., da Costa Lopes, A. M. & Bogel-Łukasik, R. Carbon Dioxide in Biomass Processing: Contributions to the Green Biorefinery Concept. *Chem. Rev.* **115,** 3–27 (2015).
9. Niranjan, E. The Food versus Fuel Debate. 11 (2017).
10. Gay, H., M'Barek, R., Hélaine, S. & Institute for Prospective Technological Studies. *Impacts of the EU biofuel policy on agricultural markets and land use: modelling assessment with AGLINK-COSIMO (2012 version).*
11. Wang, W.-C. & Tao, L. Bio-jet fuel conversion technologies. *Renew. Sustain. Energy Rev.* **53,** 801–822 (2016).
12. *Bioenergy – Chances and Limits*. 124 (German National Academy of Sciences Leopoldina, 2012).

13. Cherubini, F. The biorefinery concept: Using biomass instead of oil for producing energy and chemicals. *Energy Convers. Manag.* **51,** 1412–1421 (2010).
14. Wagemann, K. & Tippkötter, N. in *Biorefineries* (eds. Wagemann, K. & Tippkötter, N.) 1–11 (Springer International Publishing, 2019).
15. Balan, V. Current Challenges in Commercially Producing Biofuels from Lignocellulosic Biomass. *ISRN Biotechnol.* **2014,** (2014).
16. *Standard Terminology. Relating to Biotechnology.* (ASTM International, 2015).
17. Daza Serna, L. V., Orrego Alzate, C. E. & Cardona Alzate, C. A. Supercritical fluids as a green technology for the pretreatment of lignocellulosic biomass. *Bioresour. Technol.* **199,** 113–120 (2016).
18. Sinistore, J. C., Reinemann, D. J., Izaurralde, R. C., Cronin, K. R., Meier, P. J., Runge, T. M. & Zhang, X. Life Cycle Assessment of Switchgrass Cellulosic Ethanol Production in the Wisconsin and Michigan Agricultural Contexts. *BioEnergy Res.* **8,** 897–909 (2015).
19. *Renewable Fuel Standard: Potential Economic and Environmental Effects of U.S. Biofuel Policy*. (National Academies Press, 2011).
20. Ahmad, A. L., Yasin, N. H. M., Derek, C. J. C. & Lim, J. K. Microalgae as a sustainable energy source for biodiesel production: A review. *Renew. Sustain. Energy Rev.* **15,** 584–593 (2011).
21. Subramaniam, B., Chaudhari, R. V., Chaudhari, A. S., Akien, G. R. & Xie, Z. Supercritical fluids and gas-expanded liquids as tunable media for multiphase catalytic reactions. *Chem. Eng. Sci.* **115,** 3–18 (2014).
22. *Renewable 2018 Global Status Report*. 325 (Renewable Energy Policy Network for the 21st Century, 2018).

23. Schutyser, W., Renders, T., Bosch, S. V. den, Koelewijn, S.-F., Beckham, G. T. & Sels, B. F. Chemicals from lignin: an interplay of lignocellulose fractionation, depolymerisation, and upgrading. *Chem. Soc. Rev.* **47,** 852–908 (2018).

24. Bajpai, P. *Pretreatment of Lignocellulosic Biomass for Biofuel Production*. (Springer Singapore, 2016).

25. *Cellulose Chemistry and Properties: Fibers, Nanocelluloses and Advanced Materials*. (Springer International Publishing, 2016).

26. Nishiyama, Y., Langan, P. & Chanzy, H. Crystal Structure and Hydrogen-Bonding System in Cellulose Iβ from Synchrotron X-ray and Neutron Fiber Diffraction. *J. Am. Chem. Soc.* **124,** 9074–9082 (2002).

27. Nishiyama, Y., Sugiyama, J., Chanzy, H. & Langan, P. Crystal Structure and Hydrogen Bonding System in Cellulose Iα from Synchrotron X-ray and Neutron Fiber Diffraction. *J. Am. Chem. Soc.* **125,** 14300–14306 (2003).

28. Lynd, L. R., Cushman, J. H., Nichols, R. J. & Wyman, C. E. Fuel Ethanol from Cellulosic Biomass. *Science* **251,** 1318–1323 (1991).

29. Gírio, F. M., Fonseca, C., Carvalheiro, F., Duarte, L. C., Marques, S. & Bogel-Łukasik, R. Hemicelluloses for fuel ethanol: A review. *Bioresour. Technol.* **101,** 4775–4800 (2010).

30. Wilkie, K. C. B. in *Adv. Carbohydr. Chem. Biochem.* (eds. Tipson, R. S. & Horton, D.) **36,** 215–264 (Academic Press, 1979).

31. Pu, Y., Zhang, D., Singh, P. M. & Ragauskas, A. J. The new forestry biofuels sector. *Biofuels Bioprod. Biorefining* **2,** 58–73 (2008).

32. Shuai, L., Amiri, M. T., Questell-Santiago, Y. M., Héroguel, F., Li, Y., Kim, H., Meilan, R., Chapple, C., Ralph, J. & Luterbacher, J. S. Formaldehyde stabilization facilitates lignin monomer production during biomass depolymerization. *Science* **354,** 329–333 (2016).

33. Zakzeski, J., Bruijnincx, P. C. A., Jongerius, A. L. & Weckhuysen, B. M. The Catalytic Valorization of Lignin for the Production of Renewable Chemicals. *Chem. Rev.* **110,** 3552–3599 (2010).

34. Werpy, T. & Petersen, G. *Top Value Added Chemicals from Biomass: Volume I -- Results of Screening for Potential Candidates from Sugars and Synthesis Gas*. (National Renewable Energy Lab., Golden, CO (US), 2004).

35. J. J. Bozell, J. E. Holladay, D. Johnson & J. F. White. *Top Value-Added Chemicals from Biomass - Volume II—Results of Screening for Potential Candidates from Biorefinery Lignin - pnnl-16983.pdf*. 87 (US Department of Energy, 2007).

36. Rinaldi, R., Jastrzebski, R., Clough, M. T., Ralph, J., Kennema, M., Bruijnincx, P. C. A. & Weckhuysen, B. M. Paving the Way for Lignin Valorisation: Recent Advances in Bioengineering, Biorefining and Catalysis. *Angew. Chem. Int. Ed.* **55,** 8164–8215 (2016).

37. Putro, J. N., Soetaredjo, F. E., Lin, S.-Y., Ju, Y.-H. & Ismadji, S. Pretreatment and conversion of lignocellulose biomass into valuable chemicals. *RSC Adv.* **6,** 46834–46852 (2016).

38. *The Biogas Handbook: Science, Production and Applications*. (Woodhead Publishing Limited, 2013).

39. Onwudili, J. A. in *Appl. Hydrothermal React. Biomass Convers.* (ed. Jin, F.) 219–246 (Springer Berlin Heidelberg, 2014).

40. Demirel, B. Major Pathway of Methane Formation From Energy Crops in Agricultural Biogas Digesters. *Crit. Rev. Environ. Sci. Technol.* **44,** 199–222 (2014).

41. Pace, S. A., Yazdani, R., Kendall, A., Simmons, C. W. & VanderGheynst, J. S. Impact of organic waste composition on life cycle energy production, global warming and Water use for treatment by anaerobic digestion followed by composting. *Resour. Conserv. Recycl.* **137,** 126–135 (2018).

42. Chisti, Y. Biodiesel from microalgae. *Biotechnol. Adv.* **25,** 294–306 (2007).

43. Kaup, F. *The Sugarcane Complex in Brazil: The Role of Innovation in a Dynamic Sector on Its Path Towards Sustainability*. (Springer, 2015).

44. Mata, T. M., Martins, A. A. & Caetano, Nidia. S. Microalgae for biodiesel production and other applications: A review. *Renew. Sustain. Energy Rev.* **14,** 217–232 (2010).

45. Slade, R. & Bauen, A. Micro-algae cultivation for biofuels: Cost, energy balance, environmental impacts and future prospects. *Biomass Bioenergy* **53,** 29–38 (2013).

46. Alonso, D. M., Bond, J. Q. & Dumesic, J. A. Catalytic conversion of biomass to biofuels. *Green Chem.* **12,** 1493–1513 (2010).

47. Wyman, C. E., Cai, C. M. & Kumar, R. in *Encycl. Sustain. Sci. Technol.* 1–27 (Springer, New York, NY, 2017).

48. Kumar, A. K. & Sharma, S. Recent updates on different methods of pretreatment of lignocellulosic feedstocks: a review. *Bioresour. Bioprocess.* **4,** 7 (2017).

49. Alonso, D. M., Hakim, S. H., Zhou, S., Won, W., Hosseinaei, O., Tao, J., Garcia-Negron, V., Motagamwala, A. H., Mellmer, M. A., Huang, K., Houtman, C. J., Labbé, N., Harper, D. P., Maravelias, C. T., Runge, T. & Dumesic, J. A. Increasing the revenue from lignocellulosic biomass: Maximizing feedstock utilization. *Sci. Adv.* **3,** e1603301 (2017).

50. Haveren, J. van, Scott, E. L. & Sanders, J. Bulk chemicals from biomass. *Biofuels Bioprod. Biorefining* **2,** 41–57 (2008).

51. Rafiqul, I. S. M. & Sakinah, A. M. M. Processes for the Production of Xylitol—A Review. *Food Rev. Int.* **29,** 127–156 (2013).

52. Dasgupta, D., Bandhu, S., Adhikari, D. K. & Ghosh, D. Challenges and prospects of xylitol production with whole cell bio-catalysis: A review. *Microbiol. Res.* **197,** 9–21 (2017).

53. Delgado Arcaño, Y., Valmaña García, O. D., Mandelli, D., Carvalho, W. A. & Magalhães Pontes, L. A. Xylitol: A review on the progress and challenges of its production by chemical route. *Catal. Today* (2018).

54. Ravella, S. R., Gallagher, J., Fish, S. & Prakasham, R. S. in -*Xylitol Ferment. Prod. Appl. Commer.* (eds. da Silva, S. S. & Chandel, A. K.) 291–306 (Springer Berlin Heidelberg, 2012).

55. European Technology and Innovation Platform - ETIP Bioenergy. All Value Chain Biofuel Fact Sheet 2016. (2016).

56. Luterbacher, J. S., Fröling, M., Vogel, F., Maréchal, F. & Tester, J. W. Hydrothermal Gasification of Waste Biomass: Process Design and Life Cycle Asessment. *Environ. Sci. Technol.* **43,** 1578–1583 (2009).

57. T. Werpy & G. Petersen. *Top Value Added Chemicals from Biomass: Volume 1—Results of Screening for Potential Candidates from Sugars and Synthesis Gas*. 76 (US Department of Energy, 2004).

58. Dry, M. E. The Fischer–Tropsch process: 1950–2000. *Catal. Today* **71,** 227–241 (2002).

59. Tien-Thao, N., Zahedi-Niaki, M. H., Alamdari, H. & Kaliaguine, S. Conversion of syngas to higher alcohols over nanosized LaCo0.7Cu0.3O3 perovskite precursors. *Appl. Catal. Gen.* **326,** 152–163 (2007).

60. Sun, J., Wan, S., Wang, F., Lin, J. & Wang, Y. Selective Synthesis of Methanol and Higher Alcohols over Cs/Cu/ZnO/Al2O3 Catalysts. *Ind. Eng. Chem. Res.* **54,** 7841–7851 (2015).

61. Bach, Q.-V., Tran, K.-Q., Khalil, R. A., Skreiberg, Ø. & Seisenbaeva, G. Comparative Assessment of Wet Torrefaction. *Energy Fuels* **27,** 6743–6753 (2013).

62. Torrefaction of biomass and 'biocoal' technologies. *Eur. Biofuels Technol. Platf.* (2016).

63. Oh, Y. H., Eom, I. Y., Joo, J. C., Yu, J. H., Song, B. K., Lee, S. H., Hong, S. H. & Park, S. J. Recent advances in development of biomass pretreatment technologies used in biorefinery for the production of bio-based fuels, chemicals and polymers. *Korean J. Chem. Eng.* **32,** 1945–1959 (2015).

64. Seidl, P. R. & Goulart, A. K. Pretreatment processes for lignocellulosic biomass conversion to biofuels and bioproducts. *Curr. Opin. Green Sustain. Chem.* **2,** 48–53 (2016).

65. Bergius, F. Conversion of Wood To Carbohydrates. *Ind. Eng. Chem.* **29,** 247–253 (1937).

66. Renders, T., Bosch, S. V. den, Koelewijn, S.-F., Schutyser, W. & Sels, B. F. Lignin-first biomass fractionation: the advent of active stabilisation strategies. *Energy Environ. Sci.* **10,** 1551–1557 (2017).

67. Moriarty, K. L., Milbrandt, A. R., Warner, E., Lewis, J. E. & Schwab, A. A. *2016 Bioenergy Industry Status Report*. (National Renewable Energy Lab. (NREL), Golden, CO (United States), 2018).

68. Questell-Santiago, Y. M., Zambrano-Varela, R., Amiri, M. T. & Luterbacher, J. S. Carbohydrate stabilization extends the kinetic limits of chemical polysaccharide depolymerization. *Nat. Chem.* **10,** 1222 (2018).

69. Lee, Y. Y., Iyer, P. & Torget, R. W. in *Recent Prog. Bioconversion Lignocellul.* 93–115 (Springer, Berlin, Heidelberg, 1999).

70. Carvalheiro, F., Silva-Fernandes, T., Duarte, L. C. & Gírio, F. M. Wheat Straw Autohydrolysis: Process Optimization and Products Characterization. *Appl. Biochem. Biotechnol.* **153,** 84–93 (2008).

71. van Zandvoort, I., Wang, Y., Rasrendra, C. B., van Eck, E. R. H., Bruijnincx, P. C. A., Heeres, H. J. & Weckhuysen, B. M. Formation, Molecular Structure, and Morphology of Humins in Biomass Conversion: Influence of Feedstock and Processing Conditions. *ChemSusChem* **6,** 1745–1758 (2013).

72. Guadix-Montero, S. & Sankar, M. Review on Catalytic Cleavage of C–C Inter-unit Linkages in Lignin Model Compounds: Towards Lignin Depolymerisation. *Top. Catal.* **61,** 183–198 (2018).

73. Wijaya, Y. P., Putra, R. D. D., Widyaya, V. T., Ha, J.-M., Suh, D. J. & Kim, C. S. Comparative study on two-step concentrated acid hydrolysis for the extraction of sugars from lignocellulosic biomass. *Bioresour. Technol.* **164,** 221–231 (2014).

74. Timell, T. E. The Acid Hydrolysis of Glycosides: I. General Conditions and the Effect of the Nature of the Aglycone. *Can. J. Chem.* **42,** 1456–1472 (1964).

75. Esteghlalian, A., Hashimoto, A. G., Fenske, J. J. & Penner, M. H. Modeling and optimization of the dilute-sulfuric-acid pretreatment of corn stover, poplar and switchgrass. *Bioresour. Technol.* **59,** 129–136 (1997).

76. Jin, Q., Zhang, H., Yan, L., Qu, L. & Huang, H. Kinetic characterization for hemicellulose hydrolysis of corn stover in a dilute acid cycle spray flow-through reactor at moderate conditions. *Biomass Bioenergy* **35,** 4158–4164 (2011).

77. Fagan, R. D., Grethlein, H. E., Converse, A. O. & Porteous, A. Kinetics of the acid hydrolysis of cellulose found in paper refuse. **5,** 545–547 (1971).

78. Saeman, J. F. Kinetics of Wood Saccharification - Hydrolysis of Cellulose and Decomposition of Sugars in Dilute Acid at High Temperature. *Ind. Eng. Chem.* **37,** 43–52 (1945).

79. Wyman, C. E. & Yang, B. in *Hydrothermal Process. Biorefineries Prod. Bioethanol High Added-Value Compd. Second Third Gener. Biomass* (eds. Ruiz, H. A., Hedegaard Thomsen, M. & Trajano, H. L.) 161–180 (Springer International Publishing, 2017).

80. Neuman, R. P. & Walker, L. P. Solute exclusion from cellulose in packed columns: Experimental investigation and pore volume measurements. *Biotechnol. Bioeng.* **40,** 218–225 (1992).

81. Patil, S. K. R., Heltzel, J. & Lund, C. R. F. Comparison of Structural Features of Humins Formed Catalytically from Glucose, Fructose, and 5-Hydroxymethylfurfuraldehyde. *Energy Fuels* **26,** 5281–5293 (2012).

82. Hoang, T. M. C., Lefferts, L. & Seshan, K. Valorization of Humin-Based Byproducts from Biomass Processing—A Route to Sustainable Hydrogen. *ChemSusChem* **6,** 1651–1658 (2013).

83. Kang, S., Jiang, S., Peng, Z., Lu, Y., Guo, J., Li, J., Zeng, W. & Lin, X. Valorization of humins by phosphoric acid activation for activated carbon production. *Biomass Convers. Biorefinery* **8,** 889–897 (2018).

84. Boerjan, W., Ralph, J. & Baucher, M. Lignin Biosynthesis. *Annu. Rev. Plant Biol.* **54,** 519–546 (2003).

85. Ralph, J., Lundquist, K., Brunow, G., Lu, F., Kim, H., Schatz, P. F., Marita, J. M., Hatfield, R. D., Ralph, S. A., Christensen, J. H. & Boerjan, W. Lignins: Natural polymers from oxidative coupling of 4-hydroxyphenyl- propanoids. *Phytochem. Rev.* **3,** 29–60 (2004).

86. Vanholme, R., Demedts, B., Morreel, K., Ralph, J. & Boerjan, W. Lignin Biosynthesis and Structure. *Plant Physiol.* **153,** 895–905 (2010).

87. Shuai, L., Talebi Amiri, M. & Luterbacher, J. S. The influence of interunit carbon–carbon linkages during lignin upgrading. *Curr. Opin. Green Sustain. Chem.* **2,** 59–63 (2016).

88. Lan, W., Amiri, M. T., Hunston, C. M. & Luterbacher, J. S. Protection Group Effects During α,γ-Diol Lignin Stabilization Promote High-Selectivity Monomer Production. *Angew. Chem. Int. Ed.* **57,** 1356–1360 (2018).

89. Bosch, S. V. den, Schutyser, W., Vanholme, R., Driessen, T., Koelewijn, S.-F., Renders, T., Meester, B. D., J. Huijgen, W. J., Dehaen, W., M. Courtin, C., Lagrain, B., Boerjan,

W. & F. Sels, B. Reductive lignocellulose fractionation into soluble lignin-derived phenolic monomers and dimers and processable carbohydrate pulps. *Energy Environ. Sci.* **8,** 1748–1763 (2015).

90. Anderson, E. M., Stone, M. L., Katahira, R., Reed, M., Beckham, G. T. & Román-Leshkov, Y. Flowthrough Reductive Catalytic Fractionation of Biomass. *Joule* **1,** 613–622 (2017).

91. Schutyser, W., Kruger, J. S., Robinson, A. M., Katahira, R., Brandner, D. G., Cleveland, N. S., Mittal, A., Peterson, D. J., Meilan, R., Román-Leshkov, Y. & Beckham, G. T. Revisiting alkaline aerobic lignin oxidation. *Green Chem.* **20,** 3828–3844 (2018).

92. Das, A., Rahimi, A., Ulbrich, A., Alherech, M., Motagamwala, A. H., Bhalla, A., da Costa Sousa, L., Balan, V., Dumesic, J. A., Hegg, E. L., Dale, B. E., Ralph, J., Coon, J. J. & Stahl, S. S. Lignin Conversion to Low-Molecular-Weight Aromatics via an Aerobic Oxidation-Hydrolysis Sequence: Comparison of Different Lignin Sources. *ACS Sustain. Chem. Eng.* **6,** 3367–3374 (2018).

93. Rahimi, A., Azarpira, A., Kim, H., Ralph, J. & Stahl, S. S. Chemoselective Metal-Free Aerobic Alcohol Oxidation in Lignin. *J. Am. Chem. Soc.* **135,** 6415–6418 (2013).

94. Kim, S., Chmely, S. C., Nimlos, M. R., Bomble, Y. J., Foust, T. D., Paton, R. S. & Beckham, G. T. Computational Study of Bond Dissociation Enthalpies for a Large Range of Native and Modified Lignins. *J. Phys. Chem. Lett.* **2,** 2846–2852 (2011).

95. Sousa, L. da C., Jin, M., Chundawat, S. P. S., Bokade, V., Tang, X., Azarpira, A., Lu, F., Avci, U., Humpula, J., Uppugundla, N., Gunawan, C., Pattathil, S., Cheh, A. M., Kothari, N., Kumar, R., Ralph, J., Hahn, M. G., Wyman, C. E., Singh, S., Simmons, B. A., Dale, B. E. & Balan, V. Next-generation ammonia pretreatment enhances cellulosic biofuel production. *Energy Environ. Sci.* **9,** 1215–1223 (2016).

96. Riaz, A., Verma, D., Zeb, H., Lee, J. H., Kim, J. C., Kwak, S. K. & Kim, J. Solvothermal liquefaction of alkali lignin to obtain a high yield of aromatic monomers while suppressing solvent consumption. *Green Chem.* **20,** 4957–4974 (2018).

97. Bouxin, F. P., David Jackson, S. & Jarvis, M. C. Isolation of high quality lignin as a by-product from ammonia percolation pretreatment of poplar wood. *Bioresour. Technol.* **162,** 236–242 (2014).

98. Weigand, L., Mostame, S., Brandt-Talbot, A., Welton, T. & Hallett, J. P. Effect of pretreatment severity on the cellulose and lignin isolated from Salix using ionoSolv pretreatment. *Faraday Discuss.* **202,** 331–349 (2017).

99. Kim, K. H., Simmons, B. A. & Singh, S. Catalytic transfer hydrogenolysis of ionic liquid processed biorefinery lignin to phenolic compounds. *Green Chem.* **19,** 215–224 (2017).

100. Sathitsuksanoh, N., Holtman, K. M., Yelle, D. J., Morgan, T., Stavila, V., Pelton, J., Blanch, H., Simmons, B. A. & George, A. Lignin fate and characterization during ionic liquid biomass pretreatment for renewable chemicals and fuels production. *Green Chem.* **16,** 1236–1247 (2014).

101. Luterbacher, J. S., Azarpira, A., Motagamwala, A. H., Lu, F., Ralph, J. & Dumesic, J. A. Lignin monomer production integrated into the γ-valerolactone sugar platform. *Energy Environ. Sci.* **8,** 2657–2663 (2015).

102. Feghali, E., Carrot, G., Thuéry, P., Genre, C. & Cantat, T. Convergent reductive depolymerization of wood lignin to isolated phenol derivatives by metal-free catalytic hydrosilylation. *Energy Environ. Sci.* **8,** 2734–2743 (2015).

103. Lancefield, C. S., Panovic, I., Deuss, P. J., Barta, K. & Westwood, N. J. Pre-treatment of lignocellulosic feedstocks using biorenewable alcohols: towards complete biomass valorisation. *Green Chem.* **19,** 202–214 (2017).

104. Deuss, P. J., Lancefield, C. S., Narani, A., Vries, J. G. de, Westwood, N. J. & Barta, K. Phenolic acetals from lignins of varying compositions via iron(III) triflate catalysed depolymerisation. *Green Chem.* (2017).

105. Fan, L. T., Lee, Y.-H. & Beardmore, D. H. Mechanism of the enzymatic hydrolysis of cellulose: Effects of major structural features of cellulose on enzymatic hydrolysis. *Biotechnol. Bioeng.* **22,** 177–199 (1980).

106. Walker, L. P. & Wilson, D. B. Enzymatic hydrolysis of cellulose: An overview. *Bioresour. Technol.* **36,** 3–14 (1991).

107. Ezeilo, U. R., Zakaria, I. I., Huyop, F. & Wahab, R. A. Enzymatic breakdown of lignocellulosic biomass: the role of glycosyl hydrolases and lytic polysaccharide monooxygenases. *Biotechnol. Biotechnol. Equip.* **31,** 647–662 (2017).

108. Klein-Marcuschamer, D., Oleskowicz-Popiel, P., Simmons, B. A. & Blanch, H. W. The challenge of enzyme cost in the production of lignocellulosic biofuels. *Biotechnol. Bioeng.* **109,** 1083–1087 (2012).

109. Shuddhodana, Gupta, M. N. & Bisaria, V. S. Stable Cellulolytic Enzymes and Their Application in Hydrolysis of Lignocellulosic Biomass. *Biotechnol. J.* **13,** 1700633 (2018).

110. Kubicek, C. P. & Kubicek, E. M. Enzymatic deconstruction of plant biomass by fungal enzymes. *Curr. Opin. Chem. Biol.* **35,** 51–57 (2016).

111. Braconnot, H. Action de l'acide sulfurique sur la sciure de bois de charme. *Ann. Chim. Phys.* **12,** 172–195 (1819).

112. Stern, A. L. X.—Contributions to the chemistry of cellulose. I. Cellulose-sulphuric acid, and the products of its hydrolysis. *J. Chem. Soc. Trans.* **67,** 74–90 (1895).

113. Ladisch, M. R., Flickinger, M. C. & Tsao, G. T. Fuels and chemicals from biomass. *Energy* **4,** 263–275 (1979).

114. Kanchanalai, P., Temani, G., Kawajiri, Y. & Realff, M. J. Reaction Kinetics of Concentrated-Acid Hydrolysis for Cellulose and Hemicellulose and Effect of Crystallinity. *BioResources* **11,** 1672-1689–1689 (2016).

115. Moe, S. T., Janga, K. K., Hertzberg, T., Hägg, M.-B., Øyaas, K. & Dyrset, N. Saccharification of Lignocellulosic Biomass for Biofuel and Biorefinery Applications – A Renaissance for the Concentrated Acid Hydrolysis? *Energy Procedia* **20,** 50–58 (2012).

116. Cuzens, J. E. & Farone, W. A. Method of strong acid hydrolysis. (1998).

117. Liu, Z.-S., Wu, X.-L., Kida, K. & Tang, Y.-Q. Corn stover saccharification with concentrated sulfuric acid: Effects of saccharification conditions on sugar recovery and by-product generation. *Bioresour. Technol.* **119,** 224–233 (2012).

118. Ioelovich, M. Study of Cellulose Interaction with Concentrated Solutions of Sulfuric Acid. *Int. Sch. Res. Not.* (2012).

119. Song, S. K. & Lee, Y. Y. Acid hydrolysis of wood cellulose under low water condition. *Biomass* **6,** 93–100 (1984).

120. Shahbazi, A. & Zhang, B. in *Bioalcohol Prod.* (ed. Waldron, K.) 143–158 (Woodhead Publishing, 2010).

121. BlueFire Renewables | Our Technology. at <https://bfreinc.com/our-technology/>

122. Groenestijn, J. W. van, Hazewinkel, J. H. O. & Bakker, R. R. Pre-treatment of lignocellulose with biological acid recycling (the Biosulfurol process). *Int. Sugar J.* **110,** 689–692 (2008).

123. Sluiter, A., Hames, B., Ruiz, R., Scarlata, C., Sluiter, J., Templeton, D. & Crocker, D. *Determination of Structural Carbohydrates and Lignin in Biomass*. (National Renewable Energy Laboratory, 2008).

124. Shuai, L. & Luterbacher, J. Organic Solvent Effects in Biomass Conversion Reactions. *ChemSusChem* **9,** 133–155 (2016).

125. Yoo, C. G., Pu, Y. & Ragauskas, A. J. Ionic liquids: Promising green solvents for lignocellulosic biomass utilization. *Curr. Opin. Green Sustain. Chem.* **5,** 5–11 (2017).

126. Zhang, Z., Song, J. & Han, B. Catalytic Transformation of Lignocellulose into Chemicals and Fuel Products in Ionic Liquids. *Chem. Rev.* **117,** 6834–6880 (2017).

127. Brandt, A., Gräsvik, J., Hallett, J. P. & Welton, T. Deconstruction of lignocellulosic biomass with ionic liquids. *Green Chem.* **15,** 550–583 (2013).

128. Sen, S. M., Binder, J. B., Raines, R. T. & Maravelias, C. T. Conversion of biomass to sugars via ionic liquid hydrolysis: process synthesis and economic evaluation. *Biofuels Bioprod. Biorefining* **6,** 444–452 (2012).

129. Cheng, G., Varanasi, P., Li, C., Liu, H., Melnichenko, Y. B., Simmons, B. A., Kent, M. S. & Singh, S. Transition of Cellulose Crystalline Structure and Surface Morphology of Biomass as a Function of Ionic Liquid Pretreatment and Its Relation to Enzymatic Hydrolysis. *Biomacromolecules* **12,** 933–941 (2011).

130. Binder, J. B. & Raines, R. T. Fermentable sugars by chemical hydrolysis of biomass. *Proc. Natl. Acad. Sci.* **107,** 4516–4521 (2010).

131. Swatloski, R. P., Spear, S. K., Holbrey, J. D. & Rogers, R. D. Dissolution of Cellose with Ionic Liquids. *J. Am. Chem. Soc.* **124,** 4974–4975 (2002).

132. Samayam, I. P., Hanson, B. L., Langan, P. & Schall, C. A. Ionic-Liquid Induced Changes in Cellulose Structure Associated with Enhanced Biomass Hydrolysis. *Biomacromolecules* **12,** 3091–3098 (2011).

133. Liang, X., Montoya, A. & Haynes, B. S. Local Site Selectivity and Conformational Structures in the Glycosidic Bond Scission of Cellobiose. *J. Phys. Chem. B* **115,** 10682–10691 (2011).

134. Dee, S. J. & Bell, A. T. A Study of the Acid-Catalyzed Hydrolysis of Cellulose Dissolved in Ionic Liquids and the Factors Influencing the Dehydration of Glucose and the Formation of Humins. *ChemSusChem* **4,** 1166–1173 (2011).

135. Vernon C. A. & Perutz Max Ferdinand. The mechanisms of hydrolysis of glycosides and their revelance to enzyme-catalysed reactions. *Proc. R. Soc. Lond. B Biol. Sci.* **167,** 389–401 (1967).

136. Kresge, A. J. & Straub, T. S. Kinetics of hydrolysis of some sterically hindered ketene acetals. *J. Am. Chem. Soc.* **105,** 3957–3961 (1983).

137. Gschwend, F. J. V., Brandt-Talbot, A., Chambon, C. L. & Hallett, J. P. in *Ion. Liq. Curr. State Future Dir.* **1250,** 209–223 (American Chemical Society, 2017).

138. Zhou, J., Sui, H., Jia, Z., Yang, Z., He, L. & Li, X. Recovery and purification of ionic liquids from solutions: a review. *RSC Adv.* **8,** 32832–32864 (2018).

139. Konda, N. M., Shi, J., Singh, S., Blanch, H. W., Simmons, B. A. & Klein-Marcuschamer, D. Understanding cost drivers and economic potential of two variants of ionic liquid pretreatment for cellulosic biofuel production. *Biotechnol. Biofuels* **7,** 86 (2014).

140. Rogalinski, T., Liu, K., Albrecht, T. & Brunner, G. Hydrolysis kinetics of biopolymers in subcritical water. *J. Supercrit. Fluids* **46,** 335–341 (2008).

141. Peterson, A. A., Vogel, F., Lachance, R. P., Fröling, M., Michael J. Antal, J. & Tester, J. W. Thermochemical biofuel production in hydrothermal media: A review of sub- and supercritical water technologies. *Energy Environ. Sci.* **1,** 32–65 (2008).

142. Schwald, W. & Bobleter, O. Hydrothermolysis of Cellulose Under Static and Dynamic Conditions at High Temperatures. *J. Carbohydr. Chem.* **8,** 565–578 (1989).

143. Adschiri, T., Hirose, S., Malaluan, R. & Arai, K. Noncatalytic Conversion of Cellulose in Supercritical and Subcritical Water. *J. Chem. Eng. Jpn.* **26,** 676–680 (1993).

144. Mochidzuki, K., Sakoda, A. & Suzuki, M. Measurement of the hydrothermal reaction rate of cellulose using novel liquid-phase thermogravimetry. *Thermochim. Acta* **348,** 69–76 (2000).

145. Sasaki, M., Adschiri, T. & Arai, K. Kinetics of cellulose conversion at 25 MPa in sub- and supercritical water. *AIChE J.* **50,** 192–202 (2004).

146. Bobleter, O. & Pape, G. Der hydrothermale Abbau von Glucose. *Monatshefte Für Chem. Chem. Mon.* **99,** 1560–1567 (1968).

147. Amin, S. R. Reforming and decomposition of glucose in an aqueous phase. in (1975).

148. Bernard M. Kabyemela, Tadafumi Adschiri, Roberto M. Malaluan, and & Arai, K. Kinetics of Glucose Epimerization and Decomposition in Subcritical and Supercritical Water. **36,** 1552–1558 (1997).

149. Yukihiko Matsumura, Satoru Yanachi, and & Yoshida, T. Glucose Decomposition Kinetics in Water at 25 MPa in the Temperature Range of 448−673 K. **45,** 1875–1879 (2006).

150. Bandura, A. V. & Lvov, S. N. The Ionization Constant of Water over Wide Ranges of Temperature and Density. *J. Phys. Chem. Ref. Data* **35,** 15–30 (2005).

151. Sasaki, M., Fang, Z., Fukushima, Y., Adschiri, T. & Arai, K. Dissolution and Hydrolysis of Cellulose in Subcritical and Supercritical Water. *Ind. Eng. Chem. Res.* **39,** 2883–2890 (2000).

152. Cantero, D. A., Bermejo, M. D. & Cocero, M. J. Kinetic analysis of cellulose depolymerization reactions in near critical water. *J. Supercrit. Fluids* **75,** 48–57 (2013).

153. Kilambi, S. & Kadam, K. L. Production of fermentable sugars and lignin from biomass using supercritical fluids. (2018).

154. Stuart, E. Advanced biorefinery process. (2010).

155. Genta, M., Uehara, R., Fujita, K., Omoto, S., Matsubara, W. & Seiki, Y. Biomass hydrothermal decomposition apparatus and method. (2010).

156. South, C. R., Wyman, C. E. & Martin, R. L. Two-stage method for pretreatment of lignocellulosic biomass. (2010).

157. Nguyen, Q. A., Keller, F. A. & Tucker, M. P. Ethanol production with dilute acid hydrolysis using partially dried lignocellulosics. (2003).

158. Tao, L., Schell, D., Davis, R., Tan, E., Elander, R. & Bratis, A. *NREL 2012 Achievement of Ethanol Cost Targets: Biochemical Ethanol Fermentation via Dilute-Acid Pretreatment and Enzymatic Hydrolysis of Corn Stover*. (2014).

159. Luterbacher, J. S., Rand, J. M., Alonso, D. M., Han, J., Youngquist, J. T., Maravelias, C. T., Pfleger, B. F. & Dumesic, J. A. Nonenzymatic Sugar Production from Biomass Using Biomass-Derived γ-Valerolactone. *Science* **343,** 277–280 (2014).

160. Borand, M. N. & Karaosmanoğlu, F. Effects of organosolv pretreatment conditions for lignocellulosic biomass in biorefinery applications: A review. *J. Renew. Sustain. Energy* **10,** 033104 (2018).

161. Ghosh, A., Bai, X. & Brown, R. C. Solubilized Carbohydrate Production by Acid-Catalyzed Depolymerization of Cellulose in Polar Aprotic Solvents. *ChemistrySelect* **3,** 4777–4785 (2018).

162. Mellmer, M. A., Alonso, D. M., Luterbacher, J. S., Gallo, J. M. R. & Dumesic, J. A. Effects of γ-valerolactone in hydrolysis of lignocellulosic biomass to monosaccharides. *Green Chem.* **16,** 4659–4662 (2014).

163. Shuai, L., Questell-Santiago, Y. M. & Luterbacher, J. S. A mild biomass pretreatment using γ-valerolactone for concentrated sugar production. *Green Chem.* **18,** 937–943 (2016).

164. Mellmer, M. A., Sanpitakseree, C., Demir, B., Bai, P., Ma, K., Neurock, M. & Dumesic, J. A. Solvent-enabled control of reactivity for liquid-phase reactions of biomass-derived compounds. *Nat. Catal.* **1,** 199 (2018).

165. Hall, M., Bansal, P., Lee, J. H., Realff, M. J. & Bommarius, A. S. Cellulose crystallinity – a key predictor of the enzymatic hydrolysis rate. *FEBS J.* **277,** 1571–1582 (2010).

166. Sannigrahi, P., Miller, S. J. & Ragauskas, A. J. Effects of organosolv pretreatment and enzymatic hydrolysis on cellulose structure and crystallinity in Loblolly pine. *Carbohydr. Res.* **345,** 965–970 (2010).

167. Mellmer, M. A., Sener, C., Gallo, J. M. R., Luterbacher, J. S., Alonso, D. M. & Dumesic, J. A. Solvent Effects in Acid-Catalyzed Biomass Conversion Reactions. *Angew. Chem. Int. Ed.* **53,** 11872–11875 (2014).

168. Han, J., Luterbacher, J. S., Alonso, D. M., Dumesic, J. A. & Maravelias, C. T. A ligno-cellulosic ethanol strategy via nonenzymatic sugar production: Process synthesis and analysis. *Bioresour. Technol.* **182,** 258–266 (2015).

169. In *Greenes Prot. Groups Org. Synth.* 1–15 (John Wiley & Sons, Ltd, 2006).

170. Hung, S.-C. & Wang, C.-C. in *Glycochemical Synth.* 35–68 (John Wiley & Sons, Ltd, 2016).

171. *Protective Groups in Organic Chemistry*. (Springer US, 1973).

172. Fernandes, R. A. in *Prot.-Group-Free Org. Synth.* 1–9 (John Wiley & Sons, Ltd, 2018).

173. Trussardi, R. Preparation of oseltamivir phosphate. (2009).

174. Navia, J. L., Walkup, R. E., Vernon, N. M. & Neiditch, D. S. Production of sucralose without intermediate isolation of crystalline sucralose-6-ester. (1996).

175. Fischer, E. Ueber die Glucoside der Alkohole. *Berichte Dtsch. Chem. Ges.* **26,** 2400–2412 (1893).

176. Fischer, E. & Speier, A. Darstellung der Ester. *Berichte Dtsch. Chem. Ges.* **28,** 3252–3258 (1895).

177. Helferich, B. Tritylläther in der Chemie der Zucker. *Angew. Chem.* **41,** 871–875 (1928).

178. Levene, P. & Meyer, G. The Ring Structure of Diacetone Galactose. *J. Biol. Chem.* **92,** 257 (1931).

179. Mushrush, G. W. & Hardy, D. Fuel system icing inhibitor and deicing composition. (1998).

180. Haworth, W. N. The constitution of ascorbic acid. *J. Soc. Chem. Ind.* **52,** 482–485 (1933).

181. Ault, R. G., Baird, D. K., Carrington, H. C., Haworth, W. N., Herbert, R., Hirst, E. L., Percival, E. G. V., Smith, F. & Stacey, M. 332. Synthesis of d- and of l-ascorbic acid and of analogous substances. *J. Chem. Soc. Resumed* **0,** 1419–1423 (1933).

182. Codée, J. D. C., Ali, A., Overkleeft, H. S. & van der Marel, G. A. Novel protecting groups in carbohydrate chemistry. *Comptes Rendus Chim.* **14,** 178–193 (2011).

183. Hindley, N. C., O'leary, M. J. & Halder, N. Preparation of ketal sugars. (1971).

184. Sobotta, R. D. D.-C. & Klingler, F. D. D. D.-I. Method for the preparation of Isopropylidene derivatives of saccharides. (1994).

185. Protection for the Hydroxyl Group, Including 1,2- and 1,3-Diols. *Greenes Prot. Groups Org. Synth.* (2014).

186. Miljković, M. in *Carbohydr. Synth. Mech. Ster. Eff.* (ed. Miljkovic, M.) 143–167 (Springer New York, 2009).

187. Robyt, J. F. *Essentials of Carbohydrate Chemistry*. (Springer, 1998).

188. Talebi Amiri, M., Dick, G. R., Questell-Santiago, Y. M. & Luterbacher, J. S. Fractionation of lignocellulosic biomass to produce uncondensed aldehyde-stabilized lignin. *Nat. Protoc.* **14,** 921–954 (2019).

189. Lan, W., de Bueren, J. B. & Luterbacher, J. S. Highly Selective Oxidation and Depolymerization of α,γ-Diol-Protected Lignin. *Angew. Chem. Int. Ed.* **58,** 2649–2654 (2019).

190. Shuai, L., Amiri, M. T., Questell-Santiago, Y. M., Héroguel, F., Li, Y., Kim, H., Meilan, R., Chapple, C., Ralph, J. & Luterbacher, J. S. Formaldehyde stabilization facilitates lignin monomer production during biomass depolymerization. *Science* **354,** 329–333 (2016).

191. Batalha, N., da Silva, A. V., Souza, M. O. de, da Costa, B. M. C., Gomes, E. S., Silva, T. C., Barros, T. G., Gonçalves, M. L. A., Caramão, E. B., Santos, L. R. M. dos, Almeida, M. B. B., Souza, R. O. M. A. de, Lam, Y. L., Carvalho, N. M. F., Miranda, L. S. M. & Pereira, M. M. Gasoline from Biomass through Refinery-Friendly Carbohydrate-Based Bio-Oil Produced by Ketalization. *ChemSusChem* **7,** 1627–1636 (2014).

192. Paszner, L. & Chang, P.-C. Organosolv delignification and saccharification process for lignocellulosic plant materials. (1983).

193. Chernyavskaya, N. A. Method of continuous acid hydrolysis of cellulose containing substances. (2009).

194. Kan, T., Strezov, V. & Evans, T. J. Lignocellulosic biomass pyrolysis: A review of product properties and effects of pyrolysis parameters. *Renew. Sustain. Energy Rev.* **57,** 1126–1140 (2016).

195. Adkins, H. & Broderick, A. E. Hemiacetal Formation and the Refractive Indices and Densities of Mixtures of Certain Alcohols and Aldehydes. *J. Am. Chem. Soc.* **50,** 499–503 (1928).

196. Lewis, E. S. (ed). *Investigation of rates and mechanisms of reactions. Part I. General considerations and reactions at conventional rates. Third edition*. (John Wiley and Sons, Inc., New York, 1974).

197. Pétursson, S. Protecting Groups in Carbohydrate Chemistry. *J. Chem. Educ.* **74,** 1297 (1997).

198. Pagán-Torres, Y. J., Wang, T., Gallo, J. M. R., Shanks, B. H. & Dumesic, J. A. Production of 5-Hydroxymethylfurfural from Glucose Using a Combination of Lewis and Brønsted Acid Catalysts in Water in a Biphasic Reactor with an Alkylphenol Solvent. *ACS Catal.* **2,** 930–934 (2012).

199. Choudhary, V., Sandler, S. I. & Vlachos, D. G. Conversion of Xylose to Furfural Using Lewis and Brønsted Acid Catalysts in Aqueous Media. *ACS Catal.* **2,** 2022–2028 (2012).

200. Román-Leshkov, Y., Moliner, M., Labinger, J. A. & Davis, M. E. Mechanism of Glucose Isomerization Using a Solid Lewis Acid Catalyst in Water. *Angew. Chem. Int. Ed.* **49,** 8954–8957 (2010).

201. Choudhary, V., Pinar, A. B., Sandler, S. I., Vlachos, D. G. & Lobo, R. F. Xylose Isomerization to Xylulose and its Dehydration to Furfural in Aqueous Media. *ACS Catal.* **1,** 1724–1728 (2011).

202. Danon, B., Marcotullio, G. & Jong, W. de. Mechanistic and kinetic aspects of pentose dehydration towards furfural in aqueous media employing homogeneous catalysis. *Green Chem.* **16,** 39–54 (2013).

203. Robyt, J. F. *Essentials of Carbohydrate Chemistry*. (Springer-Verlag, 1998). at <//www.springer.com/de/book/9780387949512>

204. Nimlos, M. R., Qian, X., Davis, M., Himmel, M. E. & Johnson, D. K. Energetics of Xylose Decomposition as Determined Using Quantum Mechanics Modeling. *J. Phys. Chem. A* **110,** 11824–11838 (2006).

205. Moriarty, K. L., Milbrandt, A. R., Warner, E., Lewis, J. E. & Schwab, A. A. *2016 Bioenergy Industry Status Report*. (National Renewable Energy Lab. (NREL), Golden, CO (United States), 2018).

206. Mössinger, D., Scheytt, H., Uihlein, K., Wunderlich, D. & Zimmerer, B. High-tenacity viscose multifilament yarn with low yarn linear density. (2015).

207. Ronald, R., Martin, R. T. & Richardson, W. C. Filaments of regenerated cellulose. (1968).
208. Enforcement Procedure for Occupational Exposure to Formaldehyde | Occupational Safety and Health Administration.
209. Cavka, A., Stagge, S. & Jönsson, L. J. Identification of Small Aliphatic Aldehydes in Pretreated Lignocellulosic Feedstocks and Evaluation of Their Inhibitory Effects on Yeast. *J. Agric. Food Chem.* **63,** 9747–9754 (2015).
210. Klingenberg, D. J., Root, T. W., Scott, C. T., Houtman, C., Bourne, K. J. & Subramaniam, V. High temperature rheometry of lignocellulosic biomass. in (2014).
211. Vacuum distillation is a key part of the petroleum refining process - Today in Energy - U.S. Energy Information Administration (EIA).
212. Wisniak, J., Hershkowitz, M., Leibowitz, R. & Stein, S. Hydrogenation of Xylose to Xylitol. *Prod. RD* **13,** 75–79 (1974).
213. Liang, X. & Jiang, C. Atomic layer deposited highly dispersed platinum nanoparticles supported on non-functionalized multiwalled carbon nanotubes for the hydrogenation of xylose to xylitol. *J. Nanoparticle Res.* **15,** 1890 (2013).
214. Li, X., Li, G., Zang, W., Wang, L. & Zhang, X. Catalytic activity of shaped platinum nanoparticles for hydrogenation: a kinetic study. *Catal. Sci. Technol.* **4,** 3290–3297 (2014).
215. Chung, D. Y., Chung, Y.-H., Jung, N., Choi, K.-H. & Sung, Y.-E. Correlation between platinum nanoparticle surface rearrangement induced by heat treatment and activity for an oxygen reduction reaction. *Phys. Chem. Chem. Phys.* **15,** 13658–13663 (2013).
216. Lee, K., Lee, S., Jun, Y. & Choi, M. Cooperative effects of zeolite mesoporosity and defect sites on the amount and location of coke formation and its consequence in deactivation. *J. Catal.* **347,** 222–230 (2017).

217. Wang, H., Tian, P., Chen, Z., Wu, S., Yang, W., Yu, Q. & Zhou, J. Effect of coke formation on catalytic activity tests for catalytic combustion of toluene: the difficulty of measuring TOF and T98 accurately. *Chem. Eng. Commun.* **206,** 22–32 (2019).

218. Argyle, M. D. & Bartholomew, C. H. Heterogeneous Catalyst Deactivation and Regeneration: A Review. *Catalysts* **5,** 145–269 (2015).

219. *Practical Gas Chromatography*. (Springer Berlin Heidelberg, 2014).

220. Swanson, H. E. & Tatge, E. *Circular of the Bureau of Standards no. 539 volume 1: standard x-ray diffraction powder patterns*. (National Bureau of Standards, 1953).

Ydna Marie Questell-Santiago

Certified Green Belt Lean Six Sigma

Rue de la Vernie 8, 1023 Crissier, Switzerland

e-mail: ydna.questell@epfl.ch • ydna.questell@gmail.com • phone: +41 78 402 59 86

Research Interests

Production of biofuels and fine chemicals from biomass-derived carbohydrates and lignin. Catalytic upgrading of novel platform chemicals using multifunctional catalysts. Integration of high pressure systems such as CO_2 – expanded liquids as reaction media and solvent extraction/recovery.

Education

École Polytechnique Fédérale de Lausanne (EPFL), Switzerland
PhD Candidate in Chemical Engineering, Public defense in June 2019
Adviser: Professor Jeremy S. Luterbacher
Dissertation title: "Production, characterization and upgrading of biomass-derived acetal-stabilized carbohydrates"

University of Puerto Rico at Mayagüez (UPRM), Puerto Rico
Bachelor in Chemical Engineering, Graduated in June 2014
GPA: 3.62/4.00, *Magna Cum Laude*

Research Experiences

PhD Studies October 2014 – June 2019

Laboratory of Sustainable and Catalytic Processing at Lausanne, Switzerland mentored by Prof. Jeremy Luterbacher

- Stabilization of carbohydrates by protective group chemistry during the fractionation of lignocellulosic biomass and its subsequent cellulose depolymerization.
- Characterization of aldehyde-stabilized carbohydrates and their utilization as platform chemicals for the production of high-value chemicals through new reaction mechanisms.

Research Assistant August 2013 – December 2013

Glucan Biorenewables, LLC at Madison, Wisconsin USA supervised by Dr. David Alonso

- Optimization of existing processes for the production of building-block molecules such as furfural and 5-hydroxymethylfurfural for industrial applications.

Undergraduate Research May 2013 – August 2013

Catalysis Research Laboratory - University of Wisconsin at Madison, Wisconsin USA mentored by Prof. James Dumesic

- Lignocellulosic biomass depolymerization using γ-valerolactone (GVL) based processes.
- Separation of carbohydrates from GVL using phenolic solvents and liquid CO_2.

Undergraduate Research August 2011 – December 2012

Electrochemical Research Laboratory - University of Puerto Rico at Mayagüez, Puerto Rico mentored by Prof. Arnaldo Carrasquillo

- Validation of hydroquinone adsorption and its reaction kinetics on the platinum electrode interface using cyclic voltammetry. Observed new reaction kinetics on hydroquinone and platinum interface incorporating a disturbance in the equilibrium with calix[4]arene.

Industrial Experience

Intern Process Engineer January 2013 – May 2013

Merck Sharp & Dohme Química (MSDQ) at Barceloneta, Puerto Rico mentored by Eng. Glenda Ojeda, MS

- Applied Lean Six Sigma methodology, Kaizen Event, Coaching Action Plan and Standardize Work. Demonstrated completion of the approval cycle time below 10 days in order to decrease inventory by focusing on zero documentation errors, eliminating wastes and providing the organization, metrics and infrastructure to sustain results.
- Training: Good Manufacturing Practice, Lean Six Sigma, Behavior Coaching and Change and Consequence Management.

Institutional responsibilities at EPFL

Safety Delegate (COSEC) of the Laboratory of Sustainable and Catalytic Processing (LPDC) – Contact person for occupational health and safety of the unit and acquainted of the alarm system and building evacuation procedures. Management of chemical and gas inventories.

Awards/Grants

- 2019 SNSF Early Postdoc Mobility (77,700 CHF)
- 2018 Clariant CleanTech Award (5'000 CHF)
- 2018 Financial Allowance by EDCH Chemistry and Chemical Engineering (1'000 CHF)
- 2017 Chemistry Travel Award by SCNAT and SCS (1'000 CHF)
- 2016 Financial Allowance by EDCH Chemistry and Chemical Engineering (1'000 CHF)
- Research Experience for Undergraduates Summer Programs (REU - NSF) – May 2013
- Certificated Green Belt Lean Six Sigma – May 2013
- Xerox Scholarship – August 2012 (700 USD)

Conference Presentations/Poster

- Poster Session: "Carbohydrate stabilization extends the kinetic limits of chemical polysaccharide depolymerization" *Frontiers in Biorefining 2018;* St. Simons Islands, Georgia, USA.

- Flash Talk: "New routes toward biomass-derived carbohydrates upgrading" *Frontiers in Biorefining 2018;* St. Simons Islands, Georgia, USA.

- Oral Presentation: "Carbohydrate stabilization extends the kinetic limits of chemical polysaccharide depolymerization" *AIChE 2018;* Pittsburg, Pennsylvania, USA.

- Oral Presentation: "New routes toward biomass-derived carbohydrates upgrading" *Clariant Chemistry Day 2018*; Basel, Switzerland.

- Poster Session: "Carbohydrate stabilization extends the kinetic limits of chemical polysaccharide depolymerization" *Clariant Chemistry Day 2018*; Basel, Switzerland.

- Oral Presentation: "Carbohydrate stabilization extends the kinetic limits of chemical polysaccharide depolymerization" *SCS 2018*; Lausanne, Switzerland.

- Oral Presentation: "Stabilization of carbohydrates with formaldehyde during integrated biomass depolymerization" *AIChE 2017*; Minneapolis, Minnesota, USA.
- Poster Session: "Protection of carbohydrates during biomass deconstruction using formaldehyde" *AIChE 2017*; Minneapolis, Minnesota, USA.

- Poster Session: "Stabilization of carbohydrates with formaldehyde during integrated biomass depolymerization" *SCS 2017*; Bern, Switzerland.

- Poster Session: "Stabilization of carbohydrates with formaldehyde during integrated biomass depolymerization" *Frontiers in Biorefining 2016;* St. Simons Islands, Georgia, USA.

- Poster Session: "Separation of lignocellulosic biomass derivatives from gamma-valerolactone using CO_2 and organic solvents" *2013 SURE – REU Program*; UW-Madison WI, USA.

Publications

- **Questell-Santiago, Y.M.**, Komarova, A. and Luterbacher, J.S., "Mechanistic studies of the acid hydrolysis deprotection of acetal-stabilized carbohydrate". *In preparation.*

- **Questell-Santiago, Y.M.**, Barta, K. and Luterbacher, J.S., "Stabilization of reactive intermediates in biomass depolymerization by chemical functionalization". *In preparation.*

- **Questell-Santiago, Y.M.**, Yeap, J.H., Talebi Amiri, M. and Luterbacher, J.S., "Diformylxylose: A versatile reagent for the catalytic production of xylitol". *In preparation.*

- Talebi Amiri, M., Bertella, S., **Questell-Santiago, Y.M.**, and Luterbacher, J.S., "Predicting depolymerization yields from lignin structural features using quantitative ^{1}H-^{13}C heteronuclear single quantum coherence nuclear magnetic resonance spectroscopy". *In revision.*

- Rozmysłowicz, B., Yeap, J.H., Elkhaiary, A.M. I., Talebi Amiri, M., Shahab, R.L., **Questell-Santiago, Y.M.**, Xiros, C., Le Monnier, B.P., Studer, M.H. and Luterbacher, J.S., "Catalytic valorization of the acetate fraction of biomass to aromatics and its integration into the carboxylate platform", *Green Chem.,* 2019, 21, 2801-2809.

- Talebi Amiri, M., Dick, G.R., **Questell-Santiago, Y.M.,** and Luterbacher, J.S., "Fractionation of lignocellulosic biomass to produce uncondensed aldehyde-stabilized lignin", *Nature Protocols,* 14, 921–954 (2019).

- **Questell-Santiago, Y.M.,** Zambrano-Valera, R., Talebi Amiri, M., and Luterbacher, J.S., "Carbohydrate stabilization extends the kinetic limits of chemical polysaccharide depolymerization", *Nature Chemistry,* 10, 1222-1228 (2018).

- **Questell-Santiago, Y.M.,** and Luterbacher, J.S., "Chapter 2: Introduction to High Pressure CO_2 and H_2O Technologies in Sustainable Biomass Processing" in *High Pressure Technologies in Biomass Conversion*, 2017, 9-36.

- Shuai, L., Amiri, M.T., **Questell-Santiago, Y.M.**, Héroguel, F., Li, Y., Kim, H., Meilan, R, Chapple, C., Ralph, J. and Luterbacher, J.S., "Formaldehyde stabilization facilitates lignin monomer production during biomass depolymerization", *Science*, 2016, 354, 329-333.

- Shuai, L., **Questell-Santiago, Y.M.**, and Luterbacher, J.S., "A mild biomass pretreatment using γ-valerolactone for concentrated sugar production", *Green Chem.,* 2016, 18, 937-943.

- Luterbacher, J.S., Alonso, D.M., Rand, J.M., **Questell-Santiago, Y.M.**, Yeap, J.H., Pfleger, B.F. and Dumesic, J.A., "Solvent-Enabled Nonenyzmatic Sugar Production from Biomass for Chemical and Biological Upgrading", *ChemSusChem*, 2015, 8, 1317–1322.

Teaching and Mentoring Experience

Teaching Assistant – École Polytechnique Fédérale de Lausanne, Switzerland

- Chemical Engineering Lab and Project for Master Students – directed the course by combining experimental data and theoretical approaches to characterize and optimize a distillation process. Concepts include mass transport and heat transfer.
- Chemical Engineering of Heterogeneous Reaction for Master Students– discussed exercise sections about reaction elementary steps, kinetics, external and internal transport and concepts of ideal and non-ideal reactors.
- Théorie des réacteurs for Bachelor Students – introduced concepts and discussed exercises related to chemical reactors design and their operation at commercial scale.

Supervisor – École Polytechnique Fédérale de Lausanne, Switzerland

- Master thesis by Raquel Zambrano-Valera February 2017 – June 2017
  Effects of solvent and type of acid in the stabilization of carbohydrates during biomass fractionation using formaldehyde. Selective removal of the protective groups in stabilized carbohydrates. Production of furfural from stabilized carbohydrates.

- Summer internship by Alison Shapiro May 2018 – July 2018
  Organosolv pretreatment of various wood type with propionaldehyde for the production of uncondensed lignin and stabilized carbohydrates. Purification of stabilized carbohydrates.

Mentor – University of Puerto Rico at Mayagüez, Puerto Rico August 2011 – December 2011

- Mentoring and tutoring high school students emanated from public housing and low-income families through the program *Centro Universitario para el Acceso (CUA).*

Tutor – University of Puerto Rico at Ponce, Puerto Rico August 2009 – December 2009

- General Chemistry for Bachelor Students – develop exercise sessions to reinforce main subjects discussed during lectures.

Technical and non-technical skills

- Fluent in Spanish and English. Elementary proficient in French.
- Strong interpersonal and communication skills.
- Analytical Techniques: NMR, HPLC, GC, GC/MS and ESI/MS
- Catalysts Characterization Techniques: N_2 BET, TPD, TPR, FT-IR, XRD and AAS
- Programing and software: MathCad, C Language, MiniTab and Aspen Plus

Affiliations

- Member of the American Institute of Chemical Engineers – since August 2017
- Member of the Swiss Chemical Society – since January 2015
- Member of The Engineering Honor Society – Tau Beta Pi since May 2012

Extracurricular Activities

- Alto Singer: Choir of Concerts, University of Puerto Rico at Ponce, Puerto Rico
- Athlete: Taekwondo Team – Interuniversity Champion 2012, University of Puerto Rico at Mayagüez, Puerto Rico

**Ce document a été imprimé au Centre d'impression EPFL,
imprimerie climatiquement neutre, certifiée myClimate.**